Bioremediation of Polycyclic Aromatic Hydrocarbon (PAH)-Contaminated Soils in a Roller Baffled Bioreactor

A Thesis

Submitted to the College of Graduate Studies and Research

In Partial Fulfillment of the Requirements for

the Degree of Master of Science

In the Department of Chemical Engineering

University of Saskatchewan

Saskatoon, Saskatchewan

by

Ruihong Yu

PERMISSION TO USE

In presenting this thesis in partial fulfillment of the requirements for a Masters Degree from the University of Saskatchewan, I agree that the Libraries of this University may make it freely available for inspection. I further agree that permission for copying this thesis in any manner, in whole or in part, for scholarly purposes may be granted by the professors who supervised my thesis work or, in their absence, by the Head of the Department of Chemical Engineering or the Dean of the College of Graduate Studies. It is understood that due recognition shall be given to me and to the University of Saskatchewan in any scholarly use which may be made of any material in my thesis.

Requests for permission to copy or to make other use of material in this thesis in whole or in part should be addressed to:

Head of the Department of Chemical Engineering

University of Saskatchewan

Saskatoon, Saskatchewan

Canada, S7N 5A9

ABSTRACT

Contamination of soil with Polycyclic Aromatic Hydrocarbons (PAHs) is a serious environmental issue because some PAHs are toxic, carcinogenic and mutagenic. Bioremediation is a promising option to completely remove PAHs from the environment or convert them to less harmful compounds. One of the main challenges in bioremediation of PAHs in a conventional roller bioreactor is the limitation on mass transfer due to the strong hydrophobicity and low water solubility of these compounds. To address this challenge, a novel bead mill bioreactor (BMB) was developed by Riess et al. (2005) which demonstrated a significant improvement in the rates of mass transfer and biodegradation of PAHs.

In this study, to further improve mass transfer rates, baffles have been installed in both the conventional and bead mill bioreactors. Mass transfer rates of 1000 mg L^{-1} suspended naphthalene, 2-methylnaphthalene and 1,5-dimethylnaphthalene, three model compounds of PAHs, have been investigated in four bioreactors: conventional (control), baffled, BMB and baffled bead mill bioreactors. The baffled bioreactor provided mass transfer coefficients (K_La) that were up to 7 times higher than those of the control bioreactor.

Bioremediation of suspended naphthalene or 2-methylnaphthalene as a single substrate and their mixtures was studied using the bacterium *Pseudomonas putida* ATCC 17484. Both baffled and bead mill bioreactors provided maximum bioremediation rates that were 2 times higher than the control bioreactor. The maximum bioremediation rates of 2-methylnaphthalene were further increased in the presence of naphthalene by a factor of 1.5 to 2 compared to the single substrate.

Another rate-limiting step for bioremediation of PAH-contaminated soil is the strong sorption between the contaminant and soil. To find out the effect of sorption on the bioavailability of naphthalene, the appropriate sorption isotherms for three types of soils (sand, silt and clay) have been determined. It was observed that the sorption capacity of soils for naphthalene was proportional to the organic carbon content of the soils. The mass transfer of soil-bound naphthalene from the artificially prepared contaminated soils with short contamination history to the aqueous phase was studied in both the control and bead mill bioreactors. It was observed that the mass transfer was unexpectedly fast due to the increased interfacial surface area of naphthalene particles and the weak sorption between naphthalene and soils. It was concluded that artificially, naphthalene contaminated soils would likely not be any more difficult to bioremediate than pure naphthalene particles.

ACKNOWLEDGEMENT

I would like to sincerely express my great gratitude to Dr. G. A. Hill and Dr. M. Nemati for being my supervisors and supporting this work through their NSERC and PERD grants. Their patience, guidance and encouragement enabled me to overcome difficulties during the research and writing of my thesis.

I would like to extend my special appreciation to all of my advisory committee, Dr. T. Pugsley and Dr. H. Wang for their generosity in permitting me to use their instruments and their valuable advice throughout the research and thesis preparation.

Furthermore, I would like to thank all the people in the Department of Chemical Engineering: Ms. Jean Horosko, Ms. Sheryl White, Ms. Kelly Bader, Mr. Ted Wallentiny, Mr. Richard Blondin, Mr. Dale Claude and Mr. Dragan Cekic for all they have done for me for the past two years. My appreciation extends to Mr. Henry Berg in the Machine Shop for his valuable assistance.

My sincere thanks also go to my friends and colleagues. I would like to acknowledge Ryan Riess, Hossein Nikakhtari, Sachin Gadekar and Janice Paslawski for their invaluable technical advice and friendship. To Kyla Clarke, thank you very much for your precious technical assistance and your wonderful Christmas party.

My gratitude goes to my parents, who never stop wishing me the best of luck. Lastly, I would like to thank my husband Jianguo for his patience, kindness and love, without which the last two years studying in Saskatoon would not have been possible.

TABLE OF CONTENTS

LIST OF FIGURES

LIST OF TABLES

NOMENCLATURE

A	surface area of the particle (m^2)
b	sorption affinity (L mg^{-1})
C_L	dissolved concentration in liquid phase (mg L^{-1})
C_s	saturation concentration in liquid phase (mg L^{-1})
D	diffusion coefficient in liquid (m^2 h^{-1})
F	volumetric flow rate (L h^{-1})
I	toxic compound concentration (mg L^{-1})
K	soil-water partitioning coefficient (L kg^{-1})
K_a	constant indicating sorption capacity (mg naphthalene kg^{-1} soil) (mg L^{-1})$^{-N}$
K'_d	death-rate constant (h^{-1})
K_d	first-order rate constant (h^{-1})
K_I	inhibition constant (mg L^{-1})
K_L	film mass transfer coefficient (m h^{-1})
K_La	volumetric mass transfer coefficient (h^{-1})
K_p	product inhibition constant (mg L^{-1})
K_s	saturation constant (mg L^{-1})
N	flux (mg m^{-2} h^{-1})
P	product concentration (mg L^{-1})
P_m	maximum product concentration (mg L^{-1})
q	sorbed contaminant concentration (mg kg^{-1})
Q_{max}	maximum adsorption capacity of the sorbent (mg kg^{-1})

r_s rate of substrate consumption (mg L^{-1} h^{-1})

S substrate concentration (mg L^{-1})

S_0 initial substrate concentration (mg L^{-1})

S_{In} substrate concentration in the input stream (mg L^{-1})

S_L dissolved concentration of substrate (mg L^{-1})

S_{Out} substrate concentration in the output stream (mg L^{-1})

S_P substrate particle concentration (mg L^{-1})

S_s saturation concentration of substrate (mg L^{-1})

t time (h)

V liquid phase volume (L)

X biomass concentration (mg L^{-1})

X_0 initial biomass concentration (mg L^{-1})

$Y_{X/S}$ biomass yield coefficient (mg dry weight of biomass per mg of substrate)

Greek letters

γ constant

δ film thickness (m)

μ specific growth rate (h^{-1})

μ_{max} maximum specific growth rate (h^{-1})

CHAPTER 1 INTRODUCTION

1.1 Research Background

Worldwide industrial and agricultural developments have released a large number of natural and synthetic hazardous compounds into the environment due to careless waste disposal, illegal waste dumping and accidental spills. As a result, there are numerous sites in the world that require cleanup of soils and sludge. In the United States alone, it has been estimated that contaminated site treatment costs may approach 1.7 trillion dollars over the next 30 years (Mark et al., 1997).

Polycyclic aromatic hydrocarbons (PAHs) are one of the major groups of these contaminants (Da Silva et al., 2003). PAHs constitute a diverse class of organic compounds consisting of two or more aromatic rings with various structural configurations (Prabhu and Phale, 2003). Being a derivative of benzene, PAHs are thermodynamically stable. In addition, these chemicals tend to adhere to particle surfaces, such as soils, because of their low water solubility and strong hydrophobicity, and this results in greater persistency under natural conditions. This persistency coupled with their potential carcinogenicity makes PAHs problematic environmental contaminants (Cerniglia, 1992; Sutherland, 1992). PAHs are widely found in high concentrations at many industrial sites, particularly those associated with petroleum, gas production and wood preserving industries (Wilson and Jones, 1993).

Conventional techniques used for polluted soil remediation include digging up the contaminated soil and removing it to a secure landfill or simply to cap and contain the

contaminated areas of a site. These methods have some drawbacks. The first method simply moves the contamination elsewhere and may create significant risks in the excavation, handling and transport of hazardous material. Additionally, it is very difficult and increasingly expensive to find new landfill sites for the final disposal of the material. The cap and containment method is only an interim solution since the contamination remains on site, requiring monitoring and maintenance of the isolation barriers long into the future, with all the associated costs and potential liability.

A better approach than these traditional methods is to completely destroy the pollutants, if possible, or at least transform them into harmless substances. Some technologies that have been used are high-temperature incineration and various types of chemical decomposition (for example, base-catalyzed dechlorination, UV oxidation). However, these methods have significant disadvantages, principally their technological complexity, the cost for small-scale application, and the lack of public acceptance. This is particularly true for incineration since it may increase the exposure to contaminants for both the workers at the site and nearby residents.

Bioremediation is a promising option for the complete removal and destruction of contaminants. Bioremediation is the use of living organisms, primarily microorganisms, to degrade or detoxify hazardous wastes into harmless substances such as carbon dioxide, water and cell biomass. As such, it uses relatively low-cost, low-technology techniques, which generally have a high public acceptance. PAHs are biodegradable (Da Silva et al., 2003; Meysami and Baheri, 2003) and bioremediation for cleanup of PAH wastes has been extensively studied at both the laboratory and commercial levels, and has been implemented at a number of contaminated sites, including the well published cleanup of the Exxon Valdez

oil spill in Prince William Sound, Alaska in 1989, the Mega Borg spill off the Texas coast in 1990 and the Burgan Oil Field, Kuwait in 1994 (Purwaningsih, 2002).

Two different strategies, *in situ* bioremediation and e*x situ* bioremediation, are employed depending on the degree of contamination and ease of aeration of an area. *In situ* bioremediation is a technique that is applied to soil and groundwater at the site with minimal disturbance. It is a very slow process and cannot be controlled effectively. Uncertainty about the fate of the contaminant and the possible toxicity of the final product is the other down side of i*n situ* bioremediation. *Ex situ* bioremediation of PAHs, on the other hand, is a technique applied to soil and groundwater which has been removed from the site via excavation (soil) or pumping (water). This technique converts these hazardous contaminants into harmless compounds in an efficient manner in controlled bioreactors.

One of the main barriers in successful *ex situ* bioremediation of PAHs is the strong hydrophobicity and low solubility of these compounds in the aqueous phase, resulting in significant mass transfer limitations within the bioreactor (Volkering et al., 1992; Volkering, et al. 1993; Mulder et al., 1998). Stirred tank reactors offer an advantage in this case since the mass transfer can be increased with agitation. On the other hand, inherent to the design of stirred tank bioreactors, particles will always cling to the agitation system, baffles and walls. This, together with the lifting and separation of particles from the liquid phase by the sparged air required for the metabolism of the microbial cells, prevents the efficient biodegradation of PAHs. Although efficient solid to liquid mass transfer can be achieved in a stirred tank bioreactor (Purwaningsih, 2002), the extensive stripping loss of PAHs due to splashing and aeration make the use of the stirred tank bioreactor for biodegradation of PAHs impractical. These problems could be circumvented in a conventional roller bioreactor (Gray et al., 1994;

Brinkmann et al., 1998; Jauhari et al., 1999; Banerjee et al., 2002), but significant mass transfer limitation prevents the efficient biodegradation of PAHs. A novel Bead Mill Bioreactor (BMB) in which inert particles (glass beads) were used as a means to create turbulence and improve the extent of mass transfer and consequently increase biodegradation rates has been developed previously (Riess et al., 2004). Comprehensive studies have shown that the BMB not only enjoys a simple and practical design but demonstrates excellent performance with respect to mass transfer rate from the solid phase to the liquid phase and biodegradation of pure PAH particles (Riess et al., 2004).

Frequently, PAH contamination in the environment is associated with sorption onto soil rather than as pure solid particles. It is known that the biodegradation rate of most PAHs sorbed onto soil is far lower than rates measured in solution cultures of microorganisms with pure solid pollutants (Alexander and Scow, 1989; Hamaker, 1972). It is generally believed that only that fraction of PAHs dissolved in the solution can be metabolized by bacteria in soil. The amount of contaminant that can be readily taken up and degraded by microorganisms is defined as bioavailability (Bosma et al., 1997; Maier, 2000). Two phenomena have been suggested to cause the low bioavailability of PAHs in soil (Danielsson, 2000). The first one is strong adsorption of the contaminants to the soil constituents which then leads to very slow release rates of contaminants to the aqueous phase. Sorption is often well correlated with soil organic matter content (Means, 1980) and significantly reduces biodegradation (Manilal and Alexander, 1991). The second phenomenon is slow mass transfer of pollutants, such as pore diffusion in the soil aggregates or diffusion in the organic matter in the soil. The complex set of these physical, chemical and biological processes is schematically illustrated in Figure1.1. As shown in Figure 1.1, biodegradation processes are

taking place in the soil solution while diffusion processes occurs in the narrow pores in and between soil aggregates. Sorption and dissolution processes originate in solid phases such as the soil aggregates and NAPLS (non-aqueous phase liquids), respectively (Danielsson, 2000).

Seemingly contradictory studies can be found in the literatures that indicate the rate and final extent of metabolism may be either lower or higher for sorbed PAHs by soil than those for pure PAHs (Van Loosdrecht et al., 1990). These contrasting results demonstrate that the bioavailability of organic contaminants sorbed onto soil is far from being well understood.

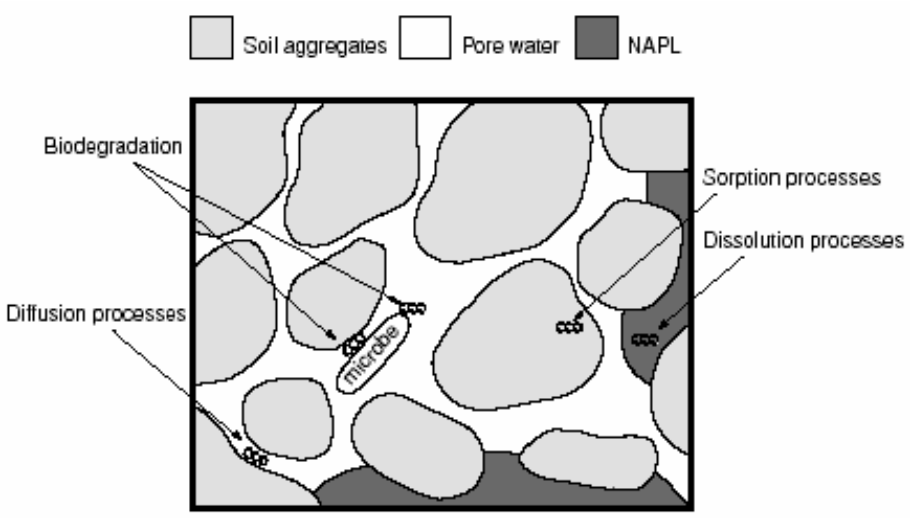

Figure 1.1: Schematic diagram showing possible rate-limiting processes during bioremediation of hydrophobic organic contaminants in a contaminated soil-water system (not to scale) (Danielsson, 2000).

Besides bioavailability, there are several other factors affecting the rate and extent of biodegradation of PAHs in soil including microbial population characteristics, physical and chemical properties of PAHs and environmental factors (temperature, moisture, pH, degree of contamination).

Attempts to overcome the slow biodegradation of PAHs in soil include the use of surfactants and water-miscible solvents. However, introduction of synthetic surfactant results in the addition of a pollutant. Furthermore the solubilization effect of cosolvents is usually not significant for volume-fraction concentrations under 10% (Wang and Brusseau, 1993). Another approach is the use of a solubility enhancer to increase the water solubility of PAHs and therefore to enhance the biodegradation rate of PAHs in soil. Unfortunately, a previous study showed that the introduction of hydropropyl-β-cyclodextrin (HPCD), a well-known PAH solubility enhancer, did not improve the biodegradation rate of PAHs, even though the solubilization of PAHs was significantly increased in the system (Mulder et al., 1998). Enhancing the extent of PAHs mass transfer from the soil phase to the liquid phase by appropriately designed reactors might prove an efficient and environmentally low-risk alternative way of addressing the problem of slow biodegradation in soil.

The major purpose of this study is to overcome the above-mentioned problems. First of all, mass transfer of PAHs from particle surfaces to the aqueous phase was studied in four different bioreactors, conventional roller, baffled, BMB and baffled bead mill bioreactors. The use of the latter three bioreactors improves the mixing of PAH particles into the liquid phase and also enhances the turbulence of the liquid, resulting in dramatically increased mass transfer rates. In this study, three PAHs: naphthalene, 2-methylnaphthalene and 1,5-dimethylnaphthalene were used as the model PAH compounds. The volumetric mass transfer coefficients of these three PAHs in different bioreactors were determined by fitting experimental data to the mathematical model of mass transfer rates. Secondly, bioremediation of suspended PAH particles, naphthalene and 2-methylnaphthalene was investigated, using *Pseudomonas putida* ATCC 17484 as the candidate bacterium in the

conventional roller, baffled and bead mill bioreactors. The co-metabolism of mixtures of naphthalene and 2-methylnaphthalene was also studied in these three bioreactors. The maximum specific growth rate, μ_{max} and yield coefficient, $Y_{X/S}$ were finally determined by applying bioremediation models to the experimental data. In addition to these suspended PAH studies, the mass transfer and bioremediation of naphthalene-contaminated soils has been studied in the conventional roller and bead mill bioreactors. For the most coverage, three types of soils: sand, silt and clay, were selected. Prior to the mass transfer and bioremediation of PAH-contaminated soils, the sorption of naphthalene to each soil was studied and the appropriate sorption isotherms and their correlation coefficients have been determined. In order to find out the relationship between sorption capacity and organic carbon contents of soils, the total organic carbon content of three soils was also determined.

1.2 Research Objectives

The objectives of this research are:

- To study mass transfer rate of suspended PAH particles in roller bioreactors. The experimental variables include the types of PAHs and the configuration of roller bioreactors.
- To calculate the volumetric mass transfer coefficients by fitting experimental data to the mathematical model that can predict the mass transfer rate of suspended PAH particles in the bioreactors.

- To investigate bioremediation rate of pure PAHs in different bioreactor configurations.
- To determine the maximum specific growth rate, μ_{max} and yield coefficient, $Y_{X/S}$, of the candidate bacterium for the prediction of biodegradation of pure PAH particles.
- To study the relationship between sorption capacity of three soils for naphthalene and organic carbon content of three soils.
- To observe mass transfer behaviour of naphthalene-contaminated soils (three types) in the conventional roller and the bead mill bioreactors.
- To study the bioremediation of naphthalene-contaminated soils (three types) in the conventional roller and the bead mill bioreactors.

1.3 Thesis Outline

This thesis consists of six chapters. Chapter 1, Introduction, describes the motivation, scope and objectives of this thesis. The Literature Review is organized in Chapter 2. This chapter reviews previous work and developments in the area of PAH bioremediation, including the type of microorganisms used to treat PAH-contaminated sites, the attempts to improve bioavailability of PAHs and the type of bioreactors commonly applied to deal with slurry systems. Chapter 3, Mathematical Models, presents the PAH mass transfer model, bioremediation kinetics and sorption isotherms for PAHs. Mass transfer and bioremediation models permit the prediction of dissolution and depletion rates under different environmental conditions. Sorption isotherms can predict the sorption capacity of different soils for PAHs. Chapter 4 focuses on Materials and Methods, which includes a description of the chemicals,

microorganisms, medium and soils used, the preparation of cell culture, the apparatus setup, the experimental procedures, the analytical methods and instruments used for sample quantification. Chapter 5, Results and Discussion, presents the experimental results, data analysis and discussion. Finally, the conclusions from this work and recommendations for future studies are summarized in Chapter 6, Conclusions and Recommendations.

CHAPTER 2 LITERATURE REVIEW

2.1 Polycyclic Aromatic Hydrocarbons (PAHs) and the Environment

2.1.1 Structure and Properties of PAHs

PAHs are a class of very stable organic molecules made up of two or more rings containing only carbon and hydrogen. These molecules are flat, with each carbon having three neighboring atoms much like graphite (Figure 2.1). PAHs generally exist as colorless, pale yellow or white solids (Mackay et al., 1992). Although hundreds of PAHs exist, two of the more common ones are benzo(a)pyrene and naphthalene. The physicochemical properties of selected PAHs are presented in Table 2.1 where it can be seen that they vary with molecular weight and structure. For instance, volatility and aqueous solubility decrease with increasing molecular weight (Wilson and Jones, 1993). The octanol-water coefficient is a measure of hydrophobicity of organic chemicals. PAH octanol-water coefficients are relatively high, indicating that they have a higher affinity for soil organic carbon than water.

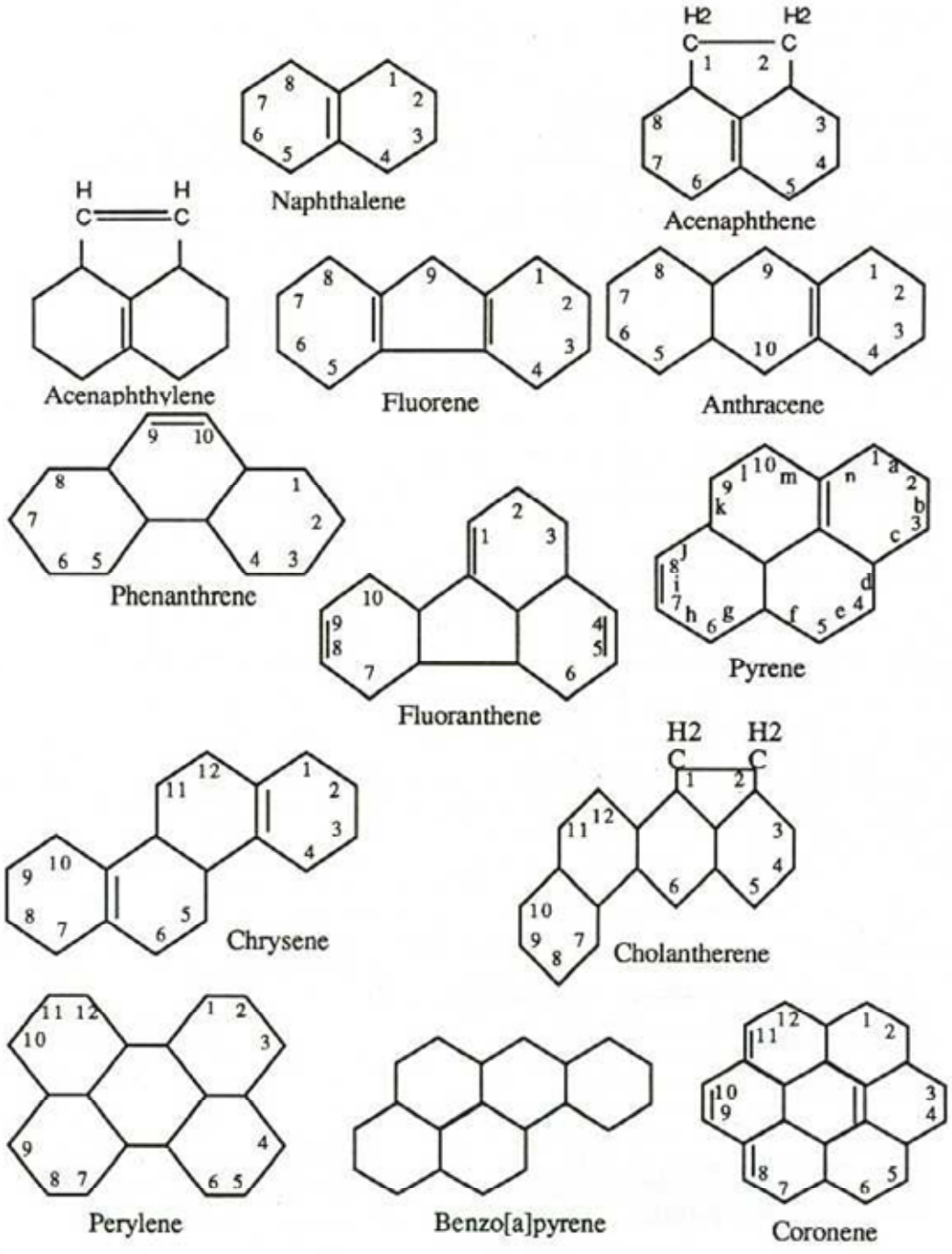

Figure 2.1: Structure and numbering of selected PAHs (Weast, 1968).

Table 2.1: Physicochemical properties of selected PAHs (Neff, 1979; Weast, 1968)

PAH	Molecular Weight (g)	Water Solubility at 25°C (µg/L)	Vapour Pressure at 25°C (mmHg)	Log $K_{octanol/water}$
Naphthalene	128.2	12500 to 34000	1.8×10^{-2}	3.37
Acenaphthylene	152.2	3420	10^{-3} - 10^{-4}	4.07 (3.40)
Acenaphthene	154.2			3.98 (3.66)
Fluorene	166.2	800		4.18 (3.86)
Anthracene	178.2	59	2.4×10^{-4}	4.5 (4.15)
Phenanthrene	178.2	435	6.8×10^{-4}	4.46 (4.15)
Fluoranthene	202.3	260		4.90 (4.58)
Pyrene	202.1	133	6.9×10^{-7}	4.88 (4.58)
Chrysene	228.3	1.9		5.63 (5.30)
Cholanthrene	254.3	2.0		6.28
Perylene	252.3	2.4		6.21
Benzo[ghi]perylene	276.4	0.3	1.0×10^{-10}	6.78 (6.20)
Coronene	300.3	0.14	1.5×10^{-11}	7.36

2.1.2 Sources and Environmental Fate of PAHs

There are two major sources of PAH emissions to the environment: natural sources and anthropogenic sources. In nature, PAHs are formed in two ways. One is high temperature pyrolysis of organic materials generally caused by fires. Forest fires, prairie fires, and agricultural burning contribute the largest volumes of PAHs from a natural source to the

atmosphere (CEPA, 1994). PAHs from fires tend to sorb to suspended particulates and eventually enter the terrestrial and aquatic environments as atmospheric fallout (Eisler, 1987). The other natural way for PAHs to occur is the formation of fossil fuels, such as coal and crude oil deposits, as a result of diagenesis (that is, low temperature, 100-150 °C, heating of organic material over a significant span of time). This process contributes a relatively small volume of PAHs to the terrestrial ecosystem because most oil deposits are trapped deep beneath layers of rock and there is little chance for PAHs to emit to the surface environment (National Research Council of Canada, NRCC, 1983).

The other source for release of PAHs into the environment is anthropogenic which is becoming more significant with the increasing worldwide industrialization. In fact, any industrial or domestic process in which organic carbon is subjected to high temperatures will result in the production of some PAHs. Industrial processes such as aluminum production, iron smelting, petroleum refining, coal coking, thermal power generation and tar paper production are all examples of major anthropogenic sources (http://www.atl.ec.gc.ca/epb/envfacts/pah.html). The contamination of the environment by PAHs is highly associated with industrial production, careless waste disposal and illegal waste dumping of PAH-containing materials. PAH-contaminated sites are also commonly associated with accidental spills, leaks from storage tanks as well as wood treatment activities involving the use of creosote and anthracene that are often used as wood treatment fungicides (Wilson and Jones, 1993). It is reported that the petroleum hydrocarbon spills cause 75 tonne/ year of PAH emissions into the environment and account for 88% of the total number of spills occurring on land (CEPA, 1994).

PAHs can remain in the air for extended periods of time adsorbed on particulate matter and can be transported over long distances before they enter soil or water by surface run-off. Since PAHs are characterized by low water solubility and strong hydrophobicity, their dissolved concentration in water is very low and most of the PAHs accumulate in sediments. Levels of PAHs in sediments vary, depending on the proximity of the sites to areas of human activity. PAHs in sediments are elevated near industrial and urban centres. In British Columbia, this trend was evident in the Greater Vancouver area. Dunn and Stich (1975) demonstrated the impact of municipal effluent on sediment PAH concentrations in samples collected near the Iona Island sewage treatment outfall when it was discharged onto Sturgeon Bank in shallow waters. Benzo(a)pyrene levels of 121 µg/g were detected at a distance of about 0.7 km from the sewage outfall. As the distance increased, however, the concentrations of benzo(a)pyrene dropped rapidly, registering a value of <1.0 µg/g past 5 km. It is generally recognized that PAHs are more environmental persistent when they are bound to particulates with a high organic carbon content (CEPA, 1994).

In addition to air and sediment, PAHs can also accumulate in biota. The level of anthracene in seaweed collected from Osaka Harbour, Japan, averaged 4 ng /g (dry weight). The average high molecular weight PAH concentrations in seaweed for this site ranged from 2 ng/g (dry weight) for dibenzo[a,h]anthracene to 72 ng/g (dry weight) for benzo[a]pyrene (Obana et al., 1981). In British Columbia, PAHs in shellfish were first reported by Dunn and Stich (1975). Levels up to 0.2 ng/g of benzo(a)pyrene were measured in mussels from the open west coast of Vancouver Island, 5 km from human activity; 42.8 ng/g of benzo(a)pyrene were found in mussels from a poorly flushed inlet (False Creek) with heavy boat and industrial use. At four out of five sites in the Vancouver Harbour, benzo(a)pyrene

uptake by mussels fluctuated seasonally. These seasonal fluctuations were attributed to variations in pollution pattern rather than physical differences such as temperature or physiological differences related to the breeding cycle of the organisms.

2.1.3 Health and Environmental Concerns

PAHs are potential carcinogens that can produce tumours in some organisms at even single doses. Other non-cancer-causing problems are not well understood, but may include adverse effects on reproduction, development, and immunity (ATSDR, 1993; Eisler, 1987b). PAH effects are wide-ranging within an organism and have been found in many types of organisms, including non-human mammals, birds, invertebrates, plants, amphibians, fish, and humans. Humans and non-human mammals can absorb PAHs by inhalation, dermal contact, or (more poorly) ingestion (Eisler, 1987b). The oral toxicity of PAHs ranges from very to moderately toxic (50 to 1000s mg/kg body weight) in rats. Plants absorb PAHs from soil, especially lower molecular weight PAHs, and readily translocate them to above-ground tissues. The concentrations in plants are substantially lower than in soil, and they are poorly correlated because of deposition and absorption of atmospheric PAHs. Eating of leaves (foliar herbivory) does not appear to be a significant route of exposure to soil PAHs. Fish exposed to PAH contamination exhibited fin erosion, liver abnormalities, cataracts, and immune system impairments leading to increased susceptibility to disease (Fabacherm, 1991; O'Conner and Huggett, 1988; Weeks. and Warinner, 1984; Weeks and Warinner, 1986). Some fish, however, increase their production of enzymes which break down PAHs, possibly reducing the chemicals' toxic effects. Organisms such as mussels and oysters lack the enzyme

systems which break down PAH compounds, and sometimes accumulate high concentrations of PAHs.

The release of PAHs is regulated under various laws, regulations and agreements designed to protect the environment and human health. PAHs are assessed for environmental and human health effects under the Canadian Environmental Protection Act's (CEPA) Priority Substances Assessment Program. PAHs are included in ocean dumping provisions of CEPA, which regulate allowable levels of contaminants in materials disposed at sea. In addition, Environment Canada administers Section 36 of the Fisheries Act which prohibits depositing harmful substances, such as PAHs, in waters used by fish. Other federal legislation which deals with the regulation of PAHs includes the Pest Control Products Act, the Transportation of Dangerous Goods Act and the Food and Drug Act. Finally, Environment Canada has published technical guidelines for the safe design and operation of wood preservation facilities which use creosote-based pesticides (http://www.atl.ec.gc.ca/epb/envfacts/pah.html).

2.2 Microorganisms

2.2.1 The Central Dogma of Biology: DNA

The primary tenet of molecular biology is the central dogma of life, which applies to all organisms. Almost all living systems have the same core approach to the storage, expression and utilization of genetic information. The information of all living cells is stored on a deoxyribonucleic acid (DNA) molecule. DNA serves as the template for its own replication as well as transcription to RNA. The information transcribed into the RNA can

then be translated into proteins using an RNA template. The proteins then perform an enzymatic role, mediating almost all the metabolic functions in the cell.

2.2.2 Growth Patterns and Kinetics

Growth of an organism can be defined as an orderly increase in all its chemical constituents (Bailey, 1977). When most single-celled organisms grow, they eventually divide. Consequently, growth of a population usually implies an increase in the number of cells as well as the mass of all cellular materials. When a liquid nutrient medium is inoculated with a seed culture, the organisms selectively take up dissolved nutrients from the medium and convert them into biomass. As a result of nutrient utilization, microbial mass increases with time and can be described simply by:

$$\text{Substrates + Cells} \longrightarrow \text{Extracellular Products + More Cells} \qquad (2.1)$$

A typical batch growth (culturing cells in a vessel with an initial charge of medium that is not altered by further nutrient addition or removal) curve includes the following phases: (1) lag phase, (2) logarithmic or exponential growth phase, (3) deceleration phase, (4) stationary phase, and (5) death phase.

The lag phase occurs immediately after inoculation and is a period of adaptation of cells to a new environment. Microorganisms reorganize their molecular constituents when they are transferred to a new medium. Depending on the composition of nutrients, new enzymes are synthesized, the synthesis of some other enzymes is repressed, and the internal machinery of cells is adapted to the new environmental conditions. During this phase, cell mass may increase a little, without an increase in cell number density.

The concentration of nutrients as well as the size and age of inoculum have a strong effect on the length of the lag phase. Low concentrations of some nutrients may cause a long lag phase. When the inoculum is small and has a low fraction of cells that are viable, there may be a pseudolag phase, which is a result not of adaptation but of the small inoculum size. The age of the inoculum culture also plays a significant role in controlling the length of the lag phase. Usually, the lag period increases with the age of the inoculum. To minimize the duration of the lag phase, cells should be adapted to the growth medium and conditions before inoculation and the cells should be young (preferably exponential phase cells) and active and the inoculum size should be large (5% to 10% by volume).

After the lag phase, cells can multiply rapidly and enter the exponential growth phase. In this phase, cell mass and cell number density increase exponentially with time. This is a period of balanced growth, in which all components of a cell grow at the same rate. The average composition of a single cell remains approximately constant during this phase of growth. During balanced growth, the net specific growth rate determined either from cell number or cell mass would be the same. A bacterial culture undergoing balanced growth mimics a first-order autocatalytic chemical reaction (Carberry, 1976; Levenspiel, 1972). Therefore, the rate of the biomass concentration increase at any particular time is proportional to the biomass concentration (X) present at that time:

$$\frac{dX}{dt} = \mu \times X \qquad (2.2)$$

where μ is the specific growth rate (h^{-1})

If μ is constant with time during the exponential growth period, Equation (2.2) can be integrated from time t_0 to t, yielding:

$$\ln \frac{X}{X_0} = \mu \times (t - t_0) \qquad (2.3)$$

As seen in Equation 2.3, the exponential growth is characterized by a straight line on a semilogarithm plot of ln X versus time.

The specific growth rate need not be a constant and there are a number of different models to predict the specific growth rate.

2.2.2.1 Substrate-Limited Growth

Since there is usually a finite amount of substrate (S) available, growth is normally substrate limited (that is, an increase in S influences growth rate while changes in other nutrient concentrations have no effect). Under these circumstances, the relationship between the specific growth rate and substrate concentration is frequently modelled using the Monod equation (Bailey and Ollis, 1986; Blanch and Clark, 1997):

$$\mu = \mu_{\max} \frac{S}{K_s + S} \qquad (2.4)$$

where μ_{max} is the maximum specific growth rate (h^{-1}). The constant K_s is known as the saturation constant (mg L^{-1}) and is equal to the substrate concentration when the specific growth rate is equal to half of maximum. That is, K_s=S when $\mu=\mu_{max}/2$. The Monod equation is semiempirical and fits a wide range of data satisfactorily. It is the most commonly applied model of substrate-limited microbial growth.

2.2.2.2 Models with Growth Inhibitors

At high concentrations of substrate or product and in the presence of inhibitory substances in the medium, growth becomes inhibited and growth rate depends on inhibitor concentration. The inhibition pattern of microbial growth is analogous to enzyme inhibition. Therefore, all the models that have been developed for enzyme inhibition can be applied to express cell growth inhibition. Some of the models are listed as follows:

2.2.2.2.1 Substrate Inhibition

At high substrate concentrations, the microbial growth rate is inhibited by the substrate. As in enzyme kinetics, substrate inhibition of growth may be competitive or noncompetitive. The major substrate-inhibition patterns and expressions are as follows (Shuler and Kargi, 2002):

Noncompetitive substrate inhibition:

$$\mu = \frac{\mu_{\max}}{\left(1+\frac{K_s}{S}\right)\left(1+\frac{S}{K_I}\right)} \tag{2.5}$$

If $K_I >> K_s$, then:

$$\mu = \frac{\mu_{\max} S}{K_s + S + S^2 / K_I} \tag{2.6}$$

which is also known as the Haldane substitute inhibition model.

For competitive substrate inhibition:

$$\mu = \frac{\mu_{\max} S}{K_s\left(1+\frac{S}{K_I}\right)+S} \qquad (2.7)$$

where K_I is the inhibition constant (mg L^{-1}).

2.2.2.2.2 Product Inhibition

High concentrations of product can be inhibitory for microbial growth. Product inhibition may be competitive or noncompetitive. Ethanol fermentation from glucose by yeasts is a good example of noncompetitive product inhibition, and ethanol is the inhibitor at concentration above about 5%. Important examples of the product inhibition rate expression are as follows (Lee, 1992; Shuler and Kargi, 2002):

Noncompetitive product inhibition:

$$\mu = \mu_{\max}\left(\frac{S}{K_s+S}\right)\left(1-\frac{P}{P_m}\right)^{\gamma} \qquad (2.8)$$

Competitive product inhibition:

$$\mu = \frac{\mu_{\max} S}{K_s\left(1+\frac{P}{K_P}\right)+S} \qquad (2.9)$$

where P is the product concentration (mg L^{-1}), P_m is the maximum product concentration (mg L^{-1}) above which cells cannot grow due to product inhibition, γ is a constant that needs to be empirically determined, and K_p is the product inhibition constant (mg L^{-1})

2.2.2.2.3 Inhibition by Toxic Compounds

The following rate expressions are used for competitive, noncompetitive and uncompetitive growth inhibition by toxic compounds other than the substrate or product, in analogy to enzyme inhibition (Shuler and Kargi, 2002):

Competitive inhibition:

$$\mu = \frac{\mu_{\max} S}{K_s\left(1+\frac{I}{K_I}\right)+S} \tag{2.10}$$

Noncompetitive inhibition:

$$\mu = \frac{\mu_{\max}}{\left(1+\frac{K_s}{S}\right)\left(1+\frac{I}{K_I}\right)} \tag{2.11}$$

Uncompetitive inhibition:

$$\mu = \frac{\mu_{\max} S}{\left(S+\frac{K_s}{\left(1+\frac{I}{K_I}\right)}\right)\left(1+\frac{I}{K_I}\right)} \tag{2.12}$$

where I is the toxic compound concentration (mg L^{-1}) and K_I is the inhibition constant.

In some cases, death occurs in the growth phase of cells. The net specific rate expression in the presence of death has the following form:

$$\mu = \frac{\mu_{\max} S}{K_s + S} - K'_d \tag{2.13}$$

where K'_d is the death-rate constant (h^{-1}).

The deceleration growth phase follows the exponential phase. In this phase, growth decelerates due to the depletion of one or more essential nutrients or the accumulation of toxic by-products of growth. For a typical culture, these changes occur over a very short period of time. The rapidly changing environment results in unbalanced growth during which cell composition and size will change. In this phase, the stresses induced by nutrient depletion or waste accumulation cause a restructuring of the cell to increase the prospects of cellular survival in a hostile environment.

The stationary phase starts at the end of the deceleration phase, when the net growth rate is zero (no cell division) or when the growth rate is equal to the death rate. Even though the net growth rate is zero during the stationary phase, cells are still metabolically active and produce secondary metabolites (nongrowth-related metabolites). During this phase, one or more of the following phenomena may take place:

1) Total cell mass concentration may stay constant, but the number of viable cells may decrease.

2) Cell lysis may occur and viable cell mass may drop. A second growth phase may take place and cells may grow on the products of lysed cells (cryptic growth).

3) Cells may not be growing but may have active metabolism to produce secondary metabolites.

During the stationary phase, the cell catabolises cellular reserves for new building blocks and for energy-producing monomers. This is called endogenous metabolism. The appropriate equation to describe the conversion of cell mass into maintenance energy (energy

expenditure to maintain an energized membrane and transport of nutrients and for essential metabolic functions) or the loss of cell mass due to cell lysis during this phase is:

$$\frac{dX}{dt} = -K_d X \qquad (2.14)$$

where K_d is a first-order rate constant for endogenous metabolism. Because S is zero, μ is zero in the stationary phase.

The death phase (or decline phase) follows the stationary phase. However, some cell death may start during the stationary phase, and a clear demarcation between these two phases is not always possible. Often, dead cell lyse and intracellular nutrients released into the medium are used by the living organism during stationary phase. At the end of the stationary phase, because of either nutrient depletion or toxic product accumulation, the dead phase begins. The rate of death usually follows first-order kinetics:

$$\frac{dN}{dt} = -K'_d N \qquad (2.15)$$

where N is the concentration of cells at the end of the stationary phase.

To better describe growth kinetics, the stoichiometric relationship between the substrate utilization and biomass production is defined as (Shuler and Kargi, 2002):

$$\frac{dX}{dt} = -Y_{X/S} \frac{dS}{dt} \qquad (2.16)$$

where $Y_{X/S}$ is the yield coefficient (mg dry weight of biomass/mg of substrate) and is defined as the ratio between the amount of biomass produced and the amount of substrate consumed.

$$Y_{X/S} = -\frac{dX}{dS} \qquad (2.17)$$

In a continuous system, yield coefficient (true growth yield) is constant for microorganisms. At the end of the batch growth, however, we have an apparent growth yield (or observed growth yield). Because culture conditions can alter patterns of substrate utilization, the apparent growth yield is not a true constant.

2.2.3 PAH-Degrading Microorganisms

Microorganisms can be isolated from almost any location and will adapt and grow over a broad range of conditions. Because of the adaptability of microbes and pervasiveness of PAHs in the environment, many different microorganisms have been used to remediate PAH-contaminated sites.

Janikowski et al. (2002) reported the use of *Sphingomonas aromaticivorans* B0695 for biodegradation of PAH compounds in a two-phase partitioning bioreactor (TPPB). *Sphingomonas aromaticivorans* B0695 was originally isolated from deep subsurface sediment of the Atlantic Coastal Plains and recently identified as possessing the ability to degrade up to seven low molecular weight (LMW) PAHs (Fredrickson et al., 1995; Fredrickson et al., 1999; Rockne and Strand, 1998). This bacterium is now available from the Subsurface Microbial Culture Collection (SMCC) as SMCC B0695 at Florida State University. In Janikowski et al.'s study, the capability of this bacterium to effectively degrade two LMW PAHs (naphthalene and phenanthrene) was firstly observed in the TPPB. It was found that the bacterium completely biodegradaed 4.5 g of both compounds in less than 75 h at a volumetric biodegradation rate of 40 $mgL^{-1}h^{-1}$. This biodegradation rate corresponded to an overall volumetric rate of 33 mg L^{-1} h^{-1} for naphthalene and 21 $mgL^{-1}h^{-1}$ for phenanthrene. The yield coefficient, $Y_{X/S}$, for this fermentation was found to be 0.55 g

cells/ g substrate which was comparable to the value reported by Saner et al. (1996) for a mixed culture. Additionally, the effect of a co-solvent (dodecane/ethanol) on the biodegradation of four LMW PAHs (naphthalene, phenanthrene, anthracene and acenaphthene) was examined in the TPPB. The yield coefficient generated in this system was 0.88 g cells / g PAHs which was higher than that achieved in the system without solvents present. The higher yield coefficient was attributed to the extra carbon sources for the bacterium from the solvents. Also, an initial lag phase of approximately 12 h for PAHs was observed in the presence of solvents, and it was believed that this lag phase occurred because the bacterium was using ethanol (one of the solvents) as the substrate before commencing to utilize the PAHs. The individual PAH degradation rates were determined to be 38 mg $L^{-1}h^{-1}$ for both naphthalene and phenanthrene and 1.6 mg $L^{-1}h^{-1}$ for both anthracene and acenaphthene. It was suspected that the lower biodegradation rates for the latter two compounds were due to a nutrient deficiency in the medium, which was confirmed by the higher biodegradation rates (85 mg $L^{-1}h^{-1}$ for both naphthalene and phenanthrene, and 11 mg L^{-1} h^{-1} for both anthracene and acenaphthene) obtained in this study after increasing the concentration of yeast extract, tryptone and salts in the medium. They also pointed out that oxygen limitation occurred during all the biodegradation experiments in the TPPB. The true capability of the bacterium, S. *aromaticivorans* B0695 to degrade PAHs should be substantially improved if oxygen limitation can be avoided.

Yeom and Ghosh (1998) discussed the use of *Pseudomonas fluorescens* DFC 50 and *Acidovorax delafieldii* in the bioremediation of artificially PAH-contaminated soils as well as the use of a mixed culture enriched from a mixture of manufactured gas plant (MGP) soil and a creosote-contaminated soil. These microorganisms, including the natural consortium

enriched from field, were reported to be able to use naphthalene and phenanthrene (rich in the MGP soil) as sole carbon and energy sources. In addition, the effect of contamination age (duration of time a soil is contact with PAHs) on the bioavailability of soil-bound PAHs was investigated using artificially contaminated soils with phenanthrene . It was concluded that in soils with recent contamination, mobilization of contaminants to the aqueous phase was not a major issue; therefore, surfactant-washing effects on such soils was not found. However, a significant retardation of biodegradation with an increase in contamination age was observed in the absence of surfactant and believed to be due to mass transfer limitations. Evidence of mass transfer limitations for soils with long contamination age were also reported earlier by other researchers (Hatzinger and Alexander, 1995; Yeom and Ghosh, 1993).

Several bacterial strains were isolated following enrichment of pristine sand and organic soils, and from eight soils chronically contaminated with crude oils, diesel, bitumen, waste lubricating oil, gasoline or gas condensate by Smith et al. (1997). In their studies, naphthalene and phenanthrene degraders were enriched from all 10 soils examined and the fastest growing bacterium (a Gram-negative rod) was designated as PD2 which metabolised both PAHs. A 4-membered bacterial consortium (designated as DC1) with the ability to degrade pyrene was obtained from the diesel-contaminated soil. The results of studies with sand and organic soils showed that the inoculation with PD2 did not accelerate the rapid natural attenuation of naphthalene by indigenous microorganisms in both soils, suggesting that naphthalene was readily available to microorganisms. Additionally, it was demonstrated that inoculation with PD2 accelerated bioremediation of phenanthrene in both soils; however, biodegradation of phenanthrene ceased in DC1-inoculated soils after a period of time compared with PD2, indicating that the PD2 species might enhance bioavailability by

producing exoenzymes or surfactants. The observation of differential bioavailability of soil-sorbed PAHs to different bacterial species was also reported by Guerin et al. (1992) and Providenti et al. (1995). In Smith et al.'s studies, inoculation of sand and organic soils with DC1 was also found to accelerate biodegradation of pyrene, but 40% and 60% of the pyrene was left undegraded in sand and organic soil, respectively. This was attributed to lower bioavailability of pyrene and its metabolites, particularly in organic soil where sorption capacity for pyrene was 47-fold greater than sand.

Many other bacteria including pure bacterial strains and mixed cultures have been reported to remediate PAH-contaminated sites. Ye et al. (1996) addressed the successful degradation of more difficult degradable PAHs such as fluoranthene, pyrene, benz[a]anthracene, chrysene, benzo[a]pyrene and benzo[b]fluoranthene by *Pseudomonas paucimobilis*. Schneider et al. (1996) reported the use of *Mycobacterium sp.* in the remediation of pyrene, benz[a]anthracene and benzo[a]pyrene. Ghoshal and Luthy (1996; 1998) and Ghoshal et al. (1996) presented kinetic data for naphthalene degradation, including the following Monod parameters for a mixed culture isolated from PAH-contaminated soil and grown on naphthalene over a long period of time in aerobic slurry systems: yield coefficient, $Y_{X/S}$, equal to 0.25±0.08 g dry biomass/ g naphthalene; maximum specific growth rate, μ_{max}, 0.067 h^{-1} and saturation constant, K_s, 3.4 mg L^{-1}.

The use of *Pseudomonas putida* in the remediation of PAH-contaminated sites has been increasingly attractive. Guerin and Boyd (1992) reported that *Pseudomonas putida* ATCC 17484 had superior characteristics in both the rate and extent of naphthalene biodegradation. Marx and Aitken (2000) suggested that bacterial chemotaxis to a pollutant can overcome the mass transfer limitations that may govern biodegradation rates in

contaminated environments. They showed that a motile wild strain of *Pseudomonas putida* exhibited better naphthalene degradation performance when compared to a nonmotile mutant or a mutant deficient in naphthalene chemotaxis.

2.3 Bioremediation and Rate-Limiting Factors

Bioremediation is the use of living microorganisms (bacteria, fungi of plant) to degrade or detoxify hazardous wastes into harmless substances such as carbon dioxide, water and cell biomass. Bioremediation can take place under both aerobic and anaerobic conditions. In aerobic conditions, microorganisms use available atmospheric oxygen as an electron acceptor to function. Under anaerobic conditions, no oxygen is present and biological activity is supported by the presence of other electron acceptors. Sometimes, during the aerobic and anaerobic processes, intermediate products which are less, equal or more toxic than the original contaminants are formed.

The control and optimization of bioremediation processes is a complex task and depends on many factors. These factors include (Vidali, 2001):

- The existence of a microbial population capable of degrading the pollutants.
- Environment factors such as temperature, pH, the presence of oxygen or other electron acceptors and nutrients to ensure the maximal growth and activity of microbes.
- Toxic or inhibitory effects of the contaminants and their degradation products.
- The bioavailability of contaminants for the microbial population.

It is not hard to enrich and/or isolate a microbial population which is capable to degrade the contaminants in the environment due to the adaptation. Environmental factors including the amount of oxygen and nutrients for the microbes, the temperature and pH in the system can often be regulated to the optimal values in *ex situ* bioremediation processes. Factors like toxicity and viability of microbes have been investigated in laboratory tests and were usually found not to be significant (Erickson et al. 1993). However, what does control the overall biodegradation rate in most cases is the bioavailability of substrate (the contaminant) to the microorganisms.

Bioavailability controls biodegradation rate because microbial cells must expend energy to induce catabolic gene systems used in the biodegradation. If the available contaminant concentration to microbes is very low, the induction will not occur. Two factors have been suggested to cause the low bioavailability of PAHs sorbed to soils and therefore lower the biodegradation rate of PAH-contaminated soil (Ashok, 1995; Bosma et al., 1997; Danielsson, 2000; Maier, 2000). First, it is difficult to provide an adequate concentration of PAHs to the bacterium in an aqueous phase because of the low water solubility of PAHs. Second, contaminant PAHs in the environment are strongly sorbed to the soil due to their strong hydrophobicity. The higher the molecular weight, the stronger is the affinity of PAH particles for the soil.

2.4 Dissolution of PAH Particles

Studies have revealed that PAHs in the solid state are consumed by microorganisms only after these compounds are transferred to the aqueous phase by dissolution (Volkering et al., 1992; Volkering et al., 1993). The dissolution of solid particles in liquids is an interfacial

mass transfer phenomenon in which the molecules on the particle surface leave the surface continuously, thus reducing the mass of particles (Purwaningsih, 2002). The simplest theory for interfacial mass transfer involves a thin film, also called an unstirred layer, and a concentration difference between the interface and the bulk. The determining factors for the diffusive transport of PAH particles across this film are the diffusion coefficient and the distance (or film thickness) over which the solute is transported (Cussler, 1997). The dissolution rate of particles can be predicted by determining the solid-liquid volumetric mass transfer coefficient which is a function of diffusion coefficient, film thickness and surface area of particles.

The dissolution rate of PAH particles can be improved by the hydrodynamic conditions of the system in the bioreactor. Riess et al. (2004) have demonstrated that the volumetric mass transfer coefficient of PAH particles was significantly enhanced in a novel BMB. The use of glass beads increased the turbulence at the interfacial surface of solid particles, reducing the film thickness and enhancing the mass transfer coefficient. On the other hand, the grinding force acting on the PAH particles by the beads broke up the PAH particles, increasing the surface area of particles and improving the mass transfer coefficient. Many other researchers also observed the effect of hydrodynamics on the mass transfer rate of PAH particles. Hixson and Sidney (1941) and Mulder et al. (1998) reported that the use of impellers in the bioreactor increased the mass transfer coefficient of naphthalene. The decrease in film thickness for naphthalene mass transfer was observed in Mulder's study as the impeller speed in the bioreactor increased. The increased agitation speed increases the turbulence of the system and therefore reduces the film thickness and enhances the mass transfer coefficient.

2.5 Sorption Mass Transfer

Due to the complexity of soil structure and constituents, there are several different sorption processes and mass transfer phenomena that control the release of contaminants in the soil. To locate possible sorbent domains and understand possible mass transfer processes involved, it is important to know the construction and the composition of the soil.

2.5.1 Soil Structure

Soil structure consists of aggregates of mineral grains that are clustered together with natural organic matter. Silt and sand particles are known to be coated with clay-sized particles (<2 μm) that are cemented to each other and to the larger particle by organic matter, mineral oxides and carbonates. The coatings of clay-sized particles can shield the organic matter from equilibrium with the bulk, which makes the sorbent organic matter (SOM) domain (see Section 2.5.2) a strong sorption site for PAHs. The coating can be thick in some places, such as in and along fissures and pits associated with the primary particle.

The void volume between the aggregates of soil is called macro pores (>50 nm). In the saturated zone, these pores will be filled with water and constitute the bulk solution. The soil aggregates also have internal pores that usually are divided into meso- (pore diameter 2-50 nm) and micro- (pore diameter < 2 nm) pores (see Figure 2.2). The meso pores will fill with sorbate at vapour pressures approaching saturation due to capillary condensation. The micro pores will influence sorbate sorption by the proximity of two solid surfaces.

2.5.2 Conceptual Model of the Geosorbent and Sorbent Domains

Various types of soils and sediments are commonly referred to as geosorbents or simply sorbents. The geosorbents consist of structurally and/or chemically different constituents that interact differently with PAHs in terms of binding energies and rates of associated sorption processes. The soil may also contain combustion residues (e.g. chars, soot and ashes) and non-aqueous phase liquids (NAPLs e.g. tars, oils and solvents) that are entrapped or adherent to the geosorbents. These types of substances can also function as sorbents for PAHs and therefore they should be included in the conceptual model of possible sorbent domains in a soil or sediment (see Figure 2.2).

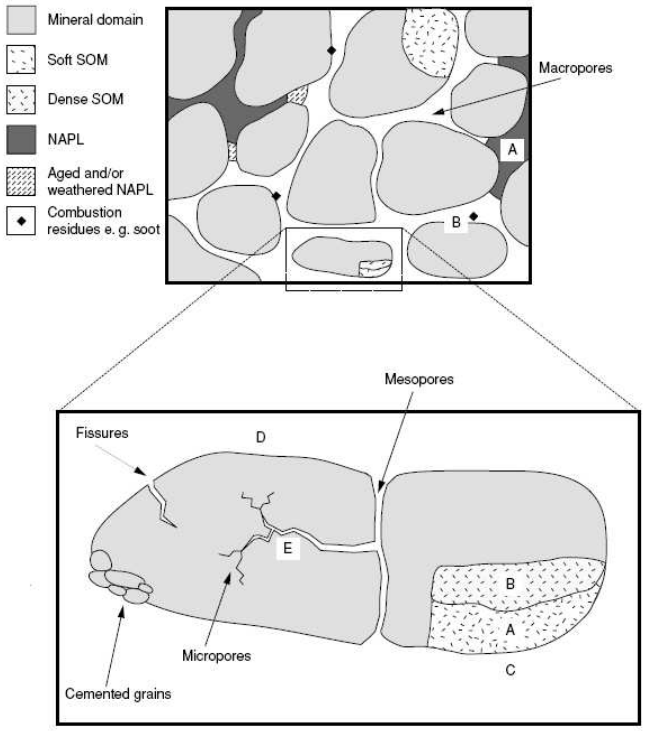

Figure 2.2: Soil structure and a conceptual model of different sorbent domains in a soil (not to scale). A: absorption into soft sorbent organic matter (SOM) or NAPLs; B: absorption into dense SOM or combustion residues; C: adsorption to water-wet nonpolar heterogeneous organic surfaces; D: adsorption onto exposed water-wet mineral surfaces; E: diffusion into hydrophobic microporous regions of minerals (Danielsson, 2000)

The conceptual model consists of three principal domains (Danielsson, 2000): the mineral domain, the sorbent organic matter (SOM) that can be divided into dense and soft SOM, and the adherent or entrapped NAPLs.

The mineral domain consists of three types of sorption sites: (i) external surfaces of the mineral grains, (ii) interlayer surfaces of swelling clays and (iii) surfaces within the pores of inorganic mineral matrices.

The SOM domain has been formed through degradation of biopolymers. During diagenesis and sedimentation these degraded biopolymers are cross-linked, forming residues (e.g. humic material) that further could be altered under metamorphic conditions. This process creates diversity in composition and structure of the SOM domain, with dense and soft carbon, and therefore different sorptive properties can be expected.

Adherent or entrapped NAPLs constitute the third domain. This sorbent domain may function as the soft SOM domain, except for highly weathered material or interfacial films. Combustion residues like soot may act as dense SOM.

2.5.3 Sorption Mechanisms

Luthy et al. (1997) summarize the possible sorption processes for hydrophobic organic contaminants (HOCs) such as PAHs in a soil from the conclusions drawn from macroscopic observations. Sorption mechanisms are usually described with respect to their exchange kinetics and type of isotherm. Table 2.2 lists these types of macroscopic experimental observations. It gives an indication of the different sorption mechanisms and sorption domain for the sorption processes.

The different proposed sorption cases, marked by letters from A to E, in the left column of Table 2.2 refer to the same letters in Figure 2.2. It should be noted that it is difficult to distinguish between the cases B and E (see Table 2.2) since they may have similar macroscopic behaviours. What also complicates the interpretation of macroscopic data is that not only one sorption mechanism dominates the sorption processes in any particular case.

Table 2.2: Possible sorption cases, regarding sorption of HOCs to soil (Cussler, 1997)

Sorption cases	**Exchange kinetics**	**Isotherm**
A: absorption into soft SOM or NAPLs	Fast (<minutes) if particles are disaggregated	Linear
B: absorption into dense SOM or combustion residues	Slow (>days); sorption-desorption hysteresis	Possible linear after very long equilibrium
C: adsorption onto water-wet organic surfaces	Fast (<minutes)	Nonlinear
D: adsorption onto exposed water-wet mineral surfaces (e.g. quartz)	Fast (<minutes)	Linear because only small energy differences among sites
E: adsorption into microporous mineral (e.g. zeolites)	Slow (>days); sorption-desorption hysteresis	Nonlinear if pore size is variable

2.5.4 Sorption Rated Mass Transfer

Mechanisms of mass transfer with the presence of soil can be characterized by soil pore size. Mass transfer in the macropores and in the bulk solution is dominated by advection and dispersion. In the meso- and micropores different types of diffusion describe the mass transfer, depending on sorption domain where the process takes place.

2.5.4.1 Advection

If the macropores are big enough for the microorganisms to move in, they are often referred to as the bulk solution. In this region, the mass transfer is controlled by advection and dispersion, which are much faster processes than diffusion and therefore not considered as rate-limiting factors for the overall rate of mass transfer. Furthermore they do not control the bioavailability since the processes are fast and often take place in the bulk phase.

2.5.4.2 Diffusion

The release of a contaminant can undergo several diffusion processes but the diffusion in soil or sediment is most reasonably explained by two mechanisms. If the solute is absorbed to SOM (case A and B), it can be assumed that the sorbate is only associated with soil organic matter and the penetration of the organic matter itself is diffusion limited. This type of diffusion is called intra organic matter diffusion or solid phase diffusion and can lead to extremely slow desorption rates of some fractions of the sorbate. The second mechanism assumes that the solutes are retarded by very slow diffusion through the intra-aggregate pores of the mineral domain (release from domain E). This is usually called retarded intra particle diffusion or diffusion into microporous regions of minerals.

2.5.4.2.1 Intra Organic Matter Diffusion

The hypothesis of intra organic matter diffusion is based on the known behaviour of small organic molecules in synthetic organic polymers (Cussler, 1997). Values of diffusion coefficients (*D*) in polymers are orders of magnitude less than in liquid solution. It is not unusual that the polymers have an internal heterogeneity. Humic polymer, for example, is

believed to be denser and more hydrophobic with distance from liquid-humic interface. This heterogeneity of the humic polymers causes a wide range of *D* values for the diffusing molecules. Intra organic matter diffusion of PAHs through a SOM-matrix is often modelled as solute transports through either a rubber polymer or a glassy polymer depending on if the diffusion is considered to occur in the soft or in the dense SOM domain. The glassy polymers are said to have a condensed and rigid structure with respect to the order and cohesive forces of the polymer chains, while the rubber polymers are more expanded and flexible. Reported *D* values, for PAHs estimated at room temperatures, range from 10^{-7} m^2 h^{-1} (in rubber polymers) to 10^{-21} m^2 h^{-1} (in glassy polymers). This gives a hint about how much slower the diffusion of solutes is in the denser regions of SOM compared to the soft regions.

2.5.4.2.2 Retarded Intra Particle Diffusion

Rapid and reversible partitioning of sorbate between the pore walls and the pore fluid retards the diffusion through the pore fluids. The pore diffusivity, D_p, will be much less than the bulk aqueous diffusivity, D_b, since tortuous pathways, dead-end pores, and variability in pore diameter reduce the diffusion rate of the solute. In addition, for very small pore diameters, pore constrictivity will also play an important role.

Two major physical differences between intra organic matter diffusion and retarded intra particle diffusion are the sizes of the pores and the pore networks. The sizes of the "pores" associated with organic matter are similar to the sizes of the sorbate molecules, whereas for porous particles the pores are much larger than the diffusing molecules, except in the case of extreme hindrance. The pore network for porous particles is fixed and is

comprised of rigid pores, while the “pore network” associated with organic matrices is dynamic and the “pores” are short-lived rather than fixed.

2.5.4.2.3 Film Diffusion

A much faster diffusion process, than the two mentioned above, is film diffusion, where the solute diffuses through a stagnant film between the particle and the bulk solution (release from domain C and D). The diffusion coefficient in the fluid film has much larger values than the diffusion coefficients in organic matter or in pores of the soil aggregates. Many researchers have shown that film diffusion resistance is generally insignificant in comparison to other mechanisms like intra organic matter diffusion and retarded intra particle diffusion regarding what is considered to be the rate-limiting step in the overall mass transfer (Weber and Miller, 1988).

2.5.5 Factors Affecting the Release Rate of Sorbed PAHs

2.5.5.1 Aging Processes

Sorption of PAHs to soils and sediments often involves an initially rapid and reversible process followed by a period of slow sorption occurring over weeks, months or even years. This slow sorption may lead to a chemical fraction that resists desorption (Ball et al., 1991). The processes by which organic compounds become increasingly desorption-resistant in soils and sediments, sometimes called chemical aging, are poorly understood. However several mechanisms have been described for the aging of chemicals in soils and sediments.

One hypothesis for aging suggests that the contaminant slowly diffuses into the small pores of the soil aggregates and becomes entrapped. Diffusion from these micro pores will be retarded by the tortuousity of the pores and by the partitioning of the chemical between pore water and organic matter on pore walls (Steinberg, et al., 1987; Wu and Geschwend, 1986). It is also possible that the formation of strong bonds between organic compounds and soil or sediment constituents may account for their resistance. Luthy et al. (1994) showed that the rate of naphthalene mass transfer from tar to water decreased with aging of the tar in slurry reactor experiments.

2.5.5.2 Pulverization or Acidification of Soil Aggregates

Pulverization of the soil aggregates can promote the release of contaminants to the aqueous phase. Contaminants in inaccessible regions become available as these regions are exposed by pulverization. Another method to enhance the release rate of the sorbate is acidification. Acidification causes dissolution of Fe oxides and Al oxides, which are believed to act as cementing agents in the formation of soil aggregates. The dissolution leads to partial disaggregation of the particles, thereby exposing sorbate in more remote regions of the matrix to bulk solution.

Pignatello (1990) believed that the slow release of HOCs was the result of diffusion limited desorption of molecules from remote regions in the soil matrix rather than breakage of specific, directed bonds between sorbate and soil components. In the experiments Pignatello pulverized contaminated soil, which greatly increased the release of residual contaminant to solution. Pignatello showed that it was difficult to rationalize this by bonding mechanisms since pulverization increased the surface area and exposed more sites for

interaction. Acidification experiments, to enhance the release of contaminants, on fractionated soil samples were also performed. The relative amount released by acid was highest for the fine sand fraction and lowest for the clay fraction.

2.6 Cometabolism of PAHs

Since most PAH contaminants are found to exist as mixtures in the environment, it is important to understand the growth behaviour of single microbial specie on mixtures of PAH compounds.

The term of cometabolism was defined as transformation of a non-growth substrate by growing cells in the presence of a growth substrate, by resting cells in the absence of a growth substrate, or by resting cells in the presence of an energy substrate (Horvarth, 1972). A growth substrate refers to an electron donor that provides reducing power and energy for cell growth and maintenance. An energy substrate is defined as an electron donor that provides reducing power and energy, but does not by itself support growth.

Walter et al. (1991) observed the cometabolism phenomenon in the bioremediation of PAHs. It was found that a pyrene-degrading Rhodococcus had the capability to cometabolically degrade naphthalene at a concentration of 250 mg L^{-1} but was unable to grow on naphthalene alone. Bouchez et al. (1995) isolated several bacterial strains from abandoned MGP sites which demonstrated cometabolism effects. A strain identified as *Pseudomonas sp.* exhibited cometabolism effect to fluoranthrene when phenanthrene was used as the main substrate. Another strain characterized as a pyrene-degrading *Rhodococcus* demonstrated cometabolism effect to fluorene after being exposed to phenanthrene and fluorene, although unable to use fluorene alone as carbon and energy sources.

2.7 Bioreactors

To construct any process, an important decision is the configuration of the bioreactor system. The choice of bioreactor and operating strategy determines product concentration, degree of substrate conversion, yields, and whether sustainable, reliable performance can be achieved. Unlike many traditionally chemical processes, the bioreactor section represents a major component (usually >50%) of the total capital expenditures. Therefore, bioreactors should be designed to minimize the costs of the product while maintaining the desired process performance and product quality (Carberry, 1976).

It has been known that the stirred tank bioreactor has its advantage to remediate PAH-contaminated soil in a slurry system (Bosma, 1997; Tabak, 1998) based on the fact that the biodegradation of suspended PAHs may be limited by the slow dissolution rate. Stirred tank bioreactors offer an advantage in this case since the dissolution rate of PAH particles can be increased with agitation. The increased dissolution rate comes from two factors both of which directly enhance the volumetric mass transfer coefficient: one is the reduced film thickness due to the intense turbulence generated by the agitation inside the bioreactor; the other one is the increased interfacial surface area of the PAH particles as a result of collision between particles and particles and impeller, again due to agitation.

In the stirred tank bioreactor, PAH-contaminated soils or pure PAH particles are mixed with water to form a slurry. Water is an essential solvent and is needed for all biochemical reactions in living system (Carberry, 1976). The growth of microorganisms is strongly dependent on the availability of water, and the nutrients used for the synthesis of microbial cells are dissolved in water.

The performance of bioreactors can be predicted by the mathematical models derived from a material balance for the reactants or products around the bioreactor as shown below:

$$R_{Accumulation}=R_{Input}-R_{Output}+R_{Prodution} \qquad (2.18)$$

2.7.1 Batch Bioreactor

Many biochemical processes involve batch growth of cell populations. Figure 2.3 shows a schematic diagram of a batch bioreactor. After seeding a liquid medium with an inoculum of living cells, nothing (except possibly some gas) is added to the culture or removed from it as growth proceeds. Typically in such a bioreactor, the concentrations of nutrients, cells and products vary with time as growth proceeds.

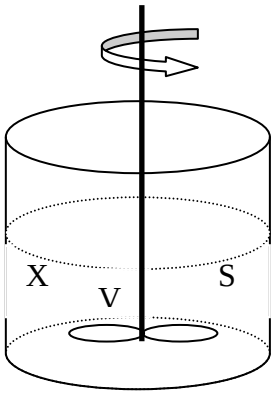

Figure 2.3: Schematic diagram of batch bioreactor

As discussed above, the performance equation of a batch bioreactor can be derived from the material balance for the substrate around the bioreactor as follows:

$$\gamma_s = \frac{dS}{dt} = -\mu \frac{X}{Y_{X/S}} \qquad (2.19)$$

where t is time and r_s is the rate of substrate consumption (mg L^{-1} h^{-1}).

For a batch bioreactor, four distinct phases are present: lag phase, exponential growth phase, harvesting, and preparation for a new batch (e.g., cleaning, sterilizing and filling).

2.7.2 Continuous Flow Stirred Tank Bioreactor (CFST)

Figure 2.4 shows a schematic diagram of a CFSTR. Such configurations for cultivation of cells are frequently called chemostats, where the concentrations of each component within the vessel are independent of time. As Figure 2.4 suggests, mixing is supplied by means of an impeller, rising gas bubbles, or both. It is assumed that the mixing in this type of system is so vigorous that each phase of the vessel contents is of uniform composition. The schematic indicates an important implication of this complete-mixing assumption: the liquid effluent has the same composition as the bioreactor contents.

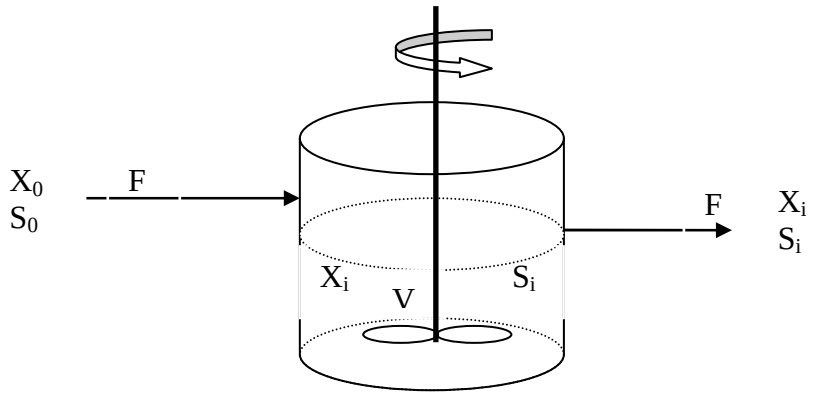

Figure 2.4: Schematic diagram of CFSTR

The performance equation of a single CFSTR can be obtained from the material balance for the substrate over the bioreactor as shown below:

$$\frac{V}{F} = \frac{S_{In} - S_{Out}}{\gamma_s} \qquad (2.20)$$

in which S_{In}= substrate concentration in the input stream (mg L^{-1})

S_{Out}=substrate concentration in the output stream (mg L^{-1})

F=volumetric flow rate of fresh media, which is normally constant (L h^{-1});

V=volume of the media in the bioreactor which is also constant at steady state (L)

Because of the complete mixing in the CFSTR, the dissolved oxygen concentration is the same throughout the bulk liquid phase. This is of crucial importance in considering aerated CFSTRs because we can often decouple the aerator or agitator design from consideration of the reaction processes. Similar logic is also usually applied to the heat-transfer problems which can accompany microbial growth. As long as the vessel is well stirred and is equipped with a satisfactory temperature controller, we can assume that it is isothermal at the desired temperature for the microbial growth.

There are several disadvantages and advantages for the batch scheme compared to the CRSRT system (Carberry, 1976; Bailey and Ollis, 1986). The first one is the operability and reliability: batch cultures can suffer great variability from one run to another. Variations in product quality and concentration create problems in downstream processing and are undesirable. However, long-term continuous culture can be problematic; pumps may break, controllers may fail, and so on. Maintenance of sterility (absence of detectable foreign organisms) can be very difficult to achieve for periods of months, and the consequences of a loss of sterility are more severe than with batch culture.

Another primary reason for the choice of batch systems over chemostats is genetic instability. The biocatalyst in most bioprocesses has undergone extensive selection. These highly “bred” organisms often grow less well than the parental strain. A chemostat imposes

strong selection pressure for the most rapidly growing cell. Back-mutation from the productive specialized strain to one similar to the less productive parental strain is always present. In the chemostat the less productive variant will become dominant, decreasing productivity. In the batch culture the number of generations available for the revertant cell to outgrow the more productive strain is limited.

One other advantage for batch bioreactor is market economics. A continuous system is dedicated to a single product. Many fermentation products are required in small amounts which is a tough requirement for the CSTR. Batch systems provide much greater flexibility because the same bioreactor can be used for two months to make product A and then for the next three for product B and the rest of the year for product C.

2.7.3 Fed-Batch Operation

In fed-batch system, nutrients are continuously or semicontinuously fed, while effluent is removed discontinuously. A schematic diagram of fed-batch system is shown in Figure 2.5.

Fed-batch culture is usually used to overcome substrate inhibition or catabolite repression by intermittent feeding of the substrate. If the substrate is inhibitory, intermittent addition of the substrate improves the productivity of the fermentation by maintaining the substrate concentration low. Fed-batch operation is also called the semicontinuous system or variable-volume continuous system.

An example of fed-batch culture is its use in some antibiotic fermentations, where a glucose solution is intermittently added to the fermentation broth due to the repression of pathways for the production of secondary metabolites caused by high initial glucose

concentrations. The fed-batch method can be applied to other secondary metabolite fermentations such as lactic acid and other plant cell and mammalian cell fermentations, where the rate of product formation is maximal at low nutrient concentrations.

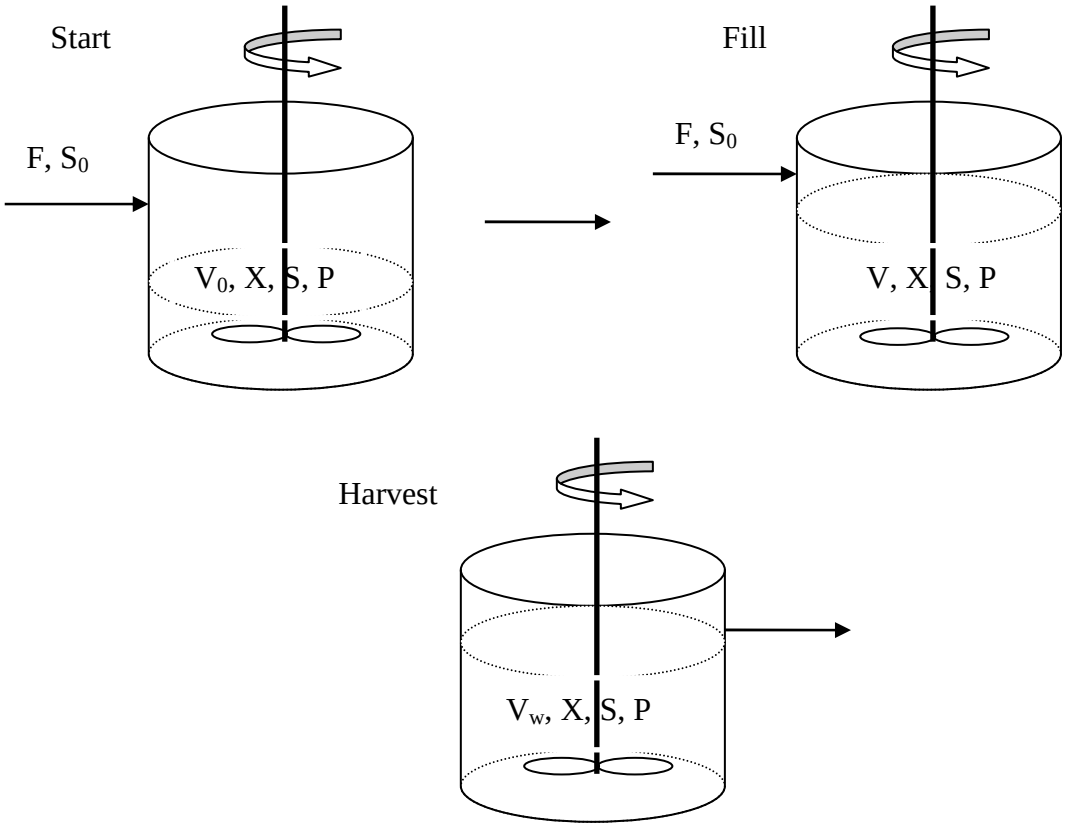

Figure 2.5: Schematic diagram of fed-batch system

2.7.4 Roller Bioreactor

Although there are benefits of using mechanical stirring in a slurry bioreactor as discussed before, the negative effects of mechanical stirring on the system in the bioreactor are not negligible. The splash of PAH particles by the mechanical stirring may take most of the particles out of the solution. Additionally, due to the strong hydrophobicity of the PAH

particles, they may stick to the various parts of the bioreactor and can not be brought back into the solution easily. Both of these two factors result in the limited presence of substrate in the solution, reducing the bioavailability of PAHs to microorganisms. The roller bioreactor, however, may offer an advantage in these cases because its rotation movement is very gentle, without splashing the particles out of the solution, and it may increase the residence time of the particles in the solution by continuously washing all the PAH particles as the vessel rotates around the fluid.

The use of a roller drum bioreactor for the bioremediation of PAH-contaminated soil has been investigated by several researchers. Gray et al. (1994) employed it for the bioremediation of anthracene-contaminated soil, Brinkmann et al. (1998) for the bioremediation of diesel fuel-contaminated sludge, and Jauhari et al. (1999) for the solid state fermentation of *Rhizobium leguminosarum*. In all these studies, the roller drum bioreactor demonstrated the ability to remediate high solid content of contaminated soil and the water content was only < 40%. It was also revealed that the oxygen supply for the microbial cells was an important factor in these processes and the oxygen uptake was enhanced by increasing the rotational speed at a constant aeration rate. The available information on the bioremediation of low solid contents of slurry solutions using roller bioreactors has not yet been reported.

Previous studies by Riess et al. (2004) showed that a novel roller BMB exhibited an excellent performance in terms of mass transfer and biodegradation of suspended PAH particles using a *Pseudomonas putida* as the degrader. In this roller bioreactor, the mass transfer rate of PAH particles was significantly enhanced in comparison to the conventional roller bioreactor and therefore the biodegradation rate was considerably increased. The

information on the bioremediation of PAH-contaminated soil slurry in this novel BMB was not available prior to the present study.

2.7.5 Roller Baffled Bioreactor

The main barrier for the use of conventional roller bioreactor (empty bottle rolling on a roller apparatus) was the slow mass transfer of PAHs from solid phase to aqueous phase because the suspended PAH particles just sat on the top of the liquid phase due to their physical properties (Bosma et al., 1997; Ashok, 1995). The employment of the BMB has a significant benefit for this case as discussed above. However, the charge of beads in the bioreactor reduced the bioreactor capacity for the contaminated media or soils in one batch compared to the conventional roller bioreactor. In the treatment of a set volume (or mass) of PAH-contaminated water (or soil), more stops and starts will be conducted in a sequencing batch operation mode, which is not very practical at the industrial scale. This disadvantage could be overcome by a roller baffled bioreactor in which baffles with a negligible volume are installed without the expense of desired mass transfer and biodegradation rates.

The application of different types of baffled bioreactors has been studied in the research area of biotechnology. Gaidhani et al. (2003; 2005) and Ni et al. (2004) reported the use of oscillatory baffled bioreactor (OBB) for the production of pullulan, a well-known extracellular polysaccharide produced by the aerobically growing yeast-like fungus *Aureobasidium pullulans*, or for the study of mass transfer in yeast, respectively. The first authors revealed that produced pullulan deposited on the outside of the fungal cells, and because of the low oxygen permeability of the pullulan, this layer acted as a barrier for the transfer of oxygen from the medium to the fungus, restricting the cultivation of the pullulan.

They also claimed that the conventional impeller-driven vessels exhibited a gradient in mixing capabilities, with high intensities at and near the impeller but low intensities in peripheral regions, inhibiting the process of pullulan generation in regions distant from the impeller and thus leading to reduced productivity. The oscillatory baffled bioreactor, however, offered enhanced and uniform mixing at very low shear rate compared with conventional mixing vessels, providing better control over the cultivation of pullulan. In their studies, they also reported that, at the optimal volumetric air flow rate of 1 vvm (volume of air per volume of liquid per min), the performance of the OBB was significantly better than the traditional stirred tank fermenter. The second authors investigated the performance of three different baffled geometries, a 50-mm-diameter column with the presence of a series of wall (orifice) baffles, the same column with central (disc) baffles, or with a mixture of both. They found that the orifice baffles gave the highest and sharpest increase in the oxygen transfer rate, and an 11% increase in the value of K_La in this bioreactor was observed compared to the stirred tank bioreactor.

The application of a simple roller baffled bioreactor in the bioremediation of PAH-contaminated water or soil has not yet been reported. Based on the capacity of holding up a full charge of contaminated water or soil and providing desirably uniform mixing of particles, this roller baffled bioreactor might be the optimum bioreactor strategy for the bioremediation of hydrophobic organic pollutants.

CHAPTER 3 MATHEMATICAL MODELS

3.1 Mass Transfer Model

The mathematical model used to calculate the dissolution rate of suspended PAH particles is developed according to film theory. The concentration gradient over the film is assumed to be established rapidly in relation to the change in concentration in the bulk solution, so the flux through the film is considered constant at any given moment (Mulder, et al., 1998). The flux of substance from the particle interface to the bulk liquid phase can be described based on a mass balance over a certain thickness of film:

$$N = \frac{D}{\delta}(C_s - C_L) \qquad (3.1)$$

where N: flux (g m^{-2} h^{-1})

D: diffusion coefficient in liquid (m^2 h^{-1})

δ: film thickness (m)

C_s: saturation concentration in liquid phase (g m^{-3})

C_L: dissolved concentration in liquid phase (g m^{-3})

By definition, the ratio of the diffusion coefficient to the film thickness can be expressed as:

$$\frac{D}{\delta} = K_L \qquad (3.2)$$

where K_L is the film mass transfer coefficient (m h^{-1}). The flux causes the change in substrate concentration with time that is observed in the bulk liquid phase, giving:

$$V\frac{dC_L}{dt} = NA \qquad (3.3)$$

in which V is the liquid phase volume (m^{-3}), and A is surface area of the particle (m^2). Equations (3.1), (3.2) and (3.3) are combined, forming:

$$\frac{dC_L}{dt} = K_L\frac{A}{V}(C_s - C_L) \qquad (3.4)$$

Since it is difficult to determine the surface area of particles, another form of mass transfer coefficient is often used (Purwaningsih, 2002):

$$K_L\frac{A}{V} = (K_L a)_{sl} \qquad (3.5)$$

where $(K_L a)_{sl}$ is the solid - liquid volumetric mass transfer coefficient (h^{-1}). If experiments are carried out at constant temperature and over a short time interval (initial rate experiments) then $(K_L a)_{sl}$ remains constant. Equation (3.5) is substituted into Equation (3.4) and integration with respect to the appropriate boundary conditions (C_L=0 at t=0) gives:

$$C_L = C_s\left[1 - \exp\left\{-(K_L a)_{sl} \times t\right\}\right] \qquad (3.6)$$

In this work, the volumetric mass transfer coefficient and saturation concentration were determined by best fitting the values of $(K_L a)_{sl}$ and C_s (least squares minimization) in Equation (3.6) to the experimental data using the Solver routine in Excel.

3.2 Bioremediation Kinetics

Although the growth of microorganisms is a complex phenomenon, it is a common practice to represent this growth by a relatively simple expression. One of the most widely employed expressions for the specific growth rate, μ, is the Monod equation which states that μ increases with the concentration of a single essential substrate (Bailey and Ollis, 1986), as

summarized in Section 2.2.2 in Chapter 2. For convenience, the Monod equation is rewritten here:

$$\mu = \mu_{\max} \frac{S}{K_s + S} \qquad (2.4)$$

As can been seen from Figure 3.1, for the Monod equation, further increases in the substrate concentration after μ reaches μ_{max} does not affect the specific growth rate. However, it has been observed that the specific growth rate decreases as the substrate concentration increases beyond a certain level, which is the situation of substrate inhibition as described in Section 2.2.2. Under such circumstances, the Haldane inhibition model has been proposed to express the specific growth rate (Shuler and Kargi, 2002):

$$\mu = \frac{\mu_{\max} S}{K_s + S + S^2 / K_I} \qquad (K_I >> K_s) \qquad (2.6)$$

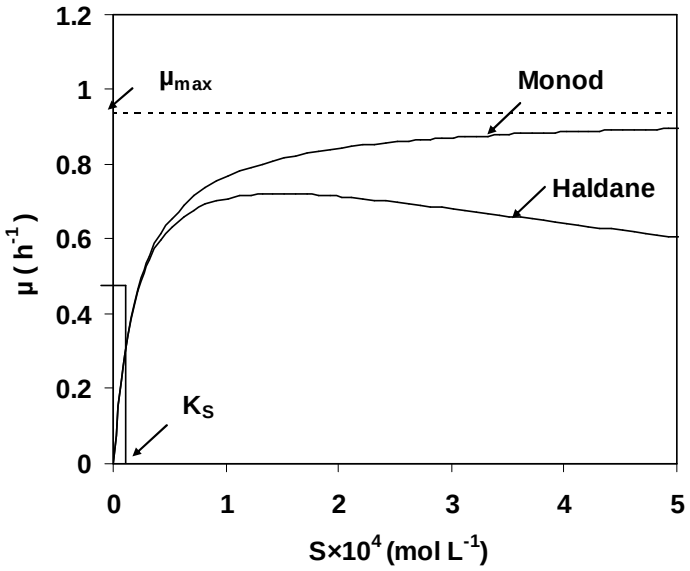

Figure 3.1: Dependence of the specific growth rate on the concentration of the growth-limiting nutrient (Schuler and Kargi, 2002)

As cells grow they produce metabolic by-products which can accumulate in the medium. The growth of microorganisms is usually inhibited by these products, whose effect can be added to the Monod equation as (Blanch and Clark, 1997; Lee, 1992):

$$\mu = \mu_{\max}\left(\frac{S}{K_s + S}\right)\left(1 - \frac{P}{P_m}\right)^{\gamma} \qquad (2.8)$$

In addition to the specific growth rate, the equations for the rate of biomass concentration increase and the stoichiometric relationship between the substrate utilization and biomass production, as described in Section 2.2.2 in Chapter 2, are also included in the bioremediation kinetics. For convenience, the latter two expressions are listed here:

$$\frac{dX}{dt} = \mu \times X \qquad (2.2)$$

$$\frac{dX}{dt} = -Y_{X/S}\frac{dS}{dt} \qquad (2.16)$$

To obtain the parameters, μ_{max}, K_S, K_I and $Y_{X/S}$, involved in Equations (2.2) to (2.16), numerical solutions of these equations was performed using Excel to fit experimental data to the models proposed. The method for the numerical modelling involves integration using a fourth-order Runga Kutta numerical scheme and best-fitting (least squares minimization) using the Solver routine in Excel.

3.3 Sorption Isotherms

The relationship between the amount of contaminant sorbed to soil and the concentration in the liquid phase can be described by linear or non-linear isotherms. The

simple linear isotherm has been frequently used in the past even though its description of many sorption processes is doubtful. It assumes that there are an infinite number of equivalent sites, independent of each other, available for sorption. The model becomes:

$$q = KC_L \qquad (3.7)$$

where q (mg kg^{-1}) is the sorbed contaminant concentration to soil, K (L kg^{-1}) is the soil-water partitioning coefficient, and C_L (mg L^{-1}) is the concentration of contaminant in the liquid phase. Examples of processes that usually show linear isotherms are absorption into soft soil organic matter (SOM) or unweathered non-aqueous phase liquids (NAPLs), while absorption into dense SOM and combustion residues may exhibit some combination of linear and nonlinear behaviour (Danielsson, 2000).

Varying adsorption energies can lead to isothermal nonlinearity (Miller and Weber, 1988; Weber and Miller, 1988) and thus adsorption cases may yield nonlinear isotherms. Adsorption onto water-wet organic surfaces should exhibit nonlinear isotherms. Another way to describe why nonlinearity occurs is the limitation in the number of available sites for sorption. The affinity for solute decreases progressively with increasing solute concentration as sites become filled. Several nonlinear isotherms have been developed, but the most common alternatives to the linear isotherm are the Langmuir and the Freundlich isotherms.

At low concentrations, monolayer adsorption at a small percentage of the available adsorption sites can be expected. This monolayer adsorption can be described by the Langmuir isotherm (Jonker and Koelmans, 2002; Paul et al., 2004):

$$q = \frac{Q_{\max} b C_L}{1 + bC_L} \qquad (3.8)$$

where Q_{max} (mg kg^{-1}) is the maximum adsorption capacity of the sorbent and b (L mg^{-1}) is the sorption affinity.

The Freundlich isotherm is expressed by Equation (3.9) (Amrith and Xing, 2003; Smith, 1997):

$$q = K_a C_L^{\ N} \qquad (3.9)$$

in which K_a (mg kg^{-1}) (mg L^{-1})$^{-N}$ is the constant indicating sorption capacity and N is a constant relating to strength of retention or sorption intensity. The value of N is often less than 1 for sorption of PAHs to soil and its organic fractions.

To compare the sorption capacity of soils for naphthalene, the experimental data were fit to these three sorption isotherms using Statistical Analysis Software (SAS) version 8 (SAS Institute Inc, 1985). This permitted the evaluation of the best-fit isotherm and its constants.

CHAPTER 4 MATERIALS AND METHODS

Since mass transfer plays a significant role in bioremediation of suspended PAHs, this research began by investigating mass transfer rates of suspended PAHs from particle surfaces to the aqueous phase in four different bioreactors. Bioremediation of suspended particles of naphthalene, 2-methylnaphthalene and mixtures of naphthalene and 2-methylnaphthalene was then investigated using *Pseudomonas putida* ATCC 17484 as the candidate bacterium. Finally, in addition to these suspended PAH studies, the sorption, mass transfer and bioremediation of naphthalene-contaminated soils (sand, silt and clay) was investigated.

4.1 Chemicals, Microorganism, Medium and Soils

The PAHs (naphthalene, 2-methylnaphthalene and 1, 5-dimethyl naphthalene) used in this study were purchased from Sigma-Aldrich (Oakville, Ontario, Canada). The characteristics of the used PAHs are given in Table 4.1. All of the PAH compounds were ground and sieved to produce a uniform particle size before they were used. The particle sizes were measured using the Malvern Mastersizer S Long Bench Particle Size Analyzer and the Sauter Mean Diameters were obtained from the analysis reports (particle size distributions are presented in Appendix B, data assumes particles were spherical).

Table 4.1: Characteristics of the used PAHs

PAHs	Molecular Formula	Molecular Weight	Water Solubility * at 25°C (mg L^{-1})	Sauter Mean Diameter (µm)
Naphthalene	$C_{10}H_8$	128.19	31	98.62
2-methyl naphthalene	$C_{11}H_{10}$	142.2	24.6	383.02
1,5-dimethyl naphthalene	$C_{10}H_6(CH_3)_2$	156.23	3	1091.58

*(Mackay et al., 1992)

Glucose was used as a carbon source for the initial growth of the bacterial cultures and was purchased from BDH (Toronto, Ontario, Canada). HPLC grade acetonitrile was employed as an eluent for HPLC analysis and was obtained from Sigma-Aldrich, Canada. Pure ethanol was used in the extraction of PAH samples and the preparation of standard solutions.

Other chemicals used included K_2HPO_4 and $Fe(NH_4)_2SO_4$ purchased from Baker Chemical; $(NH_4)_2SO_4$, $CaCl_2$ and $MgSO_4$ from BDH (Toronto, Ontario, Canada); and KH_2PO_4, NaCl, H_3BO_3, $CoCl_3$, $ZnSO_4.7H_2O$, $MnCl_2$, Na_2MoO_4, $NiCl_2$ and $CuCl_2$ from Fisher Scientific (Ottawa, Ontario, Canada).

The microorganism used in this study was *Pseudomonas putida* (ATCC 17484), obtained from the American Type Culture Collection, Rockville, Maryland, USA. These aerobic bacteria are chemoheterotrophic with an optimum growth in the temperature range of 25-30 °C and in a neutral pH environment. For short time storage, agar plates inoculated with actively growing bacterial cultures were kept at 4°C. For long term storage, 930 µL of a concentrated bacterial culture grown on glucose or naphthalene was mixed with 70 µL of di-

methyl sulfoxide (DMSO) and transferred into a 1 mL sterilized plastic tube. The tube was kept at -80°C.

Modified McKinney's medium developed by Hill (1974) was used for the growth and maintenance of *P. putida*. The composition of the minerals in one litre of growth media is shown in Table 4.2 and the composition of trace elements is shown in Table 4.3. The medium was prepared by first mixing the appropriate inorganic chemicals with one litre of Reverse Osmosis (RO) water that resulted in a buffered medium with a pH of 6.5-6.7 and which was then sterilized at 121 °C.

Table 4.2: Modified McKinney's medium in 1 litre of RO distilled water

Substance	**Mass or Volume**
KH_2PO_4	420 mg
K_2HPO_4	375 mg
$(NH_4)_2SO_4$	237 mg
NaCl	30 mg
$CaCl_2$	30 mg
$MgSO_4$	30 mg
$Fe(NH_4)_2SO_4$	10 mg
Trace element	1mL

Table 4.3: Trace element composition in l litre of reverse osmosis water

Substance	**Mass (mg)**
H_3BO_3	300
$CoCl_3$	200
$ZnSO_4.7H_2O$	100
$MnCl_2$	30
Na_2MoO_4	30
$NiCl_2$	20
$CuCl_2$	10

Three types of soils (soil composition was listed in Section 5.4) with no history of PAH contamination were obtained from the Department of Soil Science, College of Agriculture, University of Saskatchewan. Prior to use, the soils were sterilized by UV lamp overnight. Following sterilization, soil samples were kept in sterilized sealed containers at room temperature (22±1 ^{o}C).

4.2 Cell Culture

4.2.1 Shake Flask

Liquid cultures were prepared by first transferring two loops of bacteria colonies from a previously cultivated plate to a 250 mL Erlenmeyer flask with 100-150 mL of sterilized medium containing 250 mg L^{-1} of suspended naphthalene as a substrate. The shake flask was then placed on a rotary shaker at 200 rpm and maintained at 25-30 °C until the bacteria reached their exponential growth phase (20-48 hours depending on the age of the stored bacteria). When the age of stored bacteria on agar plates was more than 4 weeks, the bacteria were first grown in a shake flask with sterilized medium containing 1000 mg L^{-1} of glucose for 12-24 hours to achieve maximum growth and 5% of inoculum was then transferred to another shake flask with sterilized medium containing 250 mg L^{-1} naphthalene. The resulting culture at the mid-exponential phase was used as the inoculum sources for all experimental runs with any other substrate, and was also used to propagate the bacteria on fresh agar plates.

4.2.2 Agar Plates

The composition of agar used for the storage of bacteria is presented in Table 4.4. The ingredients were stirred while heating to almost boiling or until the solution became clear. The solution was then sterilized for 15-30 minutes (depending on the load) at 121 °C. Under the biofilter cabinet hood (Class IIA/ B3), the agar solution was poured into Petri dishes when it was still warm. To spread the bacteria on the fresh agar, several loops of broth solution from the shake flask (see Section 4.2.1) were aseptically transferred and streaked on the agar plates. The cultivated agar plates were then placed in the incubator for 24 hours at 30 °C and then stored at 4 °C. These agar plates were renewed every 4 weeks to ensure a fresh source of bacteria.

Table 4.4: Composition of agar in 100 mL of RO distilled water

Substance	**Mass (g)**
Tryptose phosphate broth	3.0
Bacto-agar	3.0

4.3 Experimental Apparatus

A number of roller bioreactors were employed for this study. The whole experimental setup included two parts: a Bellco Biotechnology roller apparatus (model 7622-S0003, New Jersey USA) and a glass bioreactor with various configurations. The roller apparatus is a two level, variable speed unit equipped with 6 roller bars and a heavy-duty DC motor. A pulley is mounted at one side of each roller bar and all of the pulleys are connected to each other with belts arranged so that once the motor starts, the rollers rotate simultaneously.

To enhance the rates of mass transfer and biodegradation, different types of bioreactor configurations, besides the conventional bioreactor (empty bottle), were employed such as baffled, BMB and baffled bead mill bioreactors. These bioreactors were 2.3 L (inside diameter of 12.8 cm, height of 26.0 cm), narrow mouthed jars and rotated on the roller apparatus at a speed of 50 rpm. The bioreactors were operated with 1 L of working volume (volume of beads plus aqueous phase) at 22±1 ^{o}C. Teflon caps, equipped with stainless steel tubing, allowed sampling and continuous injection of air into the bioreactors. The roller apparatus and bioreactor are sketched in Figure 4.1 and a picture of the roller bioreactor is shown in Figure 4.2.

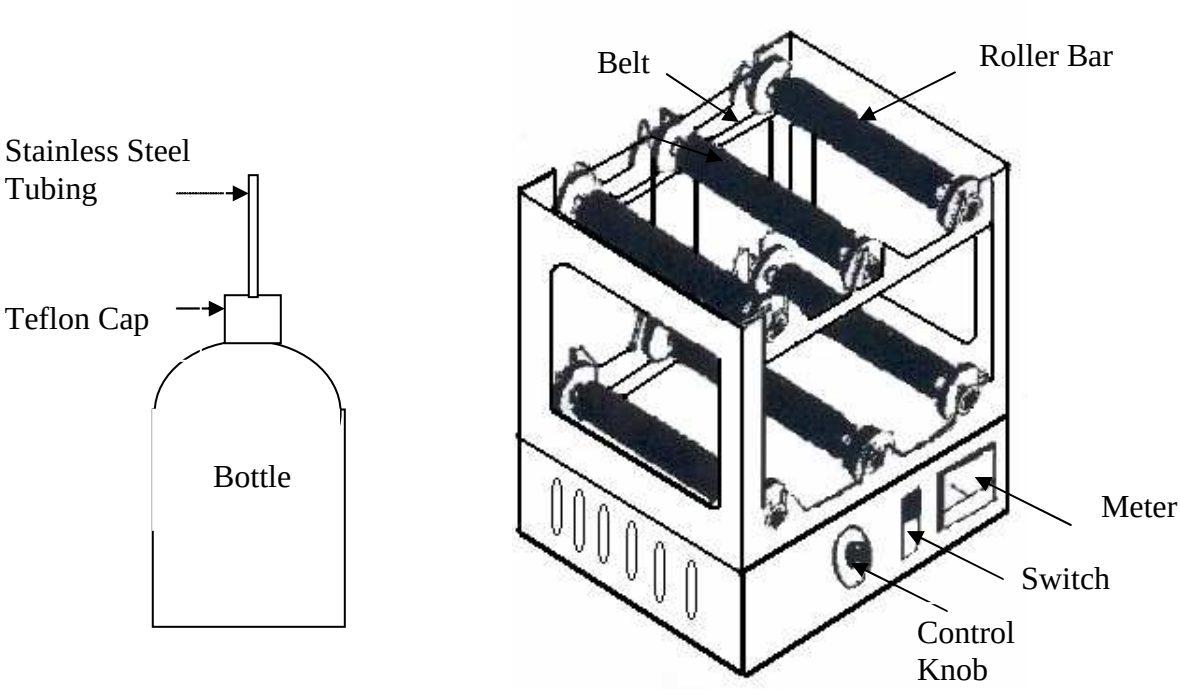

Figure 4.1: The Bellco roller apparatus and glass bottle

Figure 4.2: Photograph of the experimental setup of baffled BMB

Since the uptake of oxygen was limited during the biodegradation of suspended PAHs with intermittent injection of air, a continuous air flow system was devised to meet the oxygen demand and therefore improve the biodegradation of PAHs. The continuous addition of air was achieved through a line which was hooked up to the air supply available in the lab. The air was first filtered through glass wool and then passed through a valve where its flow rate was controlled. Before passing to the bioreactor, the rate of air flow was measured with a previously calibrated Aalborg mass flow meter. A long metal syringe needle, acting as the air supply tubing, was inserted through a 6 mm (outside diameter) stainless steel tubing mounted through the bioreactor cap. The other end of the syringe needle was linked to the air supply line. The filtered air was injected into the headspace of the bioreactor. A plastic vent tubing with an inside diameter of 2 mm was also inserted through the stainless steel tubing with one end inside the bioreactor and the other end outside. A plastic tube with an inside diameter of 6 mm was connected to the stainless steel tubing at one end and enveloped both the syringe needle and vent tubing to prevent the outflow of broth from the bioreactor during continuous

air flow. The flow meter was set to a desired air flow rate (0.025 L/min) and frequently checked during experiments to ensure a constant air flow. The lay out of this arrangement is schematically presented in Figure 4.3.

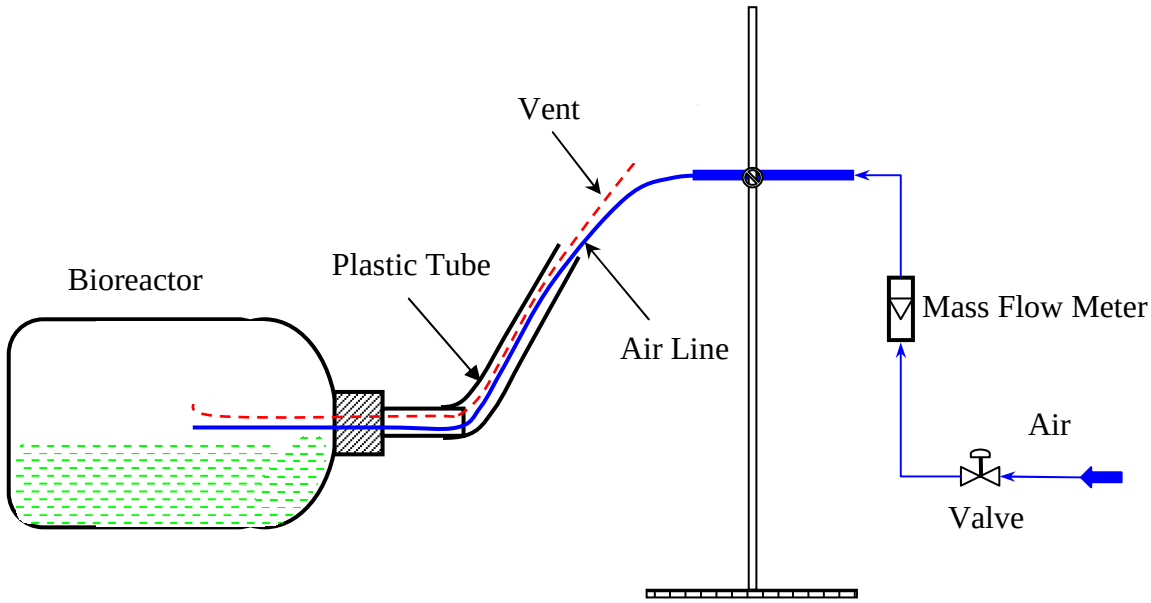

Figure 4.3: Schematic setup with a continuous air supply to the bioreactor

4.4 Experimental Procedures

4.4.1 Mass Transfer of Suspended PAHs

To determine the mass transfer rates of suspended PAH particles, experiments were carried out by inserting particles into sterilized RO water in roller bioreactors at room temperature (22±1 ^{o}C). The experimental variables tested included the bioreactor configuration and types of PAH compounds. Four configurations including conventional (control), baffled (baffles were 14 cm in length and 1.5 cm in width and were held securely to the inside circumference of the jar by four stiff stainless steel springs), BMB and baffled BMB were investigated for each of the three PAH compounds as listed in Table 4.1.

To assess the effect of glass beads and baffles on the extent of mass transfer, 5 mm sterilized glass beads at a volumetric loading of 50% (volume of beads/working volume) were added to the sterilized control and baffled bioreactors containing 500 mL of sterilized water and 500 mg of PAH particles (1000 mg L^{-1} of PAHs based on aqueous phase volume). The roller bioreactors were then operated at a rotational speed of 50 rpm and the concentration of dissolved PAHs was monitored as a function of time until the saturation level was reached. Riess et al. (2005) have shown that this bead size, bead loading and rotational rate were optimal for enhancing naphthalene mass transfer. In all cases, control experiments were carried out under similar operating conditions but without baffles or glass beads and with 1000 mL of sterilized RO water and 1000 mg of substrate. Similarly, when mass transfer runs were performed with baffles but no beads, 1000 mL of sterilized RO water and 1000 mg of substrate were again used since the baffles took up negligible volume inside the bioreactors.

4.4.2 Biodegradation of Suspended PAHs

Biodegradation of 500 mg L^{-1} (based on aqueous media volume) of naphthalene, 2-methylnaphthalene or a up to 750 mg /L of mixture of these two substrates (250 mg L^{-1} of naphthalene and 500 mg L^{-1} of 2-methyl naphthalene) was studied in the conventional, baffled and bead mill bioreactors. For runs with 50% loading (volume of beads/ working volume), the sterilized bioreactors were initially filled with 500 mL of sterilized double concentration of McKinney's modified medium. The working volume of the bioreactors was then set to 1000 mL by adding 5mm sterilized glass beads through a sterilized funnel. Measured amounts of designated substrates were then aseptically added to the glass jars. The

bioreactors were inoculated with 25 to 30 mL of a fresh, actively growing culture of *P. putida*. All the procedures were carried out inside a biosafety cabinet (Class IIA/ B3). After inoculation, the bioreactors were placed on the roller apparatus and operated at 50 rpm. The air flow meter was set to the desired low flow rate, 0.025 L min^{-1}, in which the air stripping loss of PAHs was negligible but the oxygen supply was enough for the biological reaction. Samples of 10 ml were taken at various time intervals by pouring the broth out of the well-shaken BMB through the cap tubing until the total PAH concentration reached zero. 5 ml of each sample was used to measure the total PAH concentration and the rest for the measurement of biomass concentration. Samples were always collected and analyzed in duplicate.

Control experiments were performed under similar procedures but without beads or baffles and with 1000 mL of sterilized media. Similarly, for runs with baffles, 1000 mL of sterilized media were used. Rinsing with ethanol was used for sterilization of the baffled bioreactors.

4.4.3 Sorption of PAHs to Three Soils

Sorption experiments of naphthalene were carried out using five or six concentrations of dissolved naphthalene in a system containing soil and mineral media according to a batch slurry technique (Amrith et al., 2003; Park et al., 2002; Xing et al., 1996). An aliquot of each sterilized soil and a certain volume of Mckinney's modified medium containing naphthalene stock (in ethanol) were prepared in a series of screw-cap glass vials with Teflon-lined septa. The soil/solution ratios were carefully selected to achieve approximately equal masses of naphthalene in both aqueous and solid phases at equilibrium. The soil/solution ratios were 1 g

/ 42 mL for sand, 1 g / 168 mL for silt and 1 g / 420 mL for clay. The initial naphthalene concentrations ranged from 0 to 25 mg L^{-1} (below the saturation concentration of 31.7 mg L^{-1}). The headspace of glass vials was kept less than 1 mL in volume to decrease the transfer of naphthalene from the aqueous phase to air inside the vials. Control vials without soil were also prepared for each concentration to verify the handling losses of naphthalene. Glass vials were tumbled at 150 rpm for 2 days in the dark at room temperature (22±1 ^{o}C, preliminary studies indicated that sorptive equilibrium was achieved after 48h). After shaking, each vial was centrifuged at 1200 rpm for 5 minutes to separate soil, the supernatant was then filtered through a stainless steel filter with a piece of 0.2 μm membrane using a glass syringe and then analysed by a high performance liquid chromatograph (HPLC). Sorbed naphthalene concentration was calculated by the difference between the initial and final concentrations of naphthalene in the aqueous phase.

4.4.4 Mass Transfer of Soil-Bound PAHs

4.4.4.1 Preparation of Contaminated Soil

For most coverage, three types of soils: sand, silt and clay were used. To effectively create a simulated contaminated soil, a certain amount of naphthalene was first dissolved in acetone, and the naphthalene solution was then poured onto a certain amount of air-dried soil, followed by tumbling for about 2 hours for uniform sorption of the contaminant. The contaminated soil was then placed in a flat pan and the solvent was allowed to evaporate inside a hood, leaving sorbed naphthalene on soil. Prior to use, the initial naphthalene concentration in soil was quantified by HPLC after extracting about 0.25 g of contaminated, dried soil with 37.5 mL of solution of 2:1 ratio of ethanol to water in a shaker overnight

(preliminary studies showed that the naphthalene recovery rate through the extraction was over 91%).

4.4.4.2 Experimental Procedures

The mass transfer runs of soil-bound naphthalene were carried out in both the conventional roller bioreactor and BMB. To assess the effect of glass beads on the extent of mass transfer of naphthalene from soil to water, 5 mm sterilized glass beads with 25% volumetric loading (volume of beads / working volume) were added to the sterilized control bioreactor containing 750 mL of sterilized RO water. 37.5 g of naphthalene-contaminated soil (5 g soil / 100 mL liquid) was then added to this BMB. The volume of contaminated soil was not included in the working volume since it took up a negligible volume. The bioreactor was then operated at a rotational speed of 50 rpm and the dissolved naphthalene concentration was monitored as a function of time using HPLC. To prepare the samples for analysis by HPLC, the well-mixed soil slurry was centrifuged and filtered similarly to the method used in sorption experiments. Mass transfer runs in the control bioreactor were conducted under similar operating conditions but in the absence of glass beads and with 1000 mL of sterilized RO water and 50 g of contaminated soil.

4.4.5 Biodegradation of PAH-Contaminated Soils

Biodegradation of naphthalene-contaminated soils was studied in both control and bead mill bioreactors. For the runs with 25% beads (volume of beads / working volume), the sterilized bioreactors were initially filled with 750 mL of sterilized, double concentration of nutrient media. The working volume of the bioreactors was then set to 1000 mL by adding 5

mm sterilized glass beads through a sterilized funnel. 37.5 g (5 g soil / 100 mL liquid) of naphthalene-contaminated soil was then inserted into the bioreactors through a sterilized funnel. The bioreactors were inoculated with 25-30 mL of a fresh, actively growing culture of *P. putida*. All the procedures were carried out inside the biosafety cabinet. The bioreactors were then placed on the roller apparatus and operated at 50 rpm. Filtered air with a flow rate of 0.025 L/min was injected every two hours for 20 minutes through the cap tubing during the daytime. In order to get representative samples, the bioreactor was vigorously shaken for 30 seconds. About 10 mL of soil slurry was then quickly taken into a centrifuge tube by pouring the slurry out of the roller jar through the cap tubing. Sampling was continued until the total PAH concentration reached zero. 5 ml of this sample was transferred under vigorous mixing using a vortex mixer into another tube for the measurement of total naphthalene concentration by HPLC. The remaining sample was analyzed for cell concentration using the MPN method. Samples were always collected and analyzed in duplicate. The control experiment was carried out under similar conditions but without beads and with 1000 mL of mineral media and 50 g of contaminated soil.

4.5 Analysis

4.5.1 PAH Concentration Measurements

4.5.1.1 Dissolved PAH Concentration Measurements

To determine the dissolved PAH concentrations during mass transfer of suspended PAHs, after stopping bottle rotation and waiting 15 seconds, without removing the bioreactor from the roller apparatus, samples (four mL) were withdrawn from the bottom of the aqueous phase using a stainless steel needle and glass hypodermic syringe. Using a stainless steel

cartridge, the liquid was then filtered through a 0.22 μm nylon microfilter into a special quartz cuvette. The OD of the filtered sample was then measured using a Shimadzu UV spectrophotometer (model 1240, Kyoto, Japan) at the wavelength of 276 nm for naphthalene, 220 nm for 2-methylnaphthalene and 224 nm for 1,5-dimethylnaphthalene due to their different absorbance properties. Finally, the PAH concentration was determined by relating the OD value to the previously determined calibration curves for each PAH compound.

The establishment of the calibration curve involved the preparation of standard solutions. A certain amount of PAH particles was dissolved in a certain volume of ethanol (since water solubility of PAHs is very low) to get 5000 mg L^{-1} of PAH stock solution in ethanol. The stock was then diluted with RO water resulting in a series of PAH standard solutions with concentrations ranging from 0 to 30 mg L^{-1} for naphthalene, 0 to 5 mg L^{-1} for 2-methylnaphthalene and 0 to 3 mg L^{-1} for 1,5-dimethylnaphthalene. The OD values of these series of solutions were then measured at room temperature and the measurement was repeated 3 or 4 times for each concentration. The calibration curve was then developed by plotting the PAH concentrations versus the recorded OD values.

The measurements of 2-methylnaphthalene and 1,5-dimethylnaphthalene were slightly different from naphthalene due to the absorption properties of these compounds. The relationship between the OD values of the former two chemicals and their concentrations was linear only within a small range of concentrations. This concentration range was 0 to 5 mg L^{-1} for 2-methylnaphthalene and 0 to 3 mg L^{-1} for 1,5-dimethylnaphthalene. Therefore, the filtered sample was first subjected to a series of dilutions to adjust the concentration to a desirable level. The concentration obtained by relating the measured OD to the calibration curve was then multiplied by the dilution factor to get the real dissolved PAH concentration.

The dissolved naphthalene concentration during sorption and mass transfer of soil-bound naphthalene runs was quantified by HPLC (Hewlett Packard model 1100), with a 15 cm C_{18} NovaPak column (Waters). After filtration, the supernatant was diluted in a 2:1 ratio of ethanol to liquid sample. The functions of ethanol were to make the conditions of the sample the same as standards and to suppress the bacterial activity. Ethanol in standards also acted as a PAH solvent. A 20 µl of filtered and diluted sample was then injected into the HPLC. The column temperature was set to 25 ºC. The mobile phase, a 50/50% (v/v) mixture of MiliQ-water (Millipore, USA) and a HPLC grade of acetonitrile, was pumped through the column at a flow rate of 2.1 ml/min and an average column pressure of 145 bars. A UV detector at 254 nm was used for the detection and analysis of samples. The HPLC reading was multiplied by 3 to obtain the naphthalene concentration before dilution.

4.5.1.2 Total PAH Concentration Measurements

To determine the total PAH concentration during bioremediation runs, the bioreactors were removed from the roller apparatus and vigorously shaken. 5 ml of well-mixed slurry sample was dissolved in 10 ml of ethanol. The functions of ethanol were to dissolve particulate PAHs, extract sorbed PAHs and to suppress bacteria. After being shaken on a vortex mixer for 1 minute, this slurry was then centrifuged and filtered as before to eliminate any particles including biomass or soil. 16 or 20 µl of filtered sample was then injected into the HPLC. The conditions and operation procedures of the HPLC were the same as those for the HPLC in Section 4.5.3.1.

4.5.2 Biomass Concentration Measurements

The biomass concentration during biodegradation of suspended PAHs was measured using a Shimadzu UV spectrophotometer (model 1240, Kyoto, Japan). To exclude the effect of bubbles and naphthalene particles on the OD value of sample, the sample was filtered through coarse paper (Whatman Grade 41) into a cuvette. The absorbance of the supernatant was then measured at 620 nm. The absorbance was related to dry weight of the biomass using a previously determined calibration curve.

The calibration curve was developed by determining the biomass concentration using a dry-weight method. 200 ml of bacteria broth (1000 mg L^{-1} glucose as growth substrate) in a shake flask was grown to a maximum biomass concentration. 100 ml of this broth was then transferred to centrifuge tubes and centrifuged at 9900 rpm for 15 minutes to allow the biomass to precipitate to the bottom of the tubes. The supernatant was then decanted. A few drops of RO water was added into the tubes to rinse the tube wall, followed by mixing using a vortex mixer. The procedures of centrifuging, decanting and rinsing were repeated three times. Finally, this biomass suspension was transferred to pre-weighed aluminum boats and placed into a vacuum oven at 65°C and -22 in Hg for 24 hours. The control boat holding the same amount of RO water was prepared to remove the effect of ions in water on biomass weight. Before the boats were weighed, these samples were put in a dessicator for 1 hour to bring the boats to equilibrium with room temperature. The difference in weight between the dried boat with biomass and the original boat was used to calculate the original biomass concentration (mg L^{-1}). The original broth was also subjected to a series of dilutions and analyzed for OD. These dilutions provided a range of known concentrations with measured OD and were used to plot the dry-weight calibration curve for *Pseudomonas putida*.

4.5.3 Soil Characteristics

The organic carbon contents of three soils were measured using a dichromate reduction method (HACH Company, 1994-2000). The construction of the calibration curve for total organic carbon content was started with the preparation of standard solutions. The glucose standard solution with a concentration of 3750 mg L^{-1} was prepared by mixing a certain amount of dry glucose particles with a certain volume of RO water. A series of standards with known concentration were then obtained by diluting the stock solution into different volumes of RO water. All of the standards were then completely mixed with chromate oxidant (containing Hg^{2+} as a catalyst and Ag^{+} as a remover of Cl^{-} interference) and heated at 150 ºC for 2 hours in a HACH reactor. The range of oxidant concentration used depended on the organic carbon content of the standards. Finally, a colorimetric method was used to measure the Optical Density (OD) of the standards at the wavelength of 620 nm using a UV spectrophotometer (Pharmacia LKB NovaspecII).

4.5.4 MPN Determination

The cell concentration (cell number mL^{-1}) during bioremediation of PAH-contaminated soil was determined using the MPN method (Thomas HA, 1942). First, 20 ml of sterilized bacto-peptone was prepared as a growth media and placed in a sterilized boat and 90 µL of this sterilized growth media was aseptically added to each well in a 96 well microarray plate using an 8 channel multipipettor. Secondly, serial dilutions of original sample were made by transferring 1 mL of lower diluted sample to serial sterilized test tubes containing 9 mL of sterilized saline buffer (0.45% NaCl) using sterilized pipettes. Each dilution sample was vigorously mixed for 15 seconds using a vortex mixer before being

transferred to the higher dilution tube. Thirdly, the most dilute dilution was poured into a sterilized boat and 10 µL of this dilution (starting from the most dilute sample and the pipette tips and boat were flushed with sterilized saline water for each new sample) was transferred to a row of media in the microarray plate. One of the 12 rows in the microplate was left blank to check for contamination. Fourthly, once all wells were filled, the top of the microplate was sealed with a sterilized cover to prevent cross contamination. The microplate was then placed on a Jitterbug incubator-shaker (two plates on the shaker for the balance) and the plates were vigorously mixed for one to three days at 25 ºC. For the fifth step, the plates were removed from the Jitterbug into the Biotek Reader which was connected with a laptop computer for reading the OD at 630nm of all the 96 wells. "On-off" data were measured, either growth occurred or it did not in each well. Success occurs if all growth occurs in concentrated rows (for example, all 8 wells in the row showed growth), followed by only some growth occurs in dilute rows, followed by no growth occurs in more dilute rows. Finally, the cell concentration in the original sample was computed using the Thomas' formula (Thomas HA, 1942)

$$MPN / mL = P \div (N \times T)^{0.5} \qquad (4.1)$$

where P are the number of positive results between the lowest dilution row without all positive results and the highest dilution row with at least one positive result (these are the "selected rows"), T is the total mL of sample in the selected rows and N is the total mL of sample in the selected rows that did not show growth

CHAPTER 5 RESULTS AND DISCUSSION

5.1 Mass Transfer of Suspended PAHs

Since the bioavailability of PAH particles in the slurry solution is related to the dissolved concentration and the mass transfer rate, batch dissolution experiments were performed to quantify the volumetric mass transfer rates of suspended PAHs to the aqueous phase. PAH particles were suspended in water to simulate the most concentrated condition of a suspension of polluted hydrophobic chemicals in water. Experiments were performed at room temperature (22±1 ^{o}C) with a bioreactor rotational speed of 50 rpm and an initial PAH particle concentration of 1000 mg L^{-1}. Purwaningsih et al. (2004) and Riess et al. (2005) have shown that this rotational speed and particle concentration were optimal for enhancing PAH mass transfer. In this investigation, the experimental variables included bioreactor configuration and the type of PAH compounds.

The mass transfer runs of suspended PAH particles were initiated by investigating the effect of bioreactor configurations on the mass transfer rates of solid naphthalene particles. The typical mass transfer profiles for naphthalene in the control, baffled, BMB and baffled bead mill bioreactors are shown in Figure 5.1. The symbols are the experimental data. The lines represent the simulated data using the mass transfer model (Equation 3.6) and the best-fit values for K_La and C_s. Two reproducibility runs were conducted in the control bioreactor and BMB, respectively, which resulted in a maximum scatter between data points of ± 1.0 mg L^{-1}, and error bars of that magnitude are shown for all runs in Figure 5.1. Figure 5.1 demonstrates that the baffled bioreactor provided significant improvement in mass transfer of naphthalene particles both with and without beads, compared to the control bioreactor. As

can be seen in Figure 5.1, the rate of mass transfer in the BMB was much faster than in the conventional roller bioreactor, which was also reported by Riess et al. (2005). The comparison of mass transfer profiles in the baffled bioreactor with that in the BMB indicated that the BMB provided a faster mass transfer rate than the baffled bioreactor. Additionally, the baffled BMB slightly increased the rate of mass transfer, compared to the BMB.

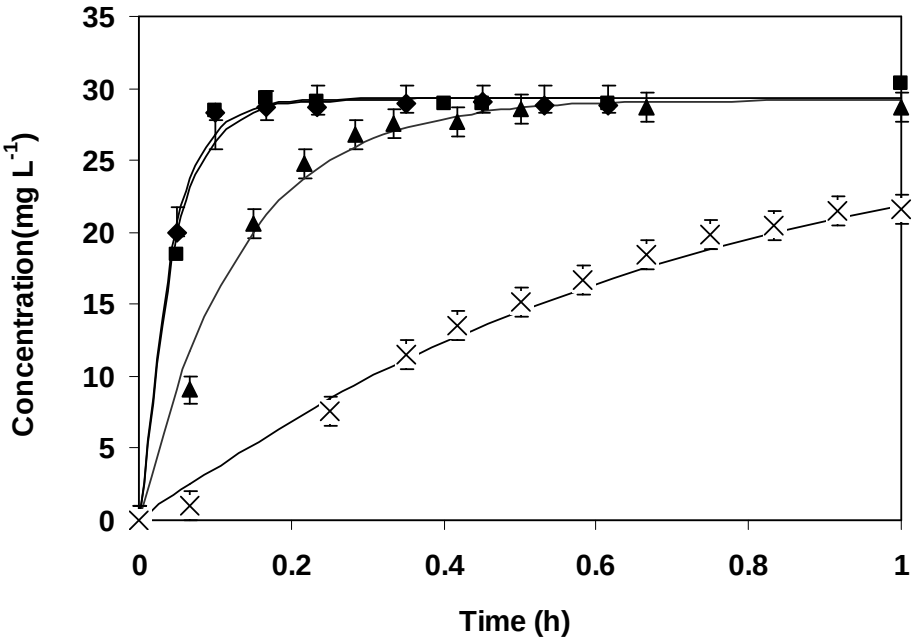

Figure 5.1: Mass transfer of 1000 mg L^{-1} suspended naphthalene particles in control (×), baffled (▲), BMB (■) and baffled BMB (♦) bioreactors (bars indicate maximum scatter between data points). Lines represent the model prediction. Symbols represent experimental data.

Values of the saturation concentration and the overall volumetric mass transfer coefficient (K_La) for each bioreactor are shown in Table 5.1. These values were determined by best-fitting the values of C_s and K_La (least squares error minimization) in the mass transfer model (Equation 3.6) to the experimental data using the Solver routine in Excel. The standard errors of these parameters, as shown in Table 5.1, were determined by Monte Carlo analyses based on a maximum fluctuation of data of ± 1 mg L^{-1} (see Section 5.3.1).

Table 5.1: Best fit values of C_s and K_La for naphthalene in four bioreactors**

Bioreactor **Parameter**	**Control**	**Baffled**	**BMB**	**Baffled BMB**
K_La (h^{-1})	1.37 ± 0.12	7.66 ± 0.37	23.0 ± 1.2	24.6 ± 2.1
C_s (mg L^{-1})	(29.3 ± 1.4)*			

* Theoretical solubility of naphthalene in water: 31 mg L^{-1} at 25°C (Mackay D. et al. 1992).
**Experimental temperature: 22±1 ^{o}C.

As can be seen from Table 5.1, the addition of baffles to the roller bioreactor increased K_La by six times compared to the control bioreactor. The function of baffles was to provide efficient mixing of the particles in the aqueous phase. To reach the bulk liquid phase, naphthalene molecules have to be transported from the solid surface through the solid-liquid film formed around each particle (Purwaningsih et al. 2004). Better mixing of the particles in the solution reduces the film thickness formed at the particle surface. According to Equation 3.2, the film mass transfer coefficient is inversely proportional to the film thickness, thus the addition of baffles enhances the volumetric mass transfer coefficient. To date, no information regarding the mass transfer of PAH particles in a baffled roller bioreactor has been published in the literature. However, Ni et al. (2004) demonstrated a similar tendency when they investigated the effect of baffled bioreactors on the mass transfer of oxygen in yeast cultures. In their study, an 11% increase in the value of K_La was observed in the baffled bioreactor compared to the stirred tank bioreactor.

Table 5.1 also indicates that the use of beads improved K_La by 16 times compared to the control bioreactor. The function of glass beads was to increase the turbulence in the PAH slurry, reducing the film thickness and enhancing the mass transfer coefficient. On the other

hand, the grinding action of the beads could break up the naphthalene particles, increasing the surface area of particles. According to Equation 3.5, the volumetric mass transfer coefficient is proportional to the surface area of particles. As a result, the crushing of naphthalene particles from the movement of beads enhances mass transfer.

The enhanced rates of mass transfer of naphthalene in the baffled bioreactor and BMB (or baffled BMB), compared to the control bioreactor, can be explicitly illustrated by the physical phenomena shown in Figures 5.2-5.4. Clearly, all the naphthalene particles were floating on the surface of the liquid medium due to their strong hydrophobicity in the control bioreactor, as shown in Figure 5.2, while they were uniformly mixed into the solution by the baffles in the baffled bioreactor, as shown in Figure 5.3, and vigorously mixed and crushed by the glass beads in the BMB as shown in Figure 5.4.

Figure 5.2: Naphthalene particles were sitting on the top of the aqueous phase in the control bioreactor (picture taken after 15 minutes from starting the roller apparatus).

Figure 5.3: Naphthalene particles were completely mixed into the solution in the baffled bioreactor (picture taken after 15 minutes).

Figure 5.4: Mixing and crushing of naphthalene particles by the glass beads in the baffled BMB (picture taken after 15 minutes).

When the overall performance was compared between the baffled bioreactor and the BMB, it was found that the baffles take up negligible volume inside the bioreactor and thus the vessel had an effective capacity of one litre of contaminated medium. Although the

optimum bead loading (50% by volume determined by Riess et al., 2005) improved the overall mass transfer coefficient by 3 times compared to the baffled bioreactor, the beads reduced the effective capacity of the bioreactor by 50%. Given the large mass transfer enhancement and the fact that a large working volume is available to maximize bioremediation productivity, it appears that the baffled bioreactor without beads provided the best overall volumetric mass transfer capacity.

The addition of baffles to the BMB provided a slight improvement, 7%, in the mass transfer rate compared to beads alone. The slight but not dramatic improvement in mass transfer rate observed in the baffled BMB, compared to the BMB, could be due to the combined effects of the beads and baffles which enhanced the turbulence in the bioreactor. Once again, the liquid volume in the baffled BMB was reduced by 50% due to the presence of the beads.

Similar trends were found for the mass transfer of 2-methyl and 1,5-dimethylnaphthalene in these four bioreactors. Figures 5.5 and 5.6 show the mass transfer profiles for 2-methylnaphthalene and 1,5-dimethylnaphthalene in four bioreactors, respectively. Since the quantification of dissolved methylnaphthalenes involved dilution of the samples before measuring the OD, the certainty of the measurement method was determined by preparing 6 diluted samples and calculating the standard errors of the measured concentrations for each of a high concentration sample and a low concentration sample. The larger standard error (5%) was selected as the magnitude of the error bars as shown in Figures 5.5 and 5.6.

As can be seen in Figures 5.5 and 5.6, the baffled bioreactor provided a significant improvement in mass transfer of both 2-methylnaphthalene and 1,5-dimethylnaphthalene

both with and without beads, compared to control bioreactor. These two Figures also demonstrate that the rates of mass transfer of 2-methylnaphthalene and 1,5-dimethylnaphthalene were much faster in the BMB than in the conventional roller bioreactors. In addition, the BMB provided faster mass transfer rates than the baffled bioreactors for both of these two methyl naphthalenes. The comparison between the baffled BMB and the BMB showed that the former provided a slight enhancement in the rates of mass transfer for methylnaphthalenes.

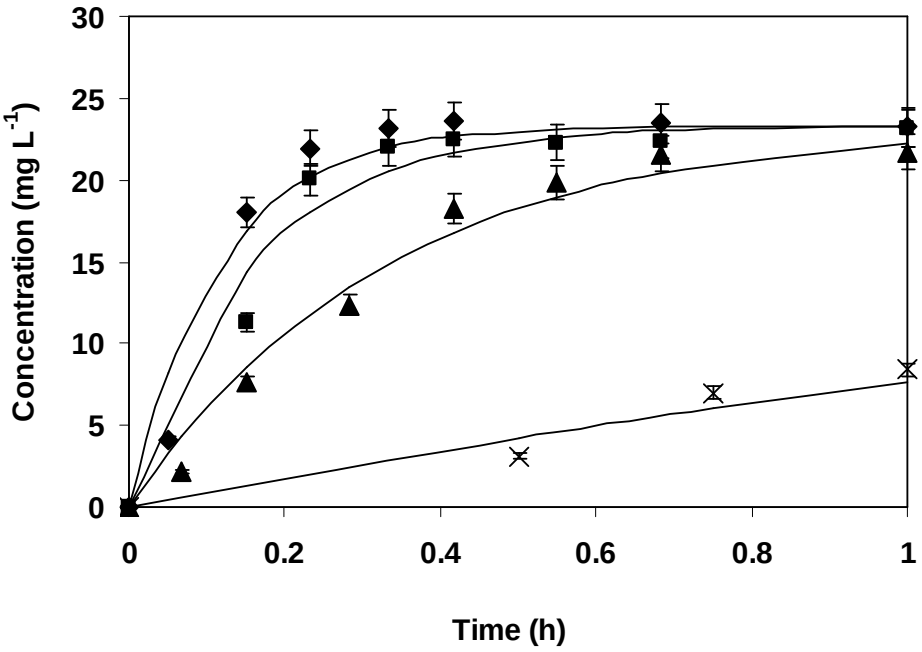

Figure 5.5: Mass transfer of 1000 mg L^{-1} suspended 2-methylnaphthalene particles in control (×), baffled (▲), BMB (■) and baffled BMB (♦) bioreactors (bars indicate standard error of measurement). Lines represent the model prediction (Equation 3.6). Symbols represent experimental data.

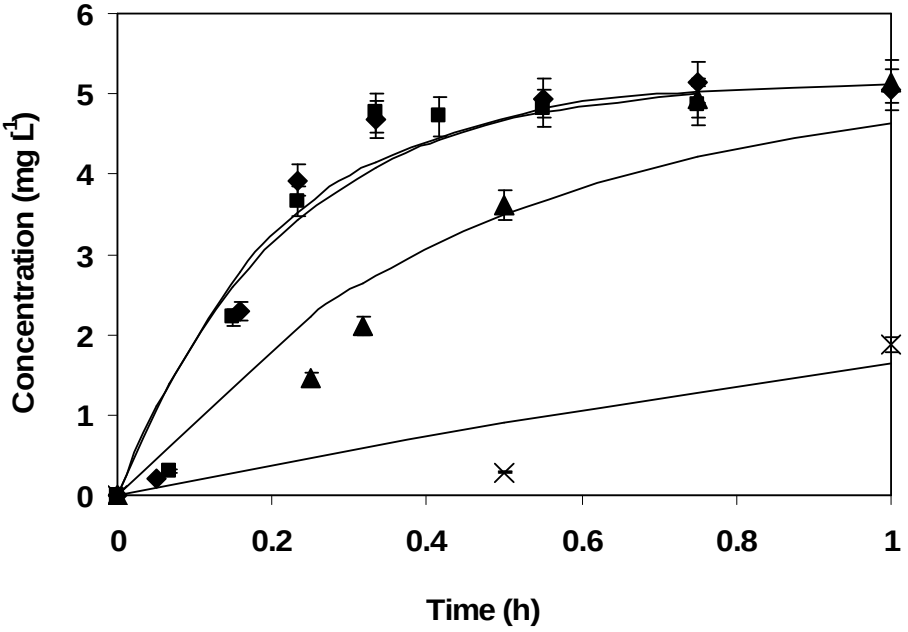

Figure 5.6: Mass transfer of 1000 mg L^{-1} suspended 1,5-dimethylnaphthalene in control (×), baffled (▲), BMB (■) and baffled BMB (♦) bioreactors (bars indicate standard error of measurement). Lines represent the model prediction (Equation 3.6). Symbols represent experimental data.

The values of the mass transfer coefficient and saturation concentration for both 2-methylnaphthalene and 1,5-dimethylnaphthalene were determined by best-fitting the mass transfer model to the experimental data and shown together with those for naphthalene in Table 5.2. Table 5.2 shows that the baffled bioreactor increased K_La by 6 to 7 times compared to the control bioreactor. Table 5.2 also demonstrates that the use of beads improved K_La by 16 times compared to the conventional roller bioreactor for 2-methylnaphthalene, and 12 times for 1,5-dimethylnaphthalene. The comparison of K_La between the BMB and the baffled bioreactor revealed that the BMB enhanced K_La by 2 times. Again, given the fact that the beads reduced the effective capacity of the bioreactor by 50% so that the baffled bioreactor had a larger effective working volume with a favourable mass transfer enhancement, it seems that the baffled bioreactor without beads was the best

choice for improving the mass transfer of PAH particles. The addition of baffles to the BMB slightly increased K_La compared to the BMB (35% increase for 2-methylnaphthalene and 5% for 1,5-dimethylnaphthalene). Once again, the baffled BMB reduced the effective capacity by 50% compared to the baffled bioreactor.

The comparison of K_La for the different chemicals in each of these four bioreactors indicated that the mass transfer of naphthalene particles from solid phase to the aqueous phase was fastest, followed by 2-methylnaphthalene and then 1,5-dimethylnaphthalene. This could be explained by the different structures of these PAH compounds which resulted in different degree of hydrophobicity. For instance, naphthalene with the most simple structure and therefore the lowest hydrophobicity had the fastest mass transfer rate, while 1,5-dimethylnaphthalene with the most complicated structure and as a result the highest hydrophobicity had the slowest mass transfer, and 2-methylnaphthalene was in the middle in terms of both complexity of structure and mass transfer rate.

Table 5.2: Best fit values of K_La and C_s for methylnaphthalenes***

Chemical: / **Parameter**	**Naphthalene**	**2-methylnaphthalene**	**1,5-dimethylnaphthalene**
K_La (h^{-1}, control)	1.37 ± 0.12	0.40 ± 0.02	0.39 ± 0.02
K_La (h^{-1}, baffled)	7.66 ± 0.37	3.04 ± 0.14	2.25 ± 0.17
K_La (h^{-1}, BMB)	23.0 ± 1.2	6.39 ± 0.31	4.67 ± 0.23
K_La (h^{-1}, baffled BMB)	24.6 ± 2.1	8.64 ± 0.41	4.88 ± 0.31
C_s (mg L^{-1})	(29.3 ± 1.4)	(23.3 ± 0.6)*	(5.17 ± 0.12)**

* Water solubility of 2-methylnaphthalene: 24.6 mg L^{-1} at 25 ˚C (Mackay D. et al. 1992)

** Water solubility of 1,5-dimethylnaphthalene: 3 mg L^{-1} at 25 ˚C (Mackay D. et al. 1992).

***Experimental temperature: 22±1 ^{o}C.

5.2 Bioremediation of Suspended PAH Particles

In this study, the experimental variables were similar to the mass transfer investigation including bioreactor configuration and the type of PAH particles. Bioremediation experiments were conducted in the control, baffled and bead mill bioreactors, since the application of the baffled BMB did not lead to a significant improvement in mass transfer, compared to the BMB. PAHs used in bioremediation runs included naphthalene, 2-methylnaphthalene and the mixtures of these two substrates since the preliminary studies indicated that *P. putida* could not metabolize 1,5-dimethylnaphthalene even when naphthalene was used as a cosubstrate. Dean-Raymond and Bartha (1975) also observed that six pure strains of marine *Pseudomonads* could not metabolize dimethylnaphthalenes.

5.2.1 Bioremediation of Single Substrate

The initial bioremediation runs were conducted to investigate the effect of bioreactor configurations on the biodegradation rates of naphthalene particles. Prior to the experimental runs with roller bioreactors, the cultures of *P. putida* 17484 were prepared in shake flasks (see Section 4.2). During the preparation of liquid cultures, it was observed that when naphthalene was the growth substrate, a yellowish-green translucent color was formed; when glucose was the sole carbon source, a white opaque solution was produced. Similar observation has been reported by Purwaningsih (2002). The experiments were started by inoculation of the bioreactor with pre-grown bacterial cultures with a biomass concentration of 9 to 10 mg dry weight L^{-1} . According to earlier experience (Hill, 1974), when the initial substrate concentration was above 350 mg L^{-1}, the nutrient concentrations in the medium shown in Tables 4.2 and 4.3 were doubled. At higher substrate concentrations, bacteria need

more mineral nutrients for metabolizing the extra organic substrate. During the experiments, the pH of the solution in the bioreactors was observed to decrease from an initial value of 6.7 to a final pH of 6.5. No attempt was made to adjust the pH.

Oxygen is an essential nutrient which is needed for the growth and activity of aerobic bacteria. The oxygen serves as an electron acceptor during the biodegradation of the organic substrate (the electron donor). It was previously assumed that the intermittent supply of oxygen to the roller bioreactors was adequate for the bacteria to oxidize all of the naphthalene particles. However, the preliminary studies demonstrated that the rate of biodegradation of naphthalene in the control and baffled bioreactors was limited by the level of oxygen, especially during the night when there was no injection of air. This finding was in agreement with that of other researchers (Ahn et al., 1998; Janikowski et al., 2002), who reported that a good oxygen supply was strongly desired for the successful biodegradation of PAHs. In this investigation, a continuous air supply system (see Figure 4.3) with a flow rate of 0.025 L min^{-1} (0.025 vvm) was employed in all bioreactors to prevent oxygen depletion during the growth of bacteria. Initial studies without microbes demonstrated negligible stripping losses at this air flow rate, with rates of stripping measured at 3.3 and 2.8 mg L^{-1} h^{-1} for naphthalene and 2-methylnaphthalene, respectively.

The results of biodegradation of 500 mg L^{-1} naphthalene in the control, baffled and BMB bioreactors are presented in Figure 5.7. The symbols stand for the experimental data. The lines represent the theoretical data generated using the bioremediation models (Equations 2.4, 2.16, 5.1 and 5.2). Section 5.3.1 describes the detailed procedures for solving these equations. Two identical bioremediation runs (same media, inoculum source and inoculum size) were undertaken in the control bioreactor at an initial naphthalene concentration of 500

mg L^{-1}. A maximum spread of ± 5% for substrate concentration and ± 10% for biomass concentration were observed and these error bars are shown for all runs in Figures 5.7, 5.8 and 5.9.

The growth curves shown in Figure 5.7 indicate that the lag phase in microbial growth was insignificant. The transferred bacteria to the bioreactors were previously grown on naphthalene as their carbon source in the shake flask, so that there was no significant time needed for the adaptation of the cells to the fresh medium. Figure 5.7 also demonstrates that bioremediation was fastest in the BMB, followed by the baffled bioreactor and then the control bioreactor. The maximum rates of biodegradation (slopes of naphthalene concentration profiles) increased from 29 to 61 to 61.5 mg L^{-1} h^{-1} (based on working volume) for the control, baffled and BMB bioreactors, respectively. Bioremediation rates increased from two to three fold with baffles and from four to five fold with beads compared to the control, but since the effective capacity of the baffled bioreactor was two times higher than that of the BMB, the total bioremediation capacity was just as good using only baffles instead of beads. Figure 5.7 also indicates that a mass transfer controlled phenomenon was observed in the control and baffled bioreactors because the substrate depletion curves were linear with time after the short lag phase in these two bioreactors. On the other hand, in the BMB the bioremediation was controlled by the bacterial growth, since the growth was exponential and the utilization rate kept increasing with time with a maximum rate occurring at the end of the bioremediation when the biomass was highest. This observation confirmed the previous mass transfer results (see Section 5.1) that the BMB provided the highest mass transfer rate so that mass transfer is not a rate-limiting step in this bioreactor, compared to the control and baffled bioreactors.

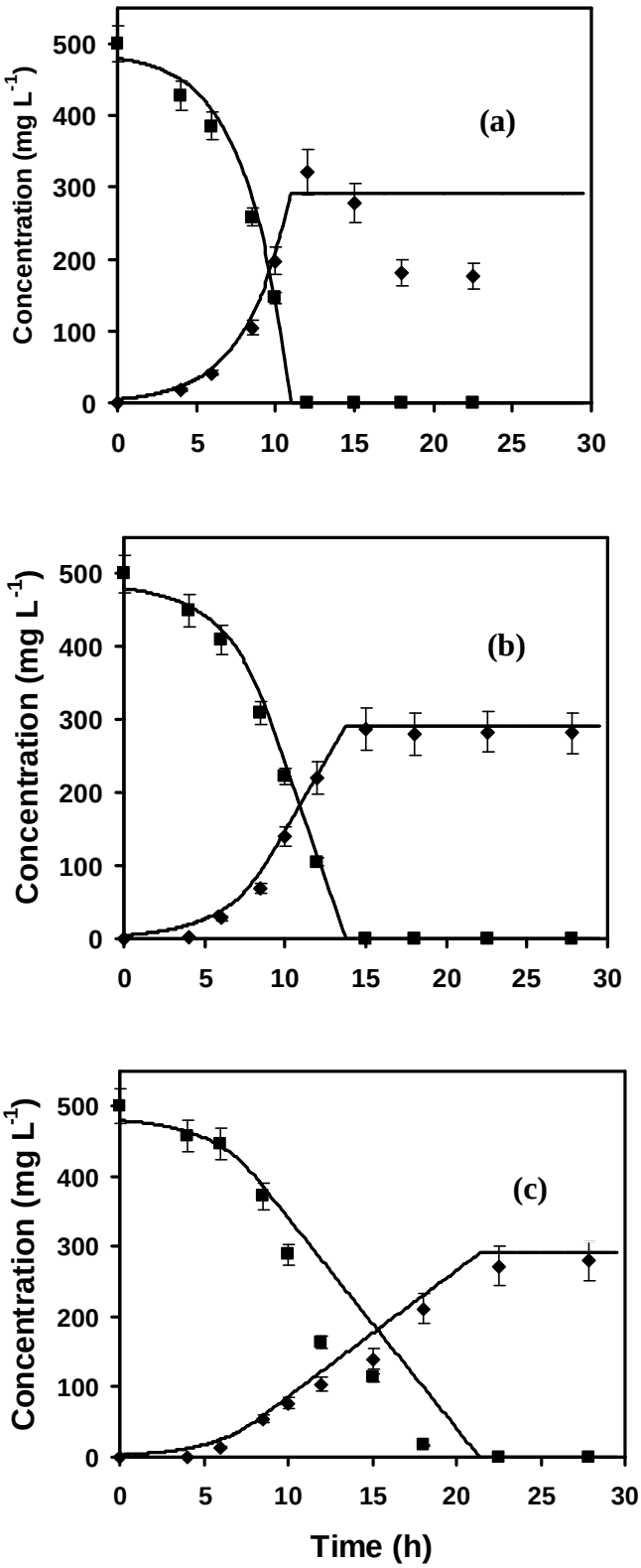

Figure 5.7: Bioremediation of 500 mg L^{-1} suspended naphthalene in BMB (a), baffled bioreactor (b) and control bioreactor (c). (Bars indicate the maximum spread of data points). Lines are model curves. Symbols are experimental data. ♦ biomass ■ total naphthalene

The bioremediation experiments for 2-methylnaphthalene were carried out under the same operational conditions as naphthalene and the results are presented in Figure 5.8. As can be seen similar to what was observed with naphthalene, the bioremediation of 2-methylnaphthalene was fastest in the BMB, followed by the baffled bioreactor and then the control bioreactor. The maximum biodegradation rates were 10, 20 and 21.7 mg L^{-1} h^{-1} (based on working volume) for the control, baffled and BMB bioreactors, respectively. Bioremediation rates increased two fold with baffles and from four to five fold with beads compared to the control, but once again since the effective capacity of the baffled bioreactor was two times higher than that of the BMB, the total bioremediation capacity was just as good using only baffles instead of beads. Similar to the bioremediation results of naphthalene, mass transfer was observed to be the rate-limiting step in the control and baffled bioreactors since the substrate depletion curves were straight lines, while the bacterial growth was found to play a more significant role than mass transfer in the BMB bioreactor, and the maximum removal rate of substrate took place at the end of experiment when the biomass concentration reached the highest.

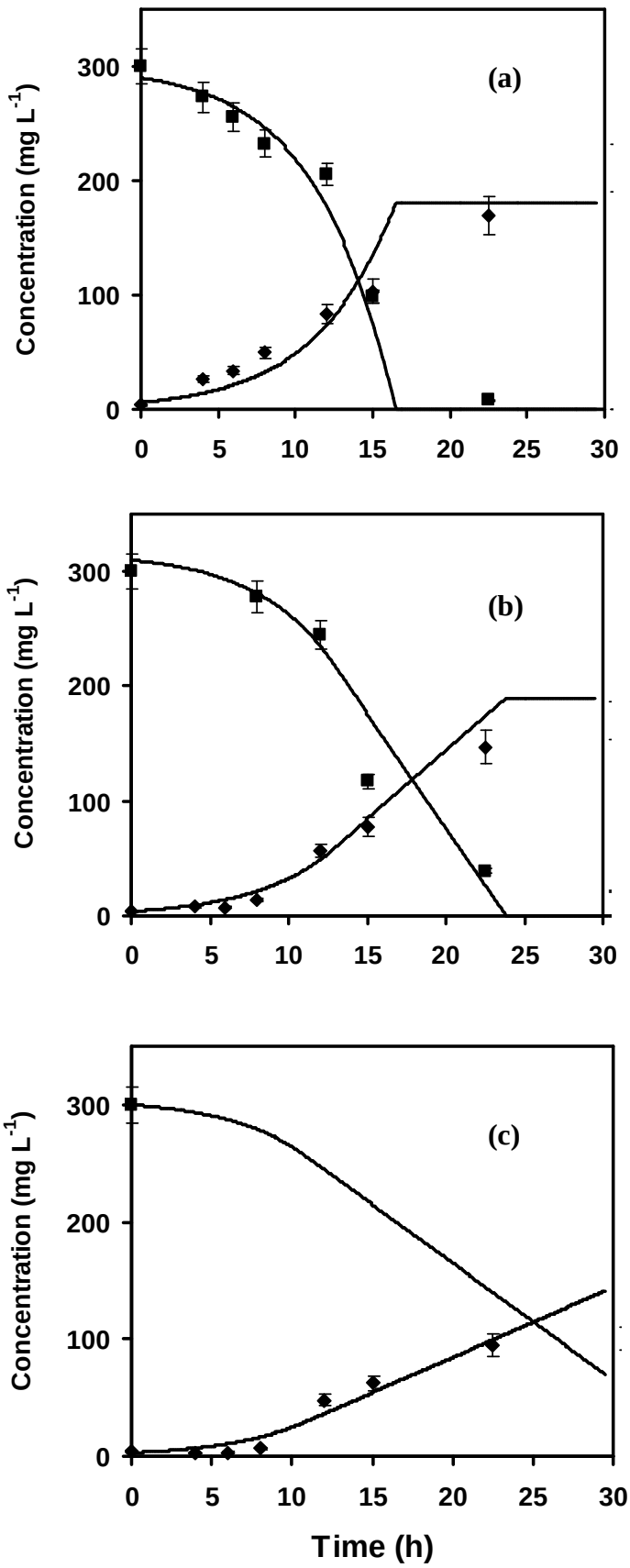

Figure 5.8: Bioremediation of 300 mg L^{-1} suspended 2-methylnaphthalene in the BMB (a), baffled bioreactor (b) and control bioreactor (c). (Bars indicate the maximum spread of data points). Lines are model curves. Symbols are experimental data. ♦ biomass ■ total naphthalene

The maximum biodegradation rates for naphthalene and 2-methylnaphthalene obtained in three types of bioreactors are reported in Table 5.3. The naphthalene removal rates were similar to those reported earlier (Riess et al., 2005). It is clear that the bioremediation rates for 2-methylnaphthalene were much lower than for naphthalene in all cases. 2-methylnaphthalene was observed to be significantly more hydrophobic than naphthalene and assembled into large clumps that floated on the surface of the liquid in the control bioreactor and to a lesser extent in the baffled bioreactor, making measurement of total substrate concentration difficult in these two types of bioreactors. The higher hydrophobicity for 2-methylnaphthalene was quantified by calculation of the octanol-water partition coefficients resulting in a value 3.5 times higher compared to naphthalene (Meylan and Howard, 1995). As shown in Figure 5.8(c), for the case of the control bioreactor, the concentration of 2-methylnaphthalene could not be measured since excessive clumping of particles made it impossible to obtain representative samples.

Table 5.3: Batch bioremediation rates (mg L^{-1} h^{-1}) of naphthalene and 2-methylnaphthalene in sole substrate in three types of bioreactors*

Bioreactor / **Substrate**	**BMB**	**Baffled**	**Control**
naphthalene	62	61	29
2-methylnaphthalene	22	20	10

* Based on working volume

5.2.2 Bioremediation of Mixed Substrates

It has been reported that bioremediation of recalcitrant compounds can be facilitated by the use of cosubstrates. For instance, phenol and glucose were shown to enhance the bioremediation of 4-chlorophenol that could not be metabolized as a sole organic substrate by *P. putida* ATCC 17484 (Tarighian et al., 2003). In this study, however, it was found that growth on naphthalene could not induce the bioremediation of 1,5-dimethylnaphthalene. But runs with mixtures of naphthalene (250 mg L^{-1}) and 2-methylnaphthalene (500 mg L^{-1}) demonstrated a significant improvement in bioremediation rates for 2-methylnaphthalene as shown in Figure 5.9 in all three bioreactors (compare to Figure 5.8). The improved rates were due to the higher biomass loading generated by the growth on naphthalene that occurred prior to the consumption of 2-methylnaphthalene. As shown in Figure 5.9, 2-methylnaphthalene was not consumed until naphthalene was used up. In the baffled bioreactor, representative slurry samples containing 2-methylnaphthalene could not be obtained, due to the severe clumping and sticking of this compound to the walls and the baffles as shown in Figure 5.10. In the control bioreactor, both naphthalene and 2-methylnaphthalene concentrations could not be measured, as shown in Figure 5.9(c), since both compounds agglomerated on the surface of the liquid medium. Accurate substrate measurements were only possible in the BMB where the crushing and mixing actions of the beads prevented substrate agglomeration, as shown in Figure 5.11.

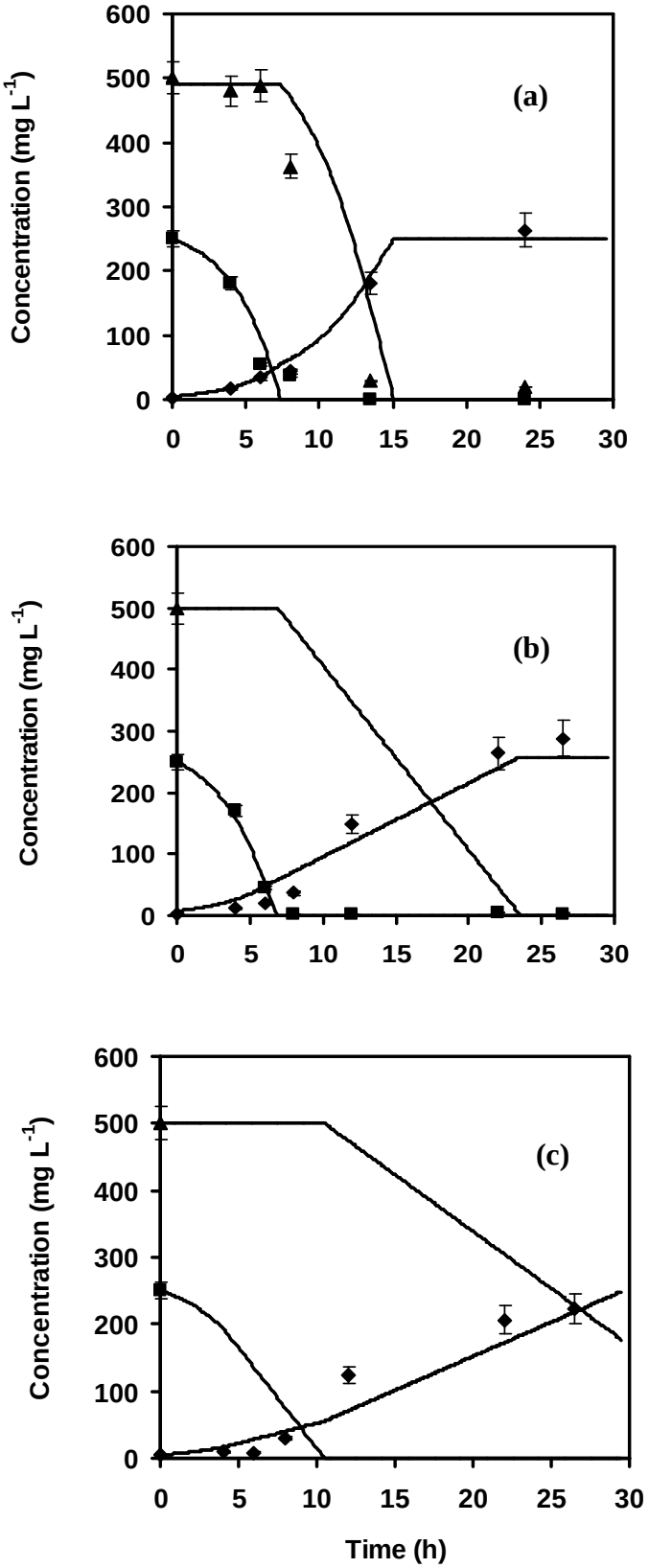

Figure 5.9: Bioremediation of mixtures of 500 mg L^{-1} suspended 2-methylnaphthalene and 250 mg L^{-1} suspended naphthalene in the BMB (a), baffled bioreactor (b) and control bioreactor (c). (Bars indicate the maximum spread of data points). Lines are model curves. Symbols are experimental data. ♦ biomass ■ total naphthalene

Figure 5.10: Mixed substrate particles clumped and stuck to the baffles in the baffled bioreactor (picture taken at 2 minutes after the start)

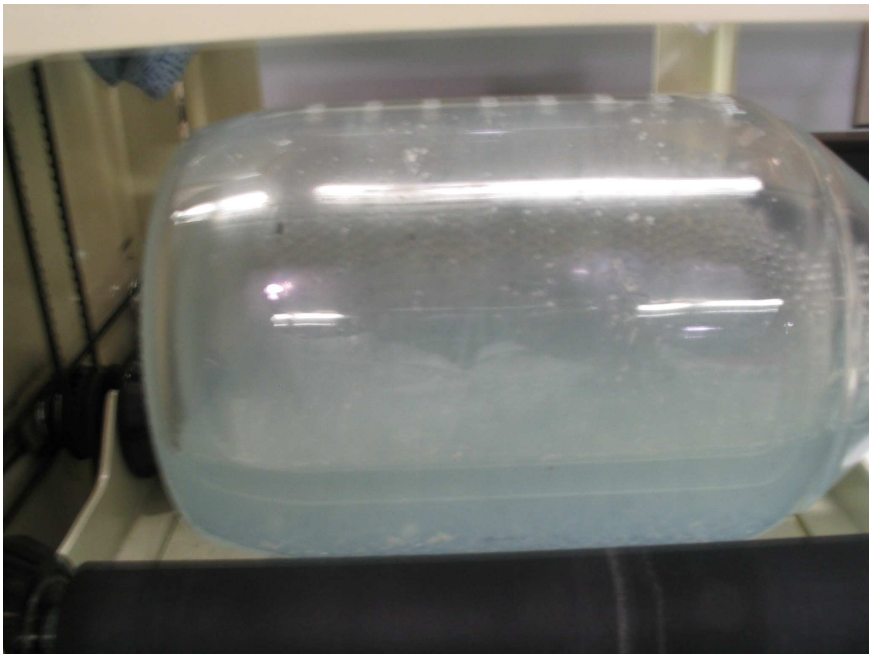

Figure 5.11: Mixed substrate particles were crushed and mixed into the solution in the BMB (picture taken at 2 minutes after the start)

Biodegradation rates of naphthalene and 2-methylnaphthalene in mixed substrate runs were obtained by taking the slopes of the substrate concentration profiles and summarized together with those obtained in sole substrate in Table 5.4. As shown in Table 5.4, the 2-methylnaphthalene removal rates generally increased two fold in the mixed substrate compared to the sole substrate for all the bioreactors. The higher removal rates of 2-methylnaphthalene was due to the higher biomass concentrations created by the growth on naphthalene. This resulted in increased demand for substrate which greatly increased 2-methylnaphthalene uptake in the growth limited condition (the BMB bioreactor) but also resulted in increased mass transfer and therefore increased 2-methylnaphthalene uptake in mass transfer limited conditions (the control and baffled bioreactors). Table 5.4 also shows that the bioremediation of 2-methylnaphthalene was much slower than naphthalene, with the bioremediation rates generally about one third those of naphthalene in the sole substrate runs and one half in the mixed substrate runs. The lower biodegradation rates were due to the higher hydrophobicity of 2-methylnaphthalene compared to naphthalene. When the overall performance was compared among different bioreactors, the simple baffled bioreactor provided good bioremediation capacity and had the significant benefit for allowing a full charge of media to be held in the roller bioreactor. In practical terms, this means that in a sequencing batch operation mode, fewer stops and starts would be necessary to treat a specific volume of hydrophobic polluted materials.

Table 5.4: Batch bioremediation rates (mg L^{-1} h^{-1}) of naphthalene and 2-methylnaphthalene in mixed substrates in three types of roller bioreactors*

Bioreactor / Substrate	BMB	Baffled	Control
naphthalene (mixed substrate)	62	61	30
2-methylnaphthalene (mixed substrate)	43	30	17
naphthalene (sole substrate)	62	61	29
2-methylnaphthalene (sole substrate)	22	20	10

* Based on working volume

5.3 Determination of Biokinetic Parameters

Knowledge and information on the kinetics of bioremediation is very important because it allows the predictions of the levels of the organic pollutants as a function of time, and permits the design of effective bioremediation systems.

The batch growth kinetics on naphthalene and 2-methylnaphthalene were simulated using first order growth kinetics (Monod equation) assuming that PAHs were the limiting substrates (see Section 3.3). First order kinetics is a reasonable assumption for the growth of *P. putida* on naphthalene since it has been shown that the saturation constant, K_s, is considerably less than 1 mg L^{-1} (Park et al., 2001; Alshafie and Ghoshal, 2003). Since mass transfer from the solid particles to the aqueous media was the rate-limiting step for almost all the cases, the maximum mass transfer rates of the particle substrates had to be considered when describing the rates of total substrate depletion. The mass balance equation for undissolved PAHs in the aqueous phase is (Purwaningsih, 2002):

$$\frac{dS_P}{dt} = -K_L a \times (S_s - S_L) \qquad (5.1)$$

where S_P is the substrate particle concentration (mg L^{-1}) ; S_s is the saturation concentration of substrate (mg L^{-1}) and S_L is the dissolved concentration of substrate (mg L^{-1}). Changes in the dissolved substrate concentration were due to particle dissolution adding to the naphthalene concentration in the water and utilization of substrate by the bacteria:

$$\frac{dS_L}{dt} = K_L a \times (S_s - S_L) - \frac{\mu \times X}{Y_{X/S}} \qquad (5.2)$$

Another two equations are imported from Chapter 2 and rewritten here for convenience:

$$\mu = \mu_{\max} \frac{S_P}{K_s + S_P} \qquad (2.4)$$

$$\frac{dX}{dt} = -Y_{X/S} \times \frac{dS_P}{dt} \qquad (2.16)$$

The numerical solution of the bioremediation models proposed was performed using a fourth-order Runga Kutta numerical scheme and best fitting the parameters (least squares minimization) by varying $\mu_{\max}$, $Y_{X/S}$ and the initial substrate (S_0) and biomass (X_0) concentrations to minimize the sum of the squared errors using the Solver routine in Excel. A Monte Carlo analysis was applied to determine the sensitivity of the proposed mathematic models (see Section 5.3.1).

The maximum specific growth rate ($\mu_{\max}$) in the case of sole substrate growth were found to be 0.33 ± 0.03 and 0.21 ± 0.02 h^{-1} for naphthalene and 2-methylnaphthalene, respectively, while $Y_{X/S}$ was equal to 0.6 ± 0.06 for each of the two substrates. The solid lines in Figures 5.7 and 5.8 demonstrate that these solved differential equations fit the bioremediation data well.

For growth on the mixed substrates (shown in Figure 5.9), it was found that *P. putida* consumed naphthalene first, and utilization of 2-methylnaphthalene proceeded after the exhaustion of naphthalene (less than 1 mg L^{-1}). *P. putida* grew on each substrate at the same rate as for pure substrates, but slightly lower biomass yields were used for modelling growth on the mixed substrates. The model (solid lines in Figure 5.9) could still reasonably predict the measured data using yield coefficients of 0.5, values which were within the 95% confidence limits of yield coefficients determined from single substrate runs.

The values of K_La listed in Table 5.2 had to be doubled for the control bioreactor simulations for both naphthalene and 2-methylnaphthalene in single substrate conditions in order to predict the growth of the cells accurately. Accurate prediction of concentration profiles during the mixed substrate runs required the values of K_La to be increased by a factor of two for naphthalene and four for 2-methylnaphthalene. Although not measured here, the increase in K_La values was likely due to natural biosurfactants excreted by *P. putida* growing on insoluble substrates. The chemical composition of biosurfactants from *P. putida* are composed of rhamnose connected to various fatty acids (Amezcua-Vega et al., 2004) and the enhancement of PAH biodegradation due to these natural biosurfactants has been extensively studied (Bonilla et al., 2005; Abalos et al., 2004; Prabhu and Phale, 2003). The increased numbers of cells during mixed substrate growth likely increased the biosurfactant concentration and resulted in a much faster removal of 2-methylnaphthalene in the control bioreactor than would have been possible had mass transfer occurred at a rate similar to that in the absence of cells.

5.3.1 Monte Carlo Analysis

Monte Carlo simulation is used to analyze the sensitivity of the proposed mathematic models. The Monte Carlo method has been successfully applied to determine uncertainty parameter of non-linear model fitting (Feller and Blaich, 2001). This procedure involves generating a number of artificial data sets consistent with the experimentally measured data. These generated data are statistically analyzed to observe how well a model performs. The evaluation of the mathematical model using Monte Carlo method is conducted according to the following procedures (Purwaningsih, 2002):

- Determining the mean and error estimate (equal to standard deviation) of experimental data based on the experimental replication. This mean remains the same throughout the procedures.
- Generating data sets of synthetic experimental results using computer generated random numbers with a uniform distribution (Excel).
- Performing the non-linear minimization procedure on 20 artificial data sets to obtain 20 different sets of kinetic parameter values.
- After carrying out the fitting procedures on each member of data sets, a distribution of kinetic parameter values is obtained whose deviation is the uncertainty range for the best-fit parameters.

The Monte Carlo analysis in this study demonstrated that the confidence limits were small with errors in the range of <6%. These small values of standard errors indicate that the precision of the mathematical models is satisfactory.

5.4 Soil Composition

Frequently, PAH contamination in the environment is highly associated with sorption to soil rather than as pure solid particles (Alexander and Scow, 1989). Sorption is often well correlated with soil organic carbon content (Means et al. 1980). As such, in this investigation, it was necessary to measure the organic carbon content of three types of soils prior to the mass transfer and bioremediation of soil-bound PAHs. The results for the organic carbon content of three soils are presented in Table 5.5.

Table 5.5: Organic carbon content of three soils

Soil	Organic carbon content (% by weight)		
	Run 1	Run 2	Mean
Sand	0.42	-	0.42
Silt	1.31	1.57	1.44
Clay	4.27	4.23	4.25

As can be seen in Table 5.5, clay had the highest organic carbon content among these three soils, followed by silt and then sand.

5.5 Sorption of Naphthalene to Three Types of Soils

The sorption data of naphthalene to sand, silt and clay were fit to Linear (Equation 3.7), Langmuir (Equation 3.8) and Freundlich (Equation 3.9) isotherms, respectively. Three reproducibility runs were conducted for both a low and a high concentration of naphthalene for each of these three soils and a larger standard error was found in the case of high concentration for each soil. These larger standard errors, 11 mg kg^{-1} with a mean of 543 mg

kg^{-1} for sand, 18mg kg^{-1} with a mean of 2185 mg kg^{-1} for silt and 159 mg kg^{-1} with a mean of 5460 mg kg^{-1} for clay, are shown in Figure 5.12 (a), (b) and (c), respectively. As shown in Figure 5.12, according to the values of correlation coefficient, R^2, the Freundlich isotherm was the best fit (R^2=0.99) model for the sorption of naphthalene to sand, while both Freundlich and Langmuir isotherms (R^2=0.99) fit the experimental data very well for the sorption of naphthalene to both silt and clay.

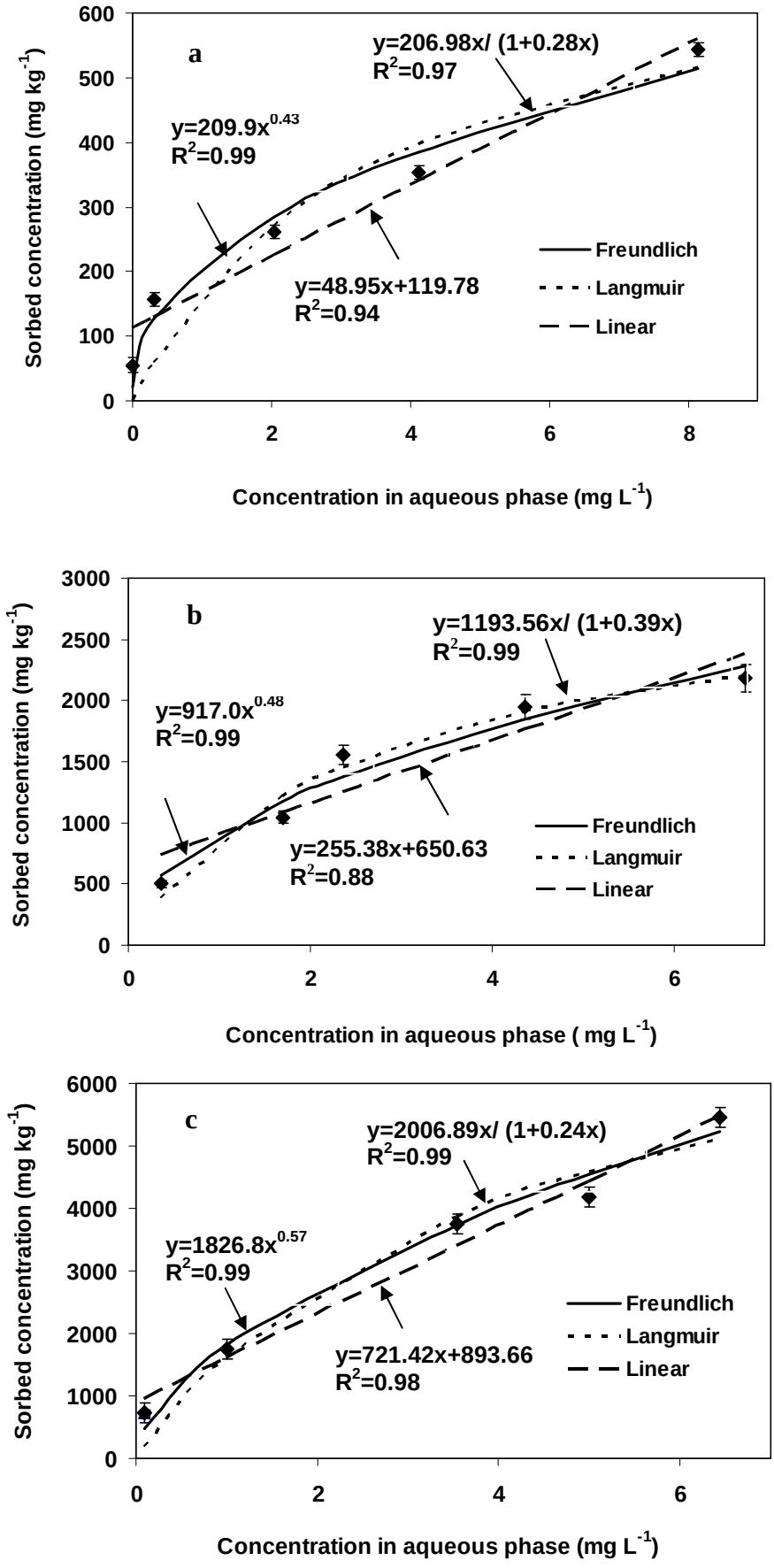

Figure 5.12: Sorption of naphthalene to sand (a), silt (b) and clay (c) at 22±1 °C**.** (Bars indicate the standard errors of experiments). Lines are model predictions. Symbols are experimental data.

In order to compare the sorption capacity of various soils for naphthalene and find out the relationship between sorption capacity and organic carbon content of soils, the sorption isotherms were analysed using the Freundlich equation. Because the units of K_a depend on the N value for a given sample (Bowman, 1981; Chen et al., 1999), K_a values cannot be compared between different isotherms. However, the K_a values from different isotherms can be compared with each other after normalizing C by the super-cooled liquid state solubility (S_{scl}) of the sorbate. S_{scl} of naphthalene is equal to 106.6 mg L^{-1} (Carmo et al., 2000). This method of normalization generated the modified Freundlich parameter, K'_a, which allowed comparison of K_a values from different isotherms. The normalized Freundlich parameter ($K_a^{'}$) and organic carbon content of three soils are summarized in Table 5.6.

Table 5.6: Comparison of sorption capacity and organic carbon content of three soils*

Soil	**K_a (mg kg^{-1}) (mg $L^{-1})^{-N}$**	**N**	**$K_a^{'}$ (mg kg^{-1})**	**Organic Carbon Content (%)**
Sand	209.90±26.71	0.43±0.073	1563	0.42
Silt	917.00±98.91	0.48±0.071	8624	1.44
Clay	1826.80±238.30	0.57±0.082	26152	4.25

*Temperature: 22±1 ^{o}C

As shown in Table 5.6, the sorption capacity of soils was proportional to the organic carbon content, which was consistent with previous research results (Manilal et al. 1991; Means et al. 1980). More specifically, clay with the highest organic carbon content had the highest sorption capacity for naphthalene, and silt was in the middle with respect to both

organic carbon content and sorption capacity, while sand with the lowest organic carbon content exhibited the lowest sorption capacity.

5.6 Mass Transfer of Soil-Bound Naphthalene

Mass transfer experiments of soil-bound naphthalene were investigated in the control and BMB bioreactors. The experimental data (as shown in Figure 5.13) indicated that the mass transfer of soil-bound naphthalene was unexpectedly fast in both the control and BMB bioreactors. This could be explained by the fact that tiny naphthalene particles were immediately released from the soils once the prepared naphthalene-contaminated soils were transferred into the solution inside the bioreactors. This increased interfacial surface area of naphthalene particles significantly enhanced the mass transfer of naphthalene to the aqueous phase.

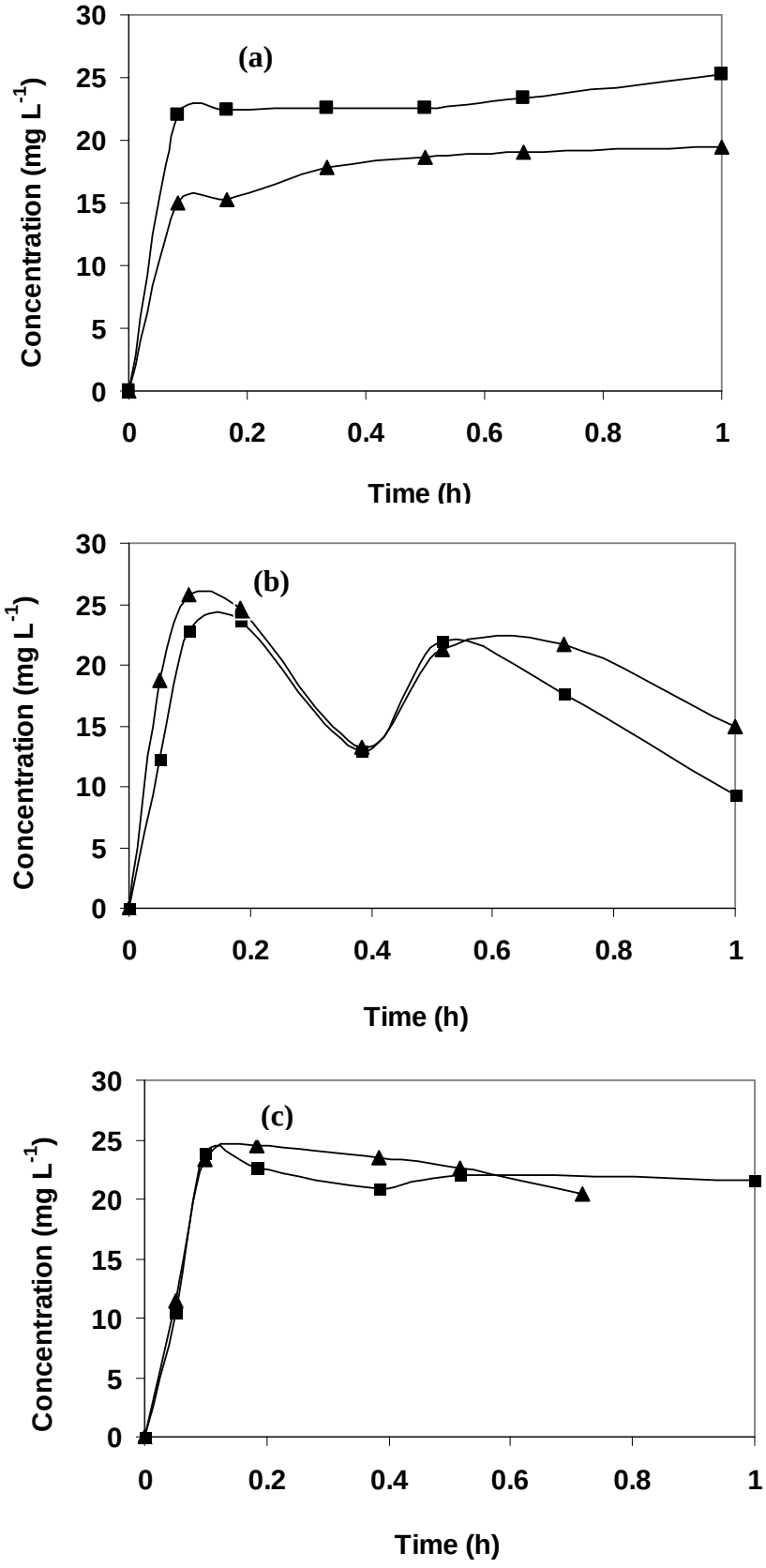

Figure 5.13: Mass transfer of sorbed naphthalene (~1% by weight) by sand (a), silt (b) and clay (c) (soil loading: 5% weight of soil (g) /volume of liquid (mL)) in control (▲) and BMB (■) bioreactors

5.7 Bioremediation of Naphthalene-Contaminated Soils

The bioremediation profiles for naphthalene-contaminated soils in the control and 25% bead mill bioreactors are presented in Figure 5.14.

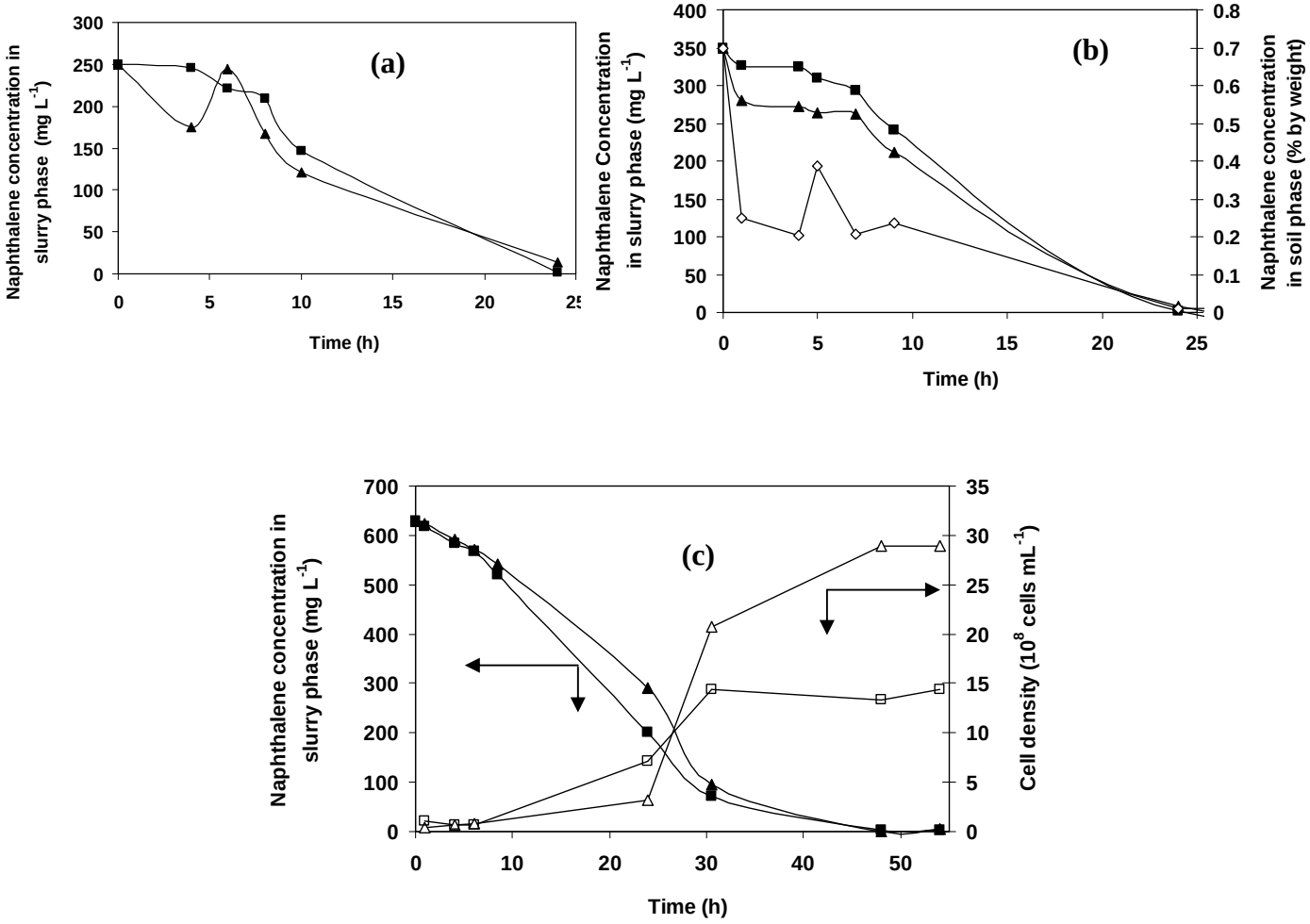

Figure 5.14: Bioremediation of naphthalene-contaminated sand (**a**), silt (**b**) and clay (**c**) in the control bioreactor (▲, Δ and ◊) and bead mill bioreactor (■ and □). Naphthalene concentration in slurry phase in the control (▲) and bead mill (■) bioreactors, naphthalene concentration in soil phase in the control bioreactor (◊), cell density in the control (Δ) and bead mill (□) bioreactors.

As shown in Figure 5.14, contrary to our expectation, biodegradation rates obtained in BMBs (with 25% bead loading) was not higher than those achieved in the control bioreactors for all three soils. It has been reported that the contamination age (duration of time a soil is in contact with dissolved PAHs) affected the bioavailability and biodegradability of soil-bound PAHs (Hatzinger et al. 1995; Yeom et al. 1993 and Yeom et al. 1998). In soils which were in contact with contaminant for a short period, mass transfer of contaminants from soil phase to the aqueous phase was not a major issue (Yeom et al. 1998), which was consistent with the mass transfer results observed in this study (Section 5.6). As a result, the enhanced biodegradation rates in the BMB may not be warranted for the soils with short history of contamination, less than 2 days in this investigation. In addition, from Figure 5.13(b), it was shown that around 64% of total naphthalene in the control bioreactor was released from soil phase to the aqueous phase within 1 hour, confirming that mass transfer was not the rate-limiting step for biodegradation of recently contaminated soil. The comparison of the average bioremediation rates among these three soils, 10.42 mg L^{-1} h^{-1} for sand, 14.58 mg L^{-1} h^{-1} for silt and 13.13 mg L^{-1} h^{-1} for clay, showed that there was no significant difference among these three soils with varying organic carbon contents. The observed pattern could be explained by the weak sorption of naphthalene on soils which resulted in the similar biodegradation rates. In order to study the effect of sorption and slow diffusion through soil pores on the bioremediation of PAH-contaminated soils and examine the performance of the BMB for the bioremediation of PAH-contaminated soils, it is strongly recommended in the future to use artificially PAH-contaminated soils with the coexistence of non-aqueous phase liquids (NAPLs), which help to build strong sorption between PAHs and soil particles, or to use industrially contaminated soils.

CHAPTER 6 CONCLUSIONS AND RECOMMENDATIONS

6.1 Conclusions

The following conclusions can be made within the limits of this investigation.

Conclusions 1 to 7 are drawn from the experiments of suspended PAHs without soil.

1. Mass transfer of suspended naphthalene, 2-methylnaphthalene and 1,5-dimethylnaphthalene has been extensively investigated in the conventional, baffled, BMB and baffled bead mill bioreactors. The baffled bioreactor provided up to 7 times higher mass transfer coefficient for these three PAH particles compared to the control bioreactor. The improved mass transfer was due to the excellent mixing of the PAH slurry by the baffles, which significantly decreased the mass transfer film and as a result increased the volumetric mass transfer coefficient. Volumetric mass transfer coefficients of these three PAH particles were also significantly enhanced by up to 16 times in the BMB, compared to the control bioreactor. The enhanced mass transfer was due to both the excellent mixing and the crushing of the PAH particles by the glass beads which significantly increased the interfacial surface area of PAH particle and therefore, increased the mass transfer coefficient.
2. The mass transfer coefficients were observed to depend on the different structures of PAH compounds which result in different degrees of hydrophobicity. For instance, the mass transfer coefficient of naphthalene, which was the least hydrophobic, was highest in all the four bioreactors,

followed by 2-methylnaphthalene and then 1,5-dimethylnaphthalene which was the most hydrophobic among these three PAH compounds.

3. 1,5-dimethylnaphthalene could not be metabolized by *Pseudomonas putida* ATCC 17484 as their carbon source. Even in the presence of naphthalene to support growth, 1,5-dimehtylnaphthalene was not utilized.
4. Bioremediation of sole substrate, naphthalene and 2-methylnaphthalene, was studied in the control, baffled and BMB bioreactors. Both baffled and BMB bioreactors provided 2 times higher maximum bioremediation rates of naphthalene and 2-methylnaphthalene compared to the control roller bioreactor. These enhanced bioremediation rates were due to the improved mass transfer in these two modified bioreactors.
5. Mass transfer was found to be the rate-limiting step for bioremediation of naphthalene and 2-methylnaphthalene in the control and baffled bioreactors, while bacterial growth was observed to be the rate-limiting step in the BMB.
6. The maximum bioremediation rates of 2-methylnaphthalene were increased in the presence of naphthalene (mixed substrates) by 1.5 to 2 times in all the control, baffled and BMB bioreactors, compared to the single substrate. The increased bioremediation rates were due to the higher biomass concentrations generated by the growth on naphthalene prior to the consumption of 2-methylnaphthalene.
7. The bioremediation of 2-methylnaphthalene was much slower than naphthalene. The maximum bioremediation rates of 2-methylnaphthalene were generally about one third those of naphthalene in the sole substrate runs and one half in

the mixed substrate runs. The lower biodegradation rates were due to the higher hydrophobicity of 2-methylnaphthalene compared to naphthalene.

The following conclusions are made from the experiments with soil.

8. Sorption capacity of soils for naphthalene was proportional to the organic carbon content of soils. For instance, sand with the lowest organic carbon content had the lowest sorption capacity for naphthalene, silt was in the middle with respect to both the organic carbon content and the sorption capacity, and clay with the highest organic carbon content had the highest sorption capacity among these three soils
9. The mass transfer of soil-bound naphthalene from the artificially prepared soils with short contamination history to the aqueous phase in both the control and BMB bioreactors was unexpectedly fast due to the increased interfacial surface area of naphthalene particles and the weak sorption between naphthalene and soils.
10. In the bioremediation of naphthalene-contaminated soils, the BMB did not provide higher bioremediation rates compared to the control bioreactor. This was again due to the weak sorption between naphthalene and soils.

6.2 Recommendations

The following recommendations are made which may be suitable for the extensions to this study.

1. The mass transfer and bioremediation of suspended PAHs in the baffled and BMB bioreactors should be expanded by investigating a larger variety of PAH compounds.
2. The mass transfer of soil-bound PAHs and the bioremediation of PAH-contaminated soils in the baffled and BMB bioreactors should be further studied by observing desorption and bioremediation of strongly adsorbed PAHs by soils in the presence of NAPLs or using industrially PAH-contaminated soils.
3. The effects of pH, temperature, mixtures of PAH and chemistry of soil on the mass transfer and bioremediation of PAH-contaminated water or soils in the baffled and BMB bioreactors should be investigated in order to be of more practical use.
4. Operation in sequential batch mode needs to be studied in the baffled and BMB bioreactors to obtain the information on the overall productivity of these bioreactors.

REFERENCES

Abalos, A., Vinas, M., Sabate, J., Manresa, M. A. and Solonas, A. M., 2004, Enhanced Biodegradation of Casablanca Crude Oil by a Microbial Consortium in Presence of a Rhamnolipid Produced by *Pseudomonas aeruginosa* AT10, Biodegradation, 15: 249-260.

Ahn, I., Ghiorse, W. C., Lion, L. W. and Shuler, M. L., 1998, Growth Kinetics of *Pseudomonas putida* G7 on Naphthalene and Occurrence of Naphthalene Toxicity During Nutrient Deprivation, Biotechnol. Bioeng, 59: 587-594.

Alexander, M. and Scow, K. M., 1989, Kinetics of Biodegradation in Soil, Soil Science Society of America Special Symposium Publication 22: Reaction and Movement of Organic Chemicals in Soils, Soil Science Society of America, Madison, WI, p. 243-269.

Allen, T., 1997, Particle Size Measurement, Vol. 1, Fifth Edition, Chapman & Hall

Alshafie, M. and Ghoshal, S., 2003, Naphthalene Biodegradation from Non-Aqueous-Phase Liquids in Batch and Column Systems: Comparison of Biokinetic Rate Coefficients, Biotechnol. Prog, 19: 844-852.

Amrith, S. G. and Xing, B., 2003, Sorption and Desorption of Naphthalene by Soil Organic Matter, Journal of Environmental Quality, 32: 240-246.

Ashok, B.T., 1995, Biodegradation of Polycyclic Aromatic Hydrocarbons- a Review, J. Sci. Ind. Res., 54: 443-451.

ATSDR, 1993, Toxicological Profile for Polycyclic Aromatic Hydrocarbons (PAHs) Draft Update, U.S. Dept. Health & Human Services, Agency for Toxic Substances and Disease Registry, Atlanta, Georgia, p. 273.

Bailey, J. E. and Ollis, D. F., 1977, Biochemical Engineering Fundamentals, McGraw-Hill, Toronto, p. 335-341.

Bailey, J. E. and Ollis, D. F., 1986, Biochemical Engineering Fundamental, 2nd ed. McGraw-Hill, Toronto, p. 382-388.

Ball, W. and P R., 1991, Long-Term Sorption of Halogenated Organic Chemicals by Aquifer Material, 2. Intraparticle Diffusion, Environ. Sci. Technol., 25: 1237-1249.

Banerjee, D. K., Fedorak, P. M., Hashimoto, A., Masliyah, J. H., Pickard, M. and Gray, M. R., 2002, Monitoring the Biological Treatment of Anthracene Contaminated Soil in a Rotating Drum Bioreactor, Appl. Microbiol. Biotechnol., 43: 521-528.

Blanch, H. W. and Clark, D. S., 1997, Biochemical Engineering, Marcel Dekker, Inc., Hong Kong.

Bonilla, M., Olivaro, C., Corona, M., Vasquez, A. and Soubes, M., 2005, Production and Characterization of a New Bioemulsifier from *Pseudomonas putida* ML2, J. Appl. Microbiol., 98: 456-463.

Bosma, T. N. P., Middeldrop, P. J. M., Schraa, G., and Zehnder, A. J. B., 1997, Mass Transfer Limitation of Biotransformation: Quantifying Bioavailability, Environ. Sci. Technol., 31: 248-252.

Bouchez, M., Blanchet, D., Vandecasteele, J. P., 1995, Degradation of Polycyclic Aromatic Hydrocarbons by Pure Strains and Defined Strain Associations: Inhibition Phenomena and Cometabolism, Appl. Microbiol. Biotechnol., 43: 156-164.

Bowman, B. T., 1981, Anomalies in the Log Freundlich Equation Resulting in Deviations in Adsorption K Values of Pesticides and Other Organic Compounds When the System of Units is Changed, J. Environ. Sci. Health. Part B, 16: 113-123.

Brinkmann, D., Rohrs, J. and Schugerl, K., 1998, Bioremediation of Diesel Fuel Contaminated Soil in a Rotating Bioreactor, Influence of Oxygen Saturation, Chem. Eng. Technol. 21: 168-172.

Carberry, J. J., 1976, Chemical and Catalytic Reaction Engineering, McGraw-Hill, New York, NY, p. 52.

Carmo, A. M., Lakhwinder, H. S. and Thompsonm, M. L., 2000, Sorption of Hydrophobic Organic Compounds by Soil Materials: Application of Unit Equivalent Freundlich Coefficients, Environ. Sci. Technol., 34: 4363-4369.

CEPA, 1994, Priority Substances List Assessment Report Polycyclic Aromatic Hydrocarbons, Government of Canada.

Cerniglia, C. E., 1992, Biodegradation of Polycyclic Aromatic Hydrocarbons, Biodegradation, 3: 351-368.

Chen, Z., Xing, B. and McGill, W. B., 1999, A Unified Sorption Variable for Environmental Applications of the Freundlich Equation, J. Environ. Qual., 28: 1422-28.

Connors, M. A., and Barnsley, E. A., 1982, Naphthalene Plasmids in Pseudomonas, J. Bacteriol., 149: 1096-1101

Cussler, E. L., 1997, Diffusion Mass Transfer in Fluid Systems, 2nd ed. University of Cambridge Press, p.580.

Da Silva, M., Cerniglia, C. E., Pothuluri, J. V., Canhos, V. P. and Espoisto, E., 2003, Screening Filamentous Fungi Isolated From Estuarine Sediments for Ability to Oxidize Polycyclic Aromatic Hydrocarbons, World J. Microbiol. Biotechnol. 19: 399-405.

Danielsson, A., 2000, Rate-Limiting Factors During Bioremediation of Soil Containing HOCs, State of the Art Report Prepared for the Board of COLDREM, Chemical Engineering II, Lund Institute of Technology, Lund, Sweden, p.1-24.

Dean-Raymond, D. and Bartha, R., 1975, Biodegradation of Some Polynuclear Aromatic Petroleum Contaminants by Marine Bacteria, Dev. Ind. Microbiol., 16: 97-110.

Dunn, B. P. and Stich, H. F., 1975, The Use of Mussels in Estimating Benzo[a]pyrene Contamination of the Marine Environment, Proc. Soc. Expt. Biol. Med. 150: 49-51.

Eisler, R., 1987, Polycyclic Aromatic Hydrocarbon Hazards to Fish, Wildlife, and Invertebrates: A Synoptic Review, United States Fish and Wild Service, Patuxent Wildlife Research Center, Laurel, MD.

Eisler, R., 1987b, Polycyclic Aromatic Hydrocarbon Hazards to Fish, Wildlife, and Invertebrates: A Synoptic Review, U.S. Fish and Wild Service, Biol. Rep. 85 (1.11).

Erickson, D., Loehr, R. and Neuhauser, E., 1993, PAH Loss during Bioremediation of Manufactured-Gas Plant Site Soils, Water Res., 27: 911-919

Fabacher, D. L., Besser, J. M. Schmitt, C. J., Harshbarger, J. C., Peterman, P. H. and Lebo J. A., 1991, Contaminated Sediments from Tributaries of the Great Lakes: Chemical Characterization and Cancer-Causing Effects in Medaka (Oryzias latipes). Arch. Environ. Contam. Toxicol., 20: 17-35.

Feller, S. E. and Blaich, C. f., 2001, Error Estimates for Fitted Parameters: Application to HCl/DCl Vibrational-Rotational Spectroscopy, J. Chem. Educ., 78: 409-412.

Fredrickson, J. K., Balkwill, D. L., Drake, G. R., Romine, M. F., Ringelberg, D. B. and White, D. C., 1995, Aromatic-Degrading Sphingomonas Isolates from the Deep Subsurface, Appl. Environ. Microbiol. 61: 1917-1922.

Fredrickson J. K., Balkwill D. L., Romine M. F., Shi T., 1999, Ecology, Physiology and Phylogeny of Deep Subsurface Sphingomonas sp., J. Ind. Microbiol. Biotechnol., 23: 273-283.

Gaidhani, H. K., McNeil, B., and Ni, X-W, 2003, Production of Pullulan Using an Oscillatory Baffled Bioreactor, J. Chem. Technol. Biotechnol., 78 (2-3): 260-264.

Gaidhani, H. K., McNeil, B. and Ni, X-W., 2005, Fermentation of Pullulan Using an Oscillatory Baffled Fermenter, 7th World Congress of Chemical Engineering, 83 (A6): 640-645.

Ghoshal, S. and Luthy, R. G., 1996, Bioavailability of Hydrophobic Organic Compounds from Nonaqueous-Phase Liquids: the Biodegradation of Naphthalene from Coal Tar. Environ. Toxicol. Chem., 15 (11): 1894-1900.

Ghoshal, S. and Luthy, R. G., 1998, Biodegradation Kinetics of Naphthalene in Nonaqueous Phase Liquid-Water Mixed Batch Systems: Comparison of Model Predictions and Experimental Results. Biotechnol. Bioeng., 57 (3): 356-366.

Ghoshal, S., Ramaswami, A. and Luthy, R. G., 1996, Biodegradation of Naphthalene from Coal Tar and Heptamethylnonane in Mixed Batch Systems. Environ. Sci. Technol. 30: 1282-1291.

Gray, M. R., Banerjee, D. K., Fedorak, P. M., Hashimoto, A., Masliyah, J. H. and Pickard, M. A., 1994, Biological Remediation of Anthracene Contaminated Soil in Rotating Bioreactors, Appl. Microbiol. Biotechnol. 40: 933-940.

Guerin, W. F. and Boyd, S. A., 1992, Bioavailability of Naphthalene Associated with Natural and Synthetic Sorbents, Water Res., 31(6): 1504-1512.

Guerin, W. F. and Boyd, S. A., 1992, Differential Bioavailability of Soil-Sorbed Naphthalene to Two Bacterial Species, Appl. Environ. Microbiol., 58: 1142-1152.

HACH Company, 1994-2000, COD Reactor Model 45600 Instrument Manual, Cat. No.45600-18

Hamaker, J. W., 1972, Decomposition: Quantitative Aspects, In Goring, C.A.I. and Hamaker, J. W. (ed.) Organic Chemicals in the Soil Environment. Marcel Dekker, New York, p. 153-240,

Hatzinger, P. B. and Alexander, M., 1995, Effect of Aging of Chemicals in Soil on their Biodegradability and Extractability, Environ. Sci. Technol., 29: 537-545.

Hill, G. A., 1974, Kinetics of Phenol Degradation by *Pseudomonas putida*, M. Sc. Thesis, University of Waterloo.

Hixson, A. W. and Sidney, J. B., 1941, Mass Transfer Coefficients in Liquid Solid Agitation System. Ind. Eng. Chem. 33: 478-485.

Horvarth, R. S., 1972, Microbial Cometabolism and the Degradation of Organic Compounds in Nature, Bacteriological Rev., 36: 146-155.

Janikowski, T. B. Velicogna, D., Punt, M. and Daugulis, A. J., 2002, Use of a Two-Phase Partitioning Bioreactor for Degrading Polycyclic Aromatic Hydrocarbons by a *Sphingomonas sp*., Appl. Microbiol. Biotechnol. 59:368-376.

Jauhari, R., Gray, M. R. and Holloway, G., 1999, Growth of *Rhizobium leguminosarum* on Peat in Rotating Bioreactors, Can. J. Chem. Eng., 77: 911-916.

Jonker, M. T. O. and Koelmans, A., 2002, Sorption of Polycyclic Aromatic Hydrocarbons and Polychlorinated Biphenyls to Soot and Soot-like Materials in the Aqueous Environment: Mechanistic Considerations, Environ. Sci. Technol., 36:3725-3734.

Lee, J. M., 1992, Biochemical Engineering, Prentice Hall, Englewood Cliffs, New Jersey, p. 145-146.

Levenspiel, O., 1972, Chemical Reaction Engineering (2nd ed.), New York, NY: John Wiley &Sons, p. 150.

Luthy, R., 1994, Remediating Tar-Contaminated Soils at Manufactured-Gas Plant Sites, Environ. Sci. Technol., 28:A266-A276.

Luthy, R., 1997, Sequestration of Hydrophobic Organic Contaminants by Geosorbents, Environ. Sci. Technol., 31:3341-3347

Mackay, D., Shiu, W. Y. and Ma, K.C., 1992, Illustrated Handbook of Physical-Chemical Properties and Environmental Fate for Organic Chemicals, V. II. Lewis, Boca Raton

Maier, R. M., 2000, Bioavailability and Its Importance to Bioremediation, in Bioremediation, editor: V.J. James, Kluwer Academic Publisher, Boston.

Manilal, V. B. and Alexander, M., 1991, Factors Affecting the Microbial Degradation of Phenanthrene in Soil: Appl. Microbiol. Biotechnol., 35: 401-405.

Mark, R., Yan, J. and Daniel, K. C., 1997, The Effect of Biosurfactants on the Fate and Transport of Nonpolar Organic Contaminants in Porous Media, Water Resources Research Grant Proposal. http://water.usgs.gov/wrri/97grants/de97ner.htm.

Marx, R. B. and Aitken, M. D., 2000, Bacterial Chemotaxis Enhances Naphthalene Degradation in a Heterogenous Aqueous System, Environ. Sci. Technol., 34:3379-3383.

Means, J. C., Wood, S. G., Hassett, J. J. and Banwart, W. L., 1980, Sorption of Polynuclear Aromatic Hydrocarbons by Sediments and Soils, Environ. Sci. Technol. 14:1524-1528.

Meylan, W. M. and Howard, P. H., 1995, Atom/Fragment Contribution Method for Estimating Octanol-Water Partition Coefficients, J. Pharm. Sci. 84: 83-92.

Meysami, P. and Baheri, H., 2003, Pre-Screening of Fungi and Bulking Agents for Contaminated Soil Remediation, Adv. Environ. Res. 7: 881-887.

Michael, J. S., Lethbridge, G., Burns, R. G., 1997, Bioavailability and Biodegradation of Polycyclic Aromatic Hydrocarbons in Soils, FEMS Microbiol. Let., 152: 141-147

Miller, C. and Weber, W. J., 1988, Modeling the Sorption of Hydrophobic Contaminants by Aquifer Materials - 2, Water Res., 22: 465-474.

Mukherji, S. and Weber, W. J. J., 1998, Mass Transfer Effects on Microbial Uptake of Naphthalene form Complex NAPLs, Biotechnol. Bioeng., 60: 750-760.

Mulder, H., Breure, A. M., Van Honschooten, D., Grotenhuis, J. T. C., Van Andel, J. G. and Rulkens, W. H., 1998, Effect of Biofilm Formation by *Pseudomonas* 8909N on the Bioavailability of Solid Naphthalene, Appl. Microbiol Biotechnol 50: 277-283.

National Research Council of Canada (NRCC), 1983, Polycyclic Aromatic Hydrocarbons in the Aquatic Environment: Formation, Sources, Fate and Effects on Aquatic Biota. NRCC Report No. 18981, p. 209.

Neff, J. M., 1979, Polycyclic Aromatic Hydrocarbons in the Aquatic Environment, Sources, Fates and Biological Effects, Applied Science Publishers Ltd., Essex, England, p.262.

Ni, X-W., Gao, S. and Pritchard, D. W., 2004, A Study of Mass Transfer in Yeast in a Pulsed Baffled Bioreactor, Biotechnol. Bioeng., 45(2): 165-175.

Obana, H., Hori, S. and Kashimoto, T., 1981, Determination of Polycyclic Aromatic Hydrocarbons in Marine Samples by High-Performance Liquid Chromatography, Bull. Environ. Contam. Toxicol. 26: 613-620.

O'Conner, J. M. and Huggett, R.J., 1988, Aquatic Pollution Problems, North Atlantic Coast, including Chesapeake Bay, Aquatic Toxicol., 11:163-190.

Park, J. H., Zhao, X. D. and Voice, T. C., 2001, Comparison of Biodegradation Kinetic Parameters for Naphthalene in Batch and Sand Column Systems by *Pseudomonas putida*, Env. Progress, 20: 93-102.

Park, J. H., Zhao, X. D. and Voice, T. C., 2002, Development of a Kinetic Basis for Bioavailability of Sorbed Naphthalene in Soil Slurries, Water Res., 36: 1620-1628.

Paul, C. M., Van, N. M., Jonker, T. O. and Ablert, A. K., 2004, Modeling Maximum Adsorption Capacities of Soot and Soot-Like Materials for PAHs and PCBs, Environ. Sci. Technol., 38(12): 3305-09.

Pignatello, J., 1990, Slowly Reversible Sorption of Aliphatic Halocarbons in Soils: 2 Mechanistic Aspects, Environ. Sci. Technol., 9: 1117-1126.

Prabhu, Y. and Phale, P. S., 2003, Biodegradation of Phenanthrene by *Pseudomonas sp*. Strain PP2: Novel Metabolic Parthway, Role of Biosurfactant and Cell Surface Hydrophobicity in Hydrocarbon Assimilation. Appl. Microbiol. Biotechnol. 61: 342-351.

Providenti, M. A., Flemming, C. A., Lee, H. and Trevors, J. T., 1995, Effect of Addition of Rhamnolipid Biosurfactants or Rhamnolipid-Producing *Pseudomonas aeruginosa* on Phenanthrene Mineralisation in Soil Slurries, FEMS Microbiol. Ecol. 17: 15-26.

Purwaningsih, I. S., 2002, Mass Transfer and Bioremediation of Solid Polycyclic Aromatic Hydrocarbon (PAH) Particles in Bioreactors, PhD Thesis, University of Saskatchewan.

Rhodes, M., 1998, Introduction to Particle Technology, John Wiley & Sons, New York.

Riess, R., Nemati, M., Hill, G. and Headley, J., 2004, Biodegradation of Methyl and Dimethyl Naphthalenes in a Bead Mill Bioreactor, Canadian International Petroleum Conference.

Riess, R., Nemati, M., Headley, J. and Hill, G. A., 2005, Improved Mass Transfer and Biodegradation Rates of Naphthalene Particles Using a Novel Bead Mill Bioreactor, J. Chem. Technol. Biotechnol., 80: 662-668.

Rockne K. J., Strand S. E., 1998, Biodegradation of Bicyclic and Polycyclic Aromatic Hydrocarbons in Anaerobic Enrichments, Environ. Sci. Technol. 32: 3962-3967.

Saner, M., Bachofen, R., Schneider, K., 1996, Simulation of Onsite Vacuum Heap Aeration and Soil Surface Enlargement by a Closed Agitated Soil Bioreactor. Microbiol Res. 151: 29-35.

SAS Institute Inc, 1985, SAS User's Guide: Statistics, SAS Institute Inc, Cary, NC.

Schneider, J., Grosser, R., Jayasimhulu, K., Xue, W. and Warshawsky, D., 1996, Degradation of Pyrene, Benz[a]anthracene, and Benzo[a]pyrene by *Mycobacterium sp*. Strain RGHII-135, Isolated from a Former Coal Gasification Site, Appl. Environ. Microbiol., 62: 13-19.

Shuler, M. L. and Kargi, F, 2002, Bioprocess Engineering: Basic Concepts, Second Edition, Prentice Hall P T R, Englewood Cliffs, New Jersey, p. 61-63.

Smith, M. J., Lethbridge, G. and Burns, R. G., 1997, Bioavailability and Biodegradation of PAHs in Soils, FEMS Microbiol. Let., 152: 141-147

Steinberg, S., Pignatello, J. and Sawhney, B., 1987, Persistence of 1, 2 Dibromoethane in Soils: Entrapment in Intraparticle Micropores, Environ. Sci. Technol., 21: 1201-1208.

Sutherland, J. B., 1992, Detoxification of Polycyclic Aromatic Hydrocarbons, J. Ind. Microbiol., 9: 53-62.

Tabak, H. H., Govind, R., Gao, C., and Fu, C., 1998, Protocol for Evaluating Biokinetics and Attainable End-Points of Polycyclic Aromatic Hydrocarbons (PAHs) in Soil Treatment, J. Environ. Sci. Health A., 33:1533-1567.

Tarighian, A., Hill, G. A., Headley, J. and Pedras, S., 2003, Enhancement of 4-Chlorophenol Biodegradation Using Glucose, Clean Technol. Environ. Policy, 5: 61-65.

Thomas H. A., 1942, Bacterial Densities from Fermentation Tube Tests, J. Am. Wat. Works Assoc., 34: 572-576.

Van Loosdrecht, M. C., Lyklema, J., Norde, W. and Zehnde, A. J. B., 1990, Influences of Interfaces on Microbial Activity, Microbiol. Rev., 54: 75-87.

Vidali, M., 2001, Bioremediation: An Overview. Pure Appl. Chem., 73(7): 1163-1172.

Volkering, F., Breure, A. M., Sterkenburg, A. and Van Andel, J. G., 1992, Microbial Degradation of Polycyclic Aromatic Hydrocarbons: Effect of Substrate Availability on Bacterial Growth Kinetics, Appl. Microbiol Biotechnol., 36: 548-552.

Volkering, F., Breure, A. M. and Van Andel, J. G., 1993, Effect of Microorganisms on the Bioavailability and Biodegradation of Crystalline Naphthalene, Appl. Microbiol Biotechnol., 40: 535-540.

Walter, U., Beyer, T. J., Klein, J. and Rehm, H. J., 1991, Degradation of Pyrene by *Rhodococcus sp*. UW 1: Appl. Microbiol. Biotechnol., 34: 671-676.

Wang, X., and Brusseau, M. J., 1993, Solubilization of Some Low-Polarity Organic Compounds by Hydroxypropyl-?-Cyclodextrin, Environ. Sci. Technol., 27: 2821-2825.

Weast, R.C., 1968, Handbook of Chemistry and Physics, 49th Edition: 1968-69, the Chemical Rubber Company, Cleveland, Ohio, U.S.A.

Weber, W. J. and Miller, C., 1988, Modeling the Sorption of Hydrophobic Contaminants by Aquifer Materials - 1, Water Res., 22: 457-464.

Weeks, B. A. and Warinner, J. E., 1984, Effects of Toxic Chemicals on Macrophage Phagocytosis in two Estuarine Fishes, Mar. Environ. Res., 14: 327-35.

Weeks, B. A. and Warinner, J. E., 1986, Functional Evaluation of Macrophages in Fish from a Polluted Estuary, Vet. Immun. Immunopathol., 12: 313-20.

Wilson, S. C. and Jones, K. C., 1993, Bioremediation of Soil Contaminated with Polycyclic Aromatic Hydrocarbons (PAHs), a Review, Environ. Pollut., 81: 229-249.

Wu, S. and Geschwend, P., 1986, Sorption Kinetics of Hydrophobic Organic Compounds to Natural Sediments and Soils, Environ. Sci. Technol., 20: 717-725.

Xing, B., Pignatello, J. J. and Gigliotti, B., 1996, Competitive Sorption between Atrazine and Other Organic Compounds in Soils and Model Sorbents, Environ. Sci. Technol. 30: 2432-2440.

Ye, D., Siddiq, M. A., Maccubbin, A., Kumar, S. and Sikka, H. C, 1996, Degradation of Polynuclear Aromatic Hydrocarbons by *Sphingomonas paucimobilis*, Environ. Sci. Technol., 30: 136-142.

Yeom, I. T. and Ghosh, M. M., 1993, Surfactants in Mobilizing Soil-Bound Polycyclic Aromatic Hydrocarbons Using Nonionic Surfactants: Proceedings CSCE-ASCE National Conference on Environmental Engineering (NCEE), 1342-1352, Montreal, Canada.

Yeom, Ick-Tae and Ghosh, M. M., 1998, Mass Transfer Limitation in PAH-Contaminated Soil Remediation, Wat. Sci. Technol., 37(8): 111-118.

APPENDIXES

A1-Calibration Curve of Dissolved PAH Concentration

The calibration curves of three dissolved PAHs are shown in Figure A1. Included in these figures are the relationships between PAH concentrations and absorbance (or ODs), as well as regression coefficients.

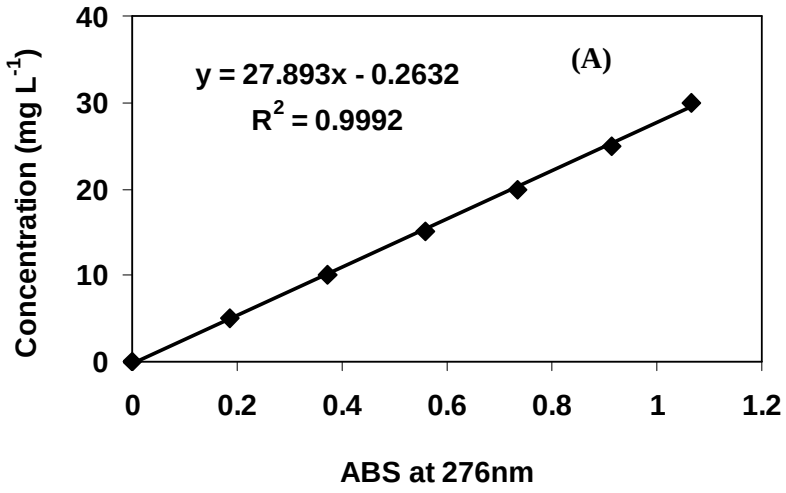

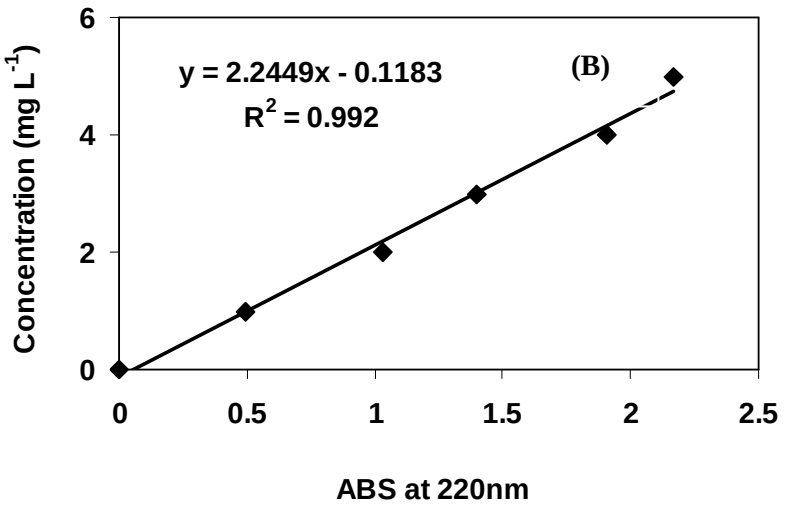

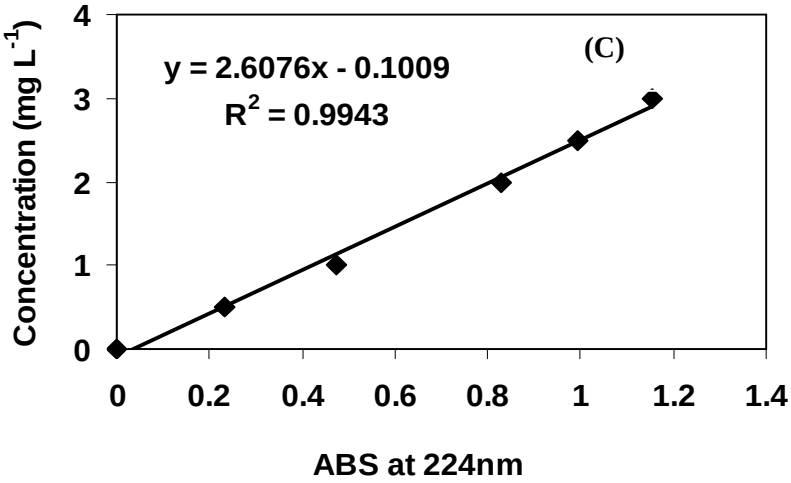

Figure A1: Calibration curves for naphthalene (A), 2-methylnaphthalene (B) and 1, 5-dimethylnaphthalene (C)

A2-Calibration Curve of Biomass Dry Weight

The calibration curve of biomass concentration was established using the spectrophotometer at a wavelength of 620nm. The calibration curve is presented in Figure A2.

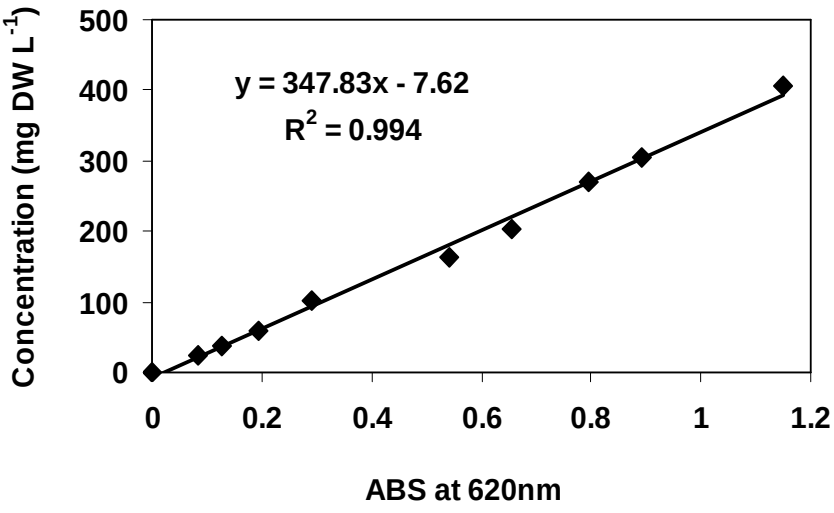

Figure A2: Calibration curve for biomass concentration

A3-Calibration Curve of Organic Carbon Mass

The calibration curve for the total organic carbon content measurement is shown in Figure A3. The relationship between organic carbon mass and ODs was linear and a least square fit gave the equation: y=2.4003x-0.0103 with a R^2=0.9994.

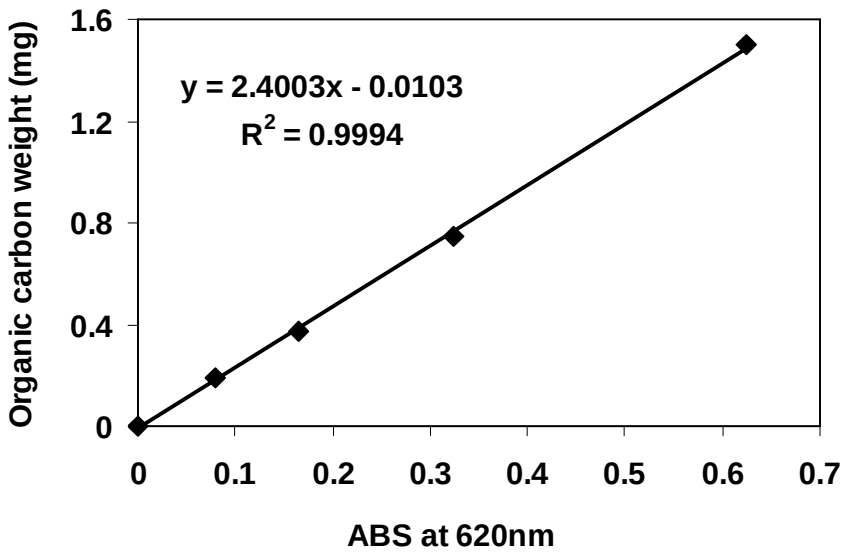

Figure A3: Calibration curve for organic carbon mass of soil

A4-Calibration Curve of Total PAH concentration

The calibration curves of naphthalene and 2-methylnaphthalene concentrations used in the bioremediation experiments were developed using HPLC and are reported in Figure A4.

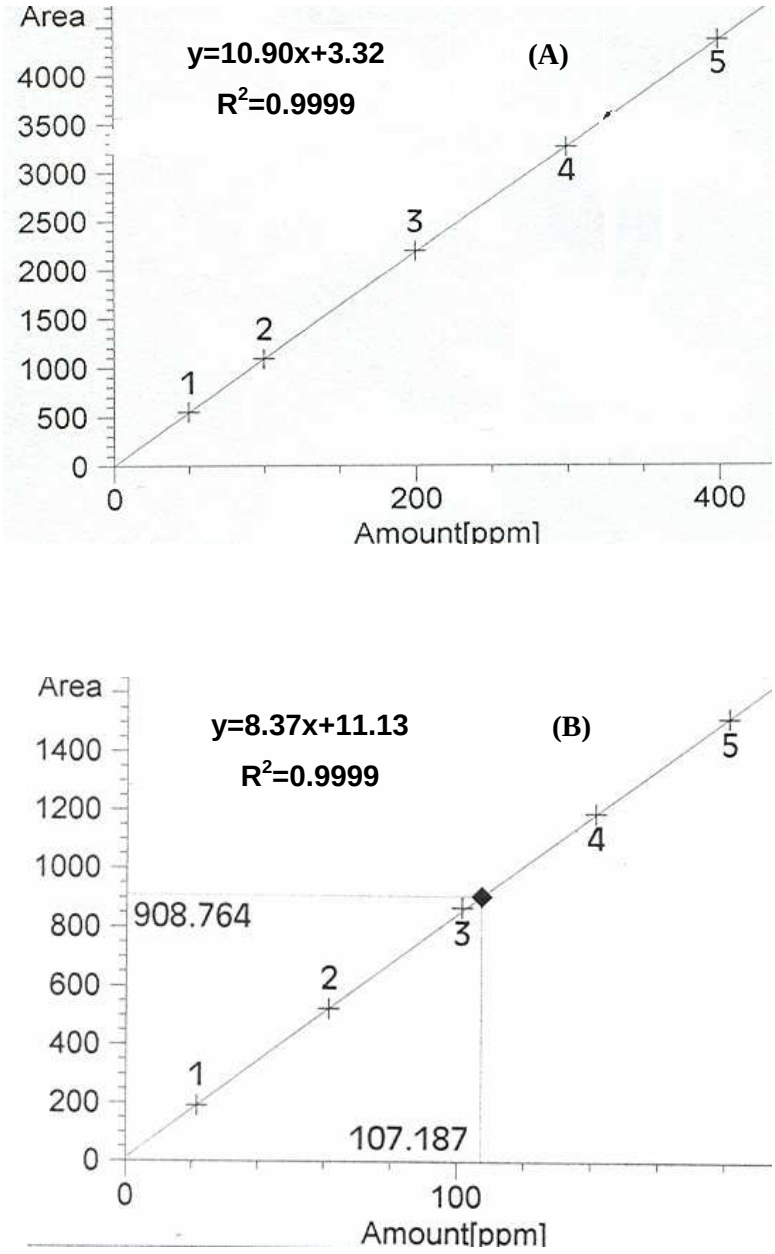

Figure A4: Calibration curves for naphthalene (A) and 2-methylnaphthalene (B) concentrations

A5-Mass Flow Meter Calibration

The Aalborg mass flow meter was used to measure the amount of air injected into the slurry solution in the roller bioreactors. It was calibrated against a volumetric displacement meter. The calibration curve is shown in Figure A5.

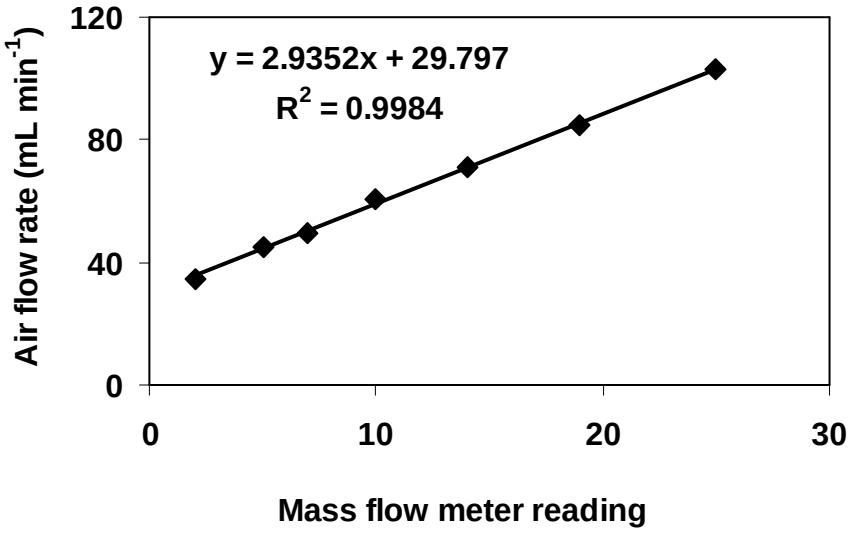

Figure A5: Calibration curve for mass flow meter

B-Particle Size Distribution

The particle size distributions of three PAH compounds were determined using a Malvern Long Bench Particle Size Analyzer (Allen, 1997; Rhodes, 1998). Before measurement for each new substance, the effect of mixing speed of the wet feeding unit on the particle size distribution was investigated using RO water as dispersant. Studies showed that 3000 rpm was the optimal mixing speed for the particles used in this study. For the wet feeder, another problem to consider was the presence of bubbles in the dispersant, which are typically recorded as 100 μm particles. Flushing of bubbles from the system was aided by pulsing the mixer from 0-3500 rpm a few times before setting the desired mixing speed. Due to different particle sizes, different lens ranges were selected for different compounds: 300 mm for naphthalene, 1000 mm for 2-methylnaphthalene and 1,5-dimethylnaphthalene.

The particle size distributions of these three PAH compounds are presented in Figure B1

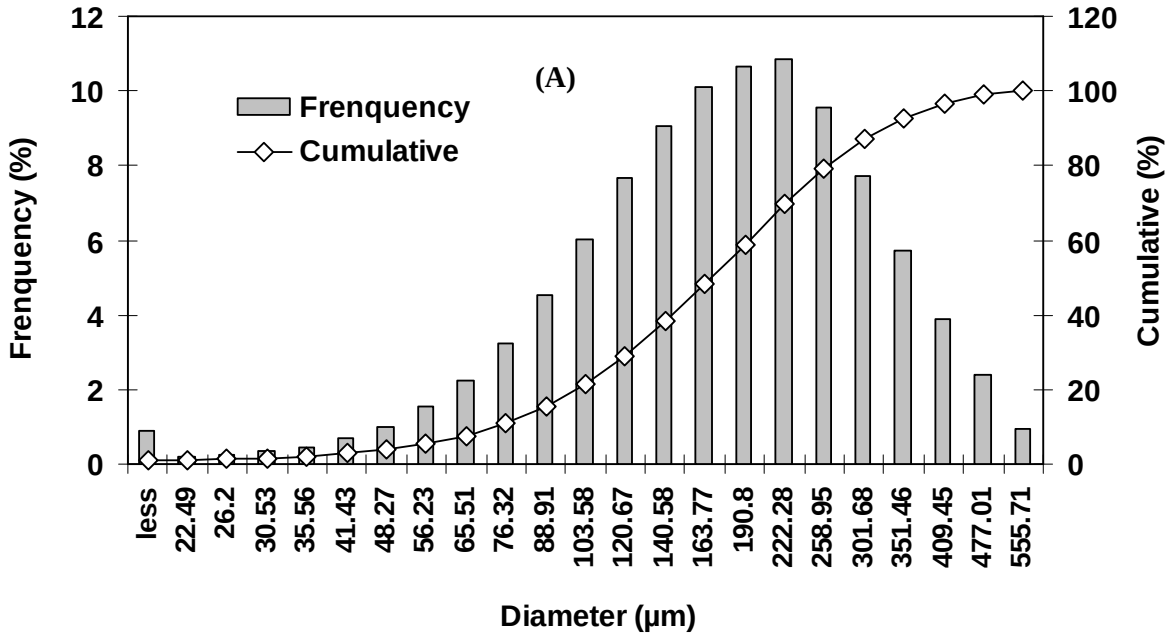

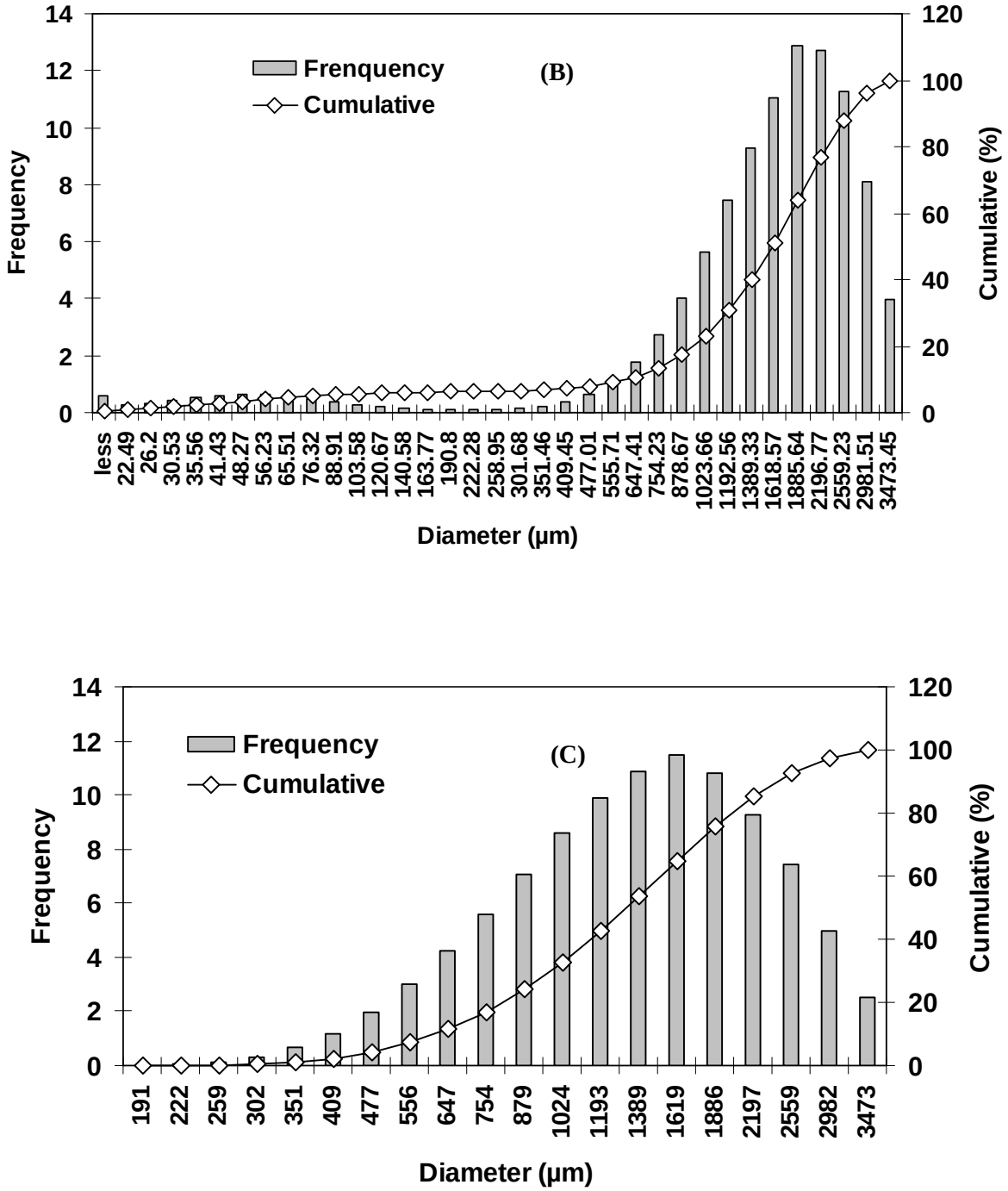

Figure B1: Particle size distributions of naphthalene (A), 2-methylnaphthalene (B) and 1,5-dimethylnaphthalene (C)

C-Raw Data Tables

1. Mass Transfer of Suspended PAHs

Table C1: Mass transfer of 1000 mg L^{-1} naphthalene in control bioreactor (22±1°C, 50 rpm)

Time (hour)	Concentration (mg L^{-1})	
	Run 1	Run 2
0	0	0
0.067	0.97	1.22
0.25	7.602	9.21
0.35	11.50	-
0.43	13.53	9.21
0.50	15.16	12.44
0.58	16.71	15.24
0.67	18.43	17.48
0.75	19.83	19.05
0.83	20.48	20.77
0.92	21.45	21.35
1.00	21.63	22.57

Table C2: Mass transfer of 1000 mg L^{-1} naphthalene in baffled bioreactor (22±1 ^{o}C**, 50 rpm)**

Time (hour)	Concentration (mg L^{-1})
0	0
0.067	9.04
0.15	20.58
0.22	24.77
0.28	26.77
0.33	27.56
0.42	27.71
0.50	28.55
0.67	28.69
1.00	28.72

Table C3: Mass transfer of 1000 mg L^{-1} naphthalene in BMB (22±1 °C, 50 rpm)

Time (hour)	Concentration (mg L^{-1})
0	0
0.050	18.50
0.10	28.40
0.17	29.35
0.23	29.03
0.40	28.89
0.45	28.89
0.62	28.88
1.00	30.28

Table C4: Mass transfer of 1000 mg L^{-1} naphthalene in baffled BMB (22±1 °C, 50 rpm)

Time (hour)	Concentration (mg L^{-1})
0	0
0.050	19.90
0.10	28.26
0.17	28.65
0.23	28.70
0.35	28.91
0.45	29.03
0.53	28.76
0.62	28.81

Table C5: Mass transfer of 1000 mg L^{-1} 2-methylnaphthalene in control bioreactor (22±1 °C, 50 rpm)

Time (hour)	Concentration (mg L^{-1})
0	0
0.50	3.10
0.75	7.01
1.00	8.40

Table C6: Mass transfer of 1000 mg L^{-1} 2-methylnaphthalene in baffled bioreactor (22±1 ^{o}C**, 50 rpm)**

Time (hour)	Concentration (mg L^{-1})
0	0
0.067	2.12
0.15	7.59
0.28	12.36
0.42	18.27
0.55	19.85
0.68	21.58
1.00	21.69

Table C7: Mass transfer of 1000 mg L^{-1} 2-methylnaphthalene in BMB (22±1 ^{o}C**, 50 rpm)**

Time (hour)	Concentration (mg L^{-1})
0	0
0.15	11.32
0.23	20.04
0.33	21.98
0.42	22.52
0.55	22.30
0.68	22.40
1.00	23.12

Table C8: Mass transfer of 1000 mg L^{-1} 2-methylnaphthalene in baffled BMB (22±1 ^{o}C**, 50 rpm)**

Time (hour)	Concentration (mg L^{-1})
0	0
0.05	4.15
0.15	18.03
0.23	21.95
0.33	23.14
0.42	23.61
0.68	23.45
1.00	23.24

Table C9: Mass transfer of 1000 mg L^{-1} 1,5-dimethylnaphthalene in control bioreactor (22±1 ^{o}C**, 50 rpm)**

Time (hour)	Concentration (mg L^{-1})
0	0
0.5	0.29
1	1.88

Table C10: Mass transfer of 1000 mg L^{-1} 1,5-dimethylnaphthalene in baffled bioreactor (22±1 ^{o}C**, 50 rpm)**

Time (hour)	Concentration (mg L^{-1})
0	0
0.25	1.45
0.32	2.11
0.50	3.61
0.75	4.94
1.00	5.15

Table C11: Mass transfer of 1000 mg L^{-1} 1,5-dimethylnaphthalene in BMB (22±1 ^{o}C**, 50 rpm)**

Time (hour)	Concentration (mg L^{-1})
0	0
0.067	0.30
0.15	2.22
0.23	3.65
0.33	4.77
0.42	4.72
0.55	4.82
0.75	4.86

Table C12: Mass transfer of 1000 mg L^{-1} 1,5-dimethylnaphthalene in baffled BMB (22±1 ^{o}C**, 50 rpm)**

Time (hour)	Concentration (mg L^{-1})
0	0
0.05	0.22
0.16	2.29
0.23	3.92
0.33	4.67
0.55	4.95
0.75	5.15
1.00	5.05

2. Bioremediation of Suspended PAHs

Table C13: Bioremediation of 500 mg L^{-1} naphthalene in three bioreactors (22±1 ^{o}C, 50 rpm)

Time (hour)	Control		Baffled		BMB	
	A*	B**	A	B	A	B
0	500	0.17	500	0.17	500	0.17
4	458.31	0.45	449.19	1.28	427.86	18.78
6	447.03	13.95	409.35	28.38	385.77	41.81
8.50	372.09	54.95	310.14	68.94	259.05	104.94
10	289.05	77.18	221.97	139.86	146.04	197.53
12	163.95	103.96	105.63	220.80	0	321.46
15	113.52	140.07	0	287.41	-	-
18	17.37	211.99	-	-	-	-
22.50	0.60	272.66	-	-	-	-
27.83	0.49	280.14	-	-	-	-

*A: Naphthalene concentration (mg L^{-1})
**B: Biomass concentration (mg L^{-1})

Table C14: Bioremediation of 300 mg L^{-1} 2-methylnaphthalene in three bioreactors (22±1 ^{o}C, 50 rpm)

Time (hour)	Control		Baffled		BMB	
	A*	B**	A	B	A	B
0	300	3.65	300	3.65	300	3.65
4	-	3.16	-	7.965	273.09	26.02
6	-	3.30	-	7.585	255.45	33.81
8	-	6.78	277.83	14.085	232.17	49.53
12	-	47.89	244.68	57.01	205.44	83.62
15	-	62.54	117.06	77.53	98.67	103.41
22.50	-	82.02	38.91	147.20	8.04	159.23
30.67	-	90.61	21.33	169.98	0	210.92

*A: 2-methylnaphthalene concentration (mg L^{-1})
**B: Biomass concentration (mg L^{-1})

Table C15: Bioremediation of Mixture of naphthalene (250 mg L^{-1}) and 2-methylnaphthalene (500 mg L^{-1}) in control and baffled bioreactors (22±1 ^{o}C**, 50 rpm)**

Time (hour)	Control			Baffled		
	A*	B**	C***	A	B	C
0	250	500	4.83	250	500	3.65
4	-	-	9.53	170.37	481.71	12.52
6	-	-	8.52	46.35	-	19.86
8	-	-	30.29	3.24	-	37.49
12	-	-	124.42	1.38	-	149.04
22	-	-	206.82	5.37	-	263.93
26.5	-	-	223.23	3.66	-	288.31
30.5	-	-	231.17	-	-	282.44

*A: Naphthalene concentration (mg L^{-1})
**B: 2-methylnaphthalene concentration (mg L^{-1})
***C: Biomass concentration (mg L^{-1})

Table C16: Bioremediation of Mixture of naphthalene (250 mg L^{-1}) and 2-methylnaphthalene (500 mg L^{-1}) in BMB (22±1 ^{o}C**, 50 rpm)**

Time (hour)	BMB		
	A*	B**	C***
0	250	500	3.65
4	180.87	480.18	16.35
6	54.9	487.74	34.36
8	37.62	362.52	43.58
13.5	0.025	28.71	180.97
24	0	19.65	263.14

*A: Naphthalene concentration (mg L^{-1})
**B: 2-methylnaphthalene concentration (mg L^{-1})
***C: Biomass concentration (mg L^{-1})

3. Sorption of Naphthalene to Three Types of Soils

Table C17: Sorption of naphthalene to three soils (22±1 ^{o}C**)**

Sand		Silt		Clay	
A*	B**	A	B	A	B
0.0042	55.39	0.36	498.16	0.092	731.99
0.31	156.06	1.7	1044.69	1.00	1747.74
2.05	261.78	2.36	1554.00	3.54	3760.66
4.13	353.30	4.36	1948.38	5.00	4174.07
8.14	543.09	6.79	2184.99	6.44	5459.98

*A: Equilibrium naphthalene concentration in aqueous phase (mg L^{-1})
**B: Equilibrium sorbed naphthalene by soil (mg kg^{-1})

4. Mass Transfer of Soil-Bound Naphthalene

Table C18: Mass transfer of sand-bound naphthalene in control and BMB bioreactors*

Time (hour)	Concentration (mg L^{-1})	
	Control	BMB
0	0	0
0.083	15.00	22.08
0.17	15.24	22.5
0.33	17.88	22.56
0.50	18.69	22.62
0.67	19.02	23.34
1.00	19.41	25.29

Table C19: Mass transfer of silt-bound naphthalene in control and BMB bioreactors*

Time (hour)	Concentration (mg L^{-1})	
	Control	BMB
0	0	0
0.05	18.69	12.27
0.10	25.74	22.80
0.18	24.66	23.64
0.38	13.26	13.02
0.52	21.3	22.02
0.72	21.75	17.67
1.00	14.91	9.27

Table C20: Mass transfer of clay-bound naphthalene in control and BMB bioreactors*

Time (hour)	Concentration (mg L^{-1})	
	Control	BMB
0	0	0
0.05	11.4	10.5
0.10	23.4	23.91
0.18	24.45	22.68
0.38	23.49	20.82
0.52	22.62	21.99
0.72	20.4	-
1.00	-	21.54

*Naphthalene: ~1% by weight; soil loading: 5% (soil mass, g)/ (liquid volume, mL); temperature: 22±1 ^{o}C; 50 rpm.

5. Bioremediation of Naphthalene-Contaminated Soils

Table C21: Bioremediation of naphthalene-contaminated sand in control and BMB bioreactors*

Time (hours)	Naphthalene concentration (mg L^{-1})	
	Control	BMB
0	249.5	249.5
4	174.76	245.17
6	244.13	221.72
8	166.86	209.67
10	121.04	147.15
24	14.14	1.33

Table C22: Bioremediation of naphthalene-contaminated silt in control and BMB bioreactors*

Time (hour)	Control		BMB
	Soil phase (%)	Slurry phase (mg L^{-1})	Slurry phase (mg L^{-1})
0	0.7	350	350
1	0.25	280.24	326.70
4	0.20	272.59	325.20
5	0.39	263.89	309.56
7	0.21	261.86	293.29
9	0.24	210.68	240.86
24	0.011	8.44	1.58

Table C23: Bioremediation of naphthalene-contaminated clay in control and BMB bioreactors*

Time (hour)	Control		BMB	
	Naphthalene (mg L^{-1})	MPN ($\times 10^8$ cells mL^{-1})	Naphthalene (mg L^{-1})	MPN ($\times 10^8$ cells mL^{-1})
0	630	-	630	-
1	624.41	0.39	618.79	1.02
4	591.83	0.71	583.73	0.71
6	570.49	0.78	567.45	0.71
8.5	542.40	-	521.33	-
24	289.54	3.13	201.75	7.07
30.5	95.78	20.7	70.80	14.4
48	0	28.9	3.863	13.4
54	4.09	28.9	1.88	14.4

*Temperature: 22±1 ^{o}C; 50 rpm